NATURAL PRODUCTS AS SELECTIVE CHEMOTHERAPEUTIC AGENTS AND AS CHEMICAL PROBES TO UNDERSTAND BIOLOGICAL PROCESSES

APPROVED BY SUPERVISORY COMMITTEE

John B. MacMillan, Ph.D.

Uttam Tambar, Ph.D.

Joseph Ready, Ph.D.

Michael Roth, Ph.D.

ACKNOWLEDGMENTS

I would like to thank my mentor Dr. John MacMillan for his guidance, patience and encouragement through out my graduate studies and for slowly allowing me to become an independent scientist. I would like to thank the members of my Graduate Committee for their insightful suggestions and encouragement through out these five years.

Finalmente, me gustaria agradecer a mis seres queridos a esas personas que gracias a su apoyo eh podido llegar a esta etapa en mi vida. A mi madre primero que nada, quien me dio el mejor ejemplo de como ser una guerrera, de luchar por tus ideales, aprender a creer en ti mismo y siempre querer ser mejor. Por ti madre estoy en el lugar en el que estoy, gracias porque a tu lado nunca me falto nada. Te amo madre y espero algun dia poder ser la mitad de mujer que eres.

A mi amado esposo, quien con su ejemplo me empuja a querer ser mejor. Gracias amor mio porque mitad de este trabajo es tuyo, gracias a tu apoyo, compresion y sobre todo amor. Te agradezco toda la paciencia que tienes hacia mi durante cualquier circumstancia y

por siempre tomarte el tiempo para estar a mi lado y ayudar en lo que sea que esta a tu alcance. Gracias por hacerme tan feliz, sin ti estaria perdida amor , eres mi luz cachito. Todos los dias espero ser mejor para poder darte la mejor version de mi para hacerte feliz como tu me haces todos los dias.

A mi hermano, la persona mas noble que conozco. Gracias hermano por tu apoyo y por tu cariño, eres el mejor hermano que pudiera haber pedido. Siempre al pendiente de mi y de mi madre, te adoro hermanito y quiero que sepas que estoy muy orgullosa de ti y te amo. A mi nena Grecia, que la siento casi como si fuera mi hija, a ti princesa que siempre llenas mis dias de alegria y te adoro changuito.

A mis kekas, a esas mujeres trinfudoras que me hacen querer ser mejor para estar a la par de ellas. Gracias por todo el cariño, las risas y el apoyo, soy muy afortunada porque Diosito me mando 9 hermanas a las que adoro con todo el corazon y que siempre estan a mi lado para darme un hombro en el cual llorar, o con quien reir, o simplemente con quien compartir el silencio, las adoro.

A mi familia politica, a mis suegros, Perla, Pancho, Emi, Viery y Dieguito quienes abrieron las puertas de su casa para mi y a quienes tengo tanto que agradecerles en muy poco tiempo. Los quiero muchisimo y gracias por apoyarnos en este el comienzo de nuestra familia, Fam. Mata guardan un lugar muy especial en mi corazon.

NATURAL PRODUCTS AS SELECTIVE CHEMOTHERAPEUTIC AGENTS AND AS CHEMICAL PROBES TO UNDERSTAND BIOLOGICAL PROCESSES

by

YAZMIN PAULINA CARRASCO

DISSERTATION

Presented to the Faculty of the Graduate School of Biomedical Sciences

The University of Texas Southwestern Medical Center at Dallas

In Partial Fulfillment of the Requirements

For the Degree of

DOCTOR OF PHILOSOPHY

The University of Texas Southwestern Medical Center at Dallas

Dallas, Texas

December, 2013

NATURAL PRODUCTS AS SELECTIVE CHEMOTHERAPEUTIC AGENTS AND AS CHEMICAL PROBES TO UNDERSTAND BIOLOGICAL PROCESSES

Publication No. _____

Yazmin Paulina Carrasco, Ph.D.

The University of Texas Southwestern Medical Center at Dallas, 2013

John B. MacMillan, Ph.D.

Aware of the important role that terrestrial microbial natural products play in the discovery of therapeutics and the decrease in rate of discovery of new natural products in the pharmaceutical industry, there is an immediate need to explore novel sources of microbial natural products with biological relevance. Marine bacteria are an excellent source of bioactive metabolites. With this idea in mind our laboratory has developed new techniques to isolate >600 species of marine actinomycetes and has created a natural product fraction library from these bacterial strains. My research efforts have focused on the isolation of natural products that exhibit selective activity against a panel of tumor derived cell lines that

include lung, colon, melanoma, pancreatic cancer and glioblastoma. In parallel to structure elucidation efforts of our active metabolite, the determination of its mode of action was ongoing in the laboratory of Dr. White. Through the use of a new screening tool, called FUSION (**Fu**nctional **Si**gnature **On**tology) we were able to determine that our active compound had similar activity to inhibitors of the TBK1 signaling pathway. Additionally, a novel polyketide was isolated from the marine-derived bacteria *Salinispora arenicola,* believed to be a key intermediate in the biosynthetic pathway of saliniketal, an inhibitor of ornithine decarboxylase induction. In addition, we have utilized the natural product leptomycin B (LMB), as a chemical tool to understand its inhibition of CRM1, a protein involved in export of cargo from the nucleus to the cytoplasm and a possible chemotherapeutic target. This work was done in collaboration with Dr. Chook. We observed that LMB irreversibly binds to CRM1 due to the hydrolysis of its lactone moiety causing stabilization of the protein-LMB complex. In contrast, compounds that lack the capability of being hydrolyzed by CRM1 are reversible inhibitors of CRM1. These research findings probe the question of designing molecules capable of reversibly inhibiting CRM1 and this perhaps will lead to reduced toxicity. This work illustrates the importance that natural products have not only as therapeutic agents for the treatment of diseases such as cancer but also as important chemical tools to understand complex biological processes.

TABLE OF CONTENTS

PRIOR PUBLICATIONS

Feng, Y.;* Carrasco, Y.P.;* MacMillan, J.B.; DeBrabander, J., Synthesis, Isolation and Biological Evaluation of Saliniketal Analog. *J Am Chem Soc*. Manuscript in progress. *Co-first authors

Potts, M.; Kim, H.; Fisher, K.W.; Hu, Y.; Carrasco, Y.P.; Ou, Y.; Herrera, M.; Cubillos, F.; Xiao, G.; Matan, H.; Ideker, T.; Xie, Y.; Lewis, R. E.; MacMillan, J.B.; White, M.A., Broad-scale mode-of-action Annotation of Natural Product Perturbations by Functional Signature Ontology (Fusion). *Science Signaling.* Manuscript accepted.

Sun, Q; Carrasco, Y.P.; Hu Y.; MacMillan, J.B.; Chook, Y.M., Nuclear export inhibition through covalent conjugation and hydrolysis of Leptomycin B by CRM1. *PNAS*. **2013**, 110 (4), 1303-1308

Varela-Ramirez, A.; Costanzo, M.; Carrasco, Y. P.; Pannell, K. H.; Aguilera, R. J., Cytotoxic effects of two organotin compounds and their mode of inflicting cell death on four mammalian cancer cells. *Cell Biol Toxicol* **2011,** *27* (3), 159-68.

Thodupunoori, S. K.; Alamudun, I. A.; Cervantes-Lee, F.; Gomez, F. D.; Carrasco, Y. P.; Pannell, K. H., Synthesis, structures and preliminary biological screening of bis(diphenyl) chlorotin complexes and adducts: Ph2ClSn-CH2-R-CH2-SnClPh2, R = p-C6H4, CH2CH2. *J Organomet Chem* **2006,** *691* (8), 1790-1796

LIST OF FIGURES

LIST OF SCHEMES

LIST OF TABLES

LIST OF APPENDICES

LIST OF DEFINITIONS

c-Abl ..... Abelson murine leukemia viral oncogene homolog 1

CLL ..... Chronic lymphocytic leukemia

COSY ..... Correlation spectroscopy

CRM1 ..... Chromosome region maintenance

DBU ..... (1,8-diazabicyclo [5.4.0] undec-7-ene)

DCM ..... Dicholoromethane

DMF ..... Dimethylformamide

DMPU ..... 1,3-Dimethyl-3,4,5,6-tetrahydro-2(1H)-pyrimidinone

DTT ..... Dithiothreitol

FDA ..... Food and Drug Administration

FOXO-3A ..... Forkhead box O3

GDP ..... Guanosine diphosphate

GST ..... Gluthathione S-transferase

GTP ..... Guanosine triphosphate

GTPase ..... Guanosine triphosphate hydrolase enzyme

HIP ..... Haploinsufficiency profiling

HMBC ..... Heteronuclear multiple bond correlation

HMPA ..... Hexamethylphosphoramide

HOP ..... Homozygous profiling

HPLC ..... High-performance liquid chromatography

^{Hs}CRM1 ..... Human CRM1

HSQC .....Heteronuclear single quantum coherence spectroscopy

Hsp90 .....Heat shock protein 90

HTS .....High-throughput screening

LCMS .....Liquid chromatography-mass spectrometry

LMB .....Leptomycin B

MDM2 .....Mouse double minute 2 homolog

mRNA .....Messenger ribonucleic acid

MSP ..... Mutlicopy suppression profiling

NBS .....N-bromosuccinimide

NES ..... Nuclear export signal

NLS ..... Nuclear localization signal

NMR .....Nuclear magnetic resonance

NPC ..... Nuclear pore complex

NOE .....Nuclear overhauser effect

NTF ..... Nuclear transport factors

p53 .....Tumor protein

Ran .....Ras-related nuclear protein

RCC1 ..... Regulator of chromosome condensation 1

RNAi ..... RNA interference

SAR .....Structure-activity relationships

^{Sc}CRM1 ..... *Saccharomyces cerevisiae* CRM1

SDS/PAGE..... Sodium dodecyl sulfate/Polyacrylamide gel electrophoresis

siRNA .....small interference RNA

TBS .....*tert*-Butyldimethyl silane

TBSCl .....*tert*-Butyldimethylsilyl chloride

THF .....Tetrahydrofuran

TLC ..... Thin layer chromatography

TOR ..... Target of rapamycin

CHAPTER ONE
Introduction

NATURAL PRODUCTS: THE NEXT FRONTIER IN DRUG DISCOVERY

1.1 Natural products in drug discovery

1.1.1 History of natural products in drug discovery

Nature has had a pivotal role in the area of drug discovery, for centuries natural products have been used as a source of medicines. The earliest record of natural products used for medicinal purposes dates back to 2600 BC when over 1000 plant-derived substances were utilized in Mesopotamia for the treatment of a variety of diseases.[1] Folk medicine continues to be utilized by different cultures for therapeutic purposes. [1] Over 200 years ago, Friedrich Sertürner isolated the first therapeutically active pure compound (morphine) from a plant. [2] The isolation of morphine from opium opened up a new area of drug discovery, where active components could be purified from their source and administered in specific dosages. [3] The modern age of natural products began with the discovery of penicillin, which opened up to a biological activity driven process for the identification of new antibiotics. [3] By 1990 an approximate of 80% of drugs were natural products or derivatives thereof. [3-4] Nevertheless, the pharmaceutical industry started to move away from natural products due to the introduction of combinatorial chemistry for the generation of what looked like an endless supply of compound libraries and a change in paradigm of high-throughput target based screening. [4-5] It was thought that the easy generation of large number of molecules would lead to faster discovery of leads compared to the traditional drug discovery process.[6] Even after pharma switched gears from natural products to synthetic medicinal chemistry, 13

natural product-derived drugs were approved from 2005 to 2007 in the United States. [4] Despite the success of natural products in drug discovery pharmaceutical companies have reduced the use of natural product in their drug discovery platforms because of the perceived limitations associated with natural products such as: meeting the supply requirements, access to the biological resource, structural complexity of natural products, and the apparent slowness associated with working with natural products (More on **section 1.1.2**). [4]

Unfortunately, the accepted approach for drug discovery by the pharmaceutical industry of high-throughput screening (HTS) of large chemical libraries against a single target, followed by optimization of lead compounds has failed to provide sufficient new drugs.[7] After the high point in the late 1980s for the discovery of new drugs (60 small molecules/year) the discovery rate has declined, over the period of 2001 and 2010 the average of new drugs discovery dropped to 23 per year. [8] Even though this drop in productivity by the pharmaceutical industry can be attributed to a number of factors, it certainly occurred at a stage where pharmaceutical companies moved away from natural products. [1]

The pharmaceutical industry is facing important challenges that can hurt their revenue which include expensive product recalls, the forthcoming patent expirations of successful products, and competition by generic drug manufacturers. [3, 7] The sum of all these factors has pushed industry to concentrate on therapies that can provide sustainable products and to re-examine the drug discovery process. In context with the latter, industry has begun to shift their focus once again to natural products and it's moving away from target-based screens concentrating instead on phenotypic screens. [7] It is becoming clearer that a disease state is a

sum of aberrant molecular signals and targeting one protein may not translate to a true therapeutic value. Instead phenotypic screens offer the ability to screen for small molecules in a complex biological system and probe an entire pathway involved in a disease state. More details on phenotypic and target-based screens are in **section 1.2**. Furthermore, natural products were evolved by nature to interact with macromolecules, representing privileged structures capable of interacting with disease relevant macromolecules.[3] Contrary to the simplified chemical scaffolds found in single-target HTS, natural products have complex structures with large number of stereocenters and several oxygenated substituents. [3, 7] Synthetic chemist Sam Danishefsky better stated this idea *"a small collection of smart compounds may be more valuable than a much larger hodgepodge collection mindlessly assembled"*. [9] The structural complexity and molecular diversity of natural products provides the perfect chemical scaffold for the interaction with macromolecules. After all they were evolutionary designed to interact with cellular determinants.

1.1.2 How to overcome the challenges of natural products in drug discovery

The arguments discussed above calls for the integration of natural products in drug discovery platforms, however there are some perceived challenges associated with natural products that need to be fully addressed for their incorporation to drug discovery efforts.

1.1.2.1 Access to biological resources

A concern in natural products research is access to a source of secondary metabolites that offers new and diverse chemistry. Plants have been a good source of natural product-derived drugs with 91 compounds in clinical trials up to 2007. [3] Only 6% of the plants have been investigated for pharmacological purposes opening up the possibility for the exploration of different species of plants in the search of new natural products. [1] However, as much as plants have contributed to the field of drug discovery microorganisms represent a more easily renewable source than plants. [10] Since the "Golden Age of Antibiotics" microorganism have been a prolific source of structurally diverse natural product-derived drugs with 130 drugs currently in use [10] treating a variety of disease areas, some examples include: rapamycin (molecular target mTOR), [11] lovastatin (molecular target HMG-CoA reductase) [12], and oxytetracycline (molecular target 30S ribosomal subunit) [13] just to mention a few (**Figure 1.1**).[1]

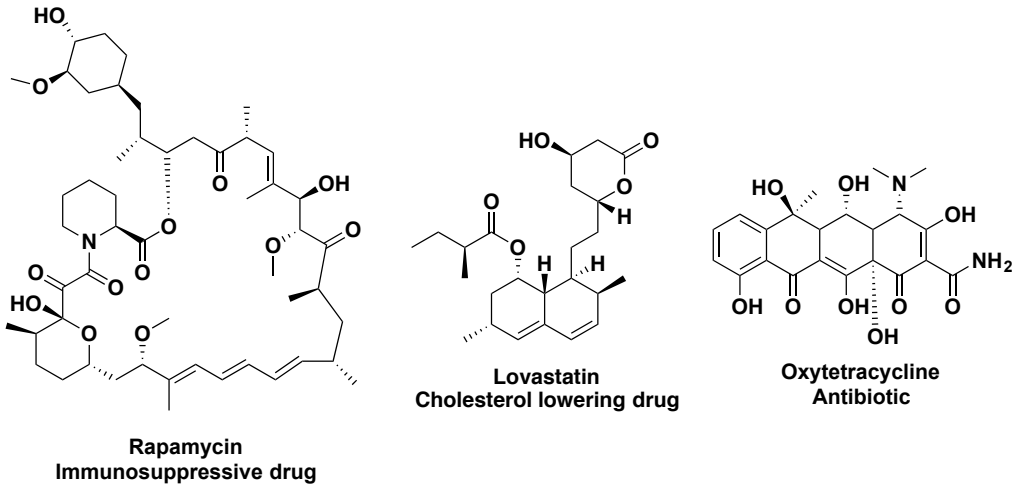

Figure 1.1. Drugs isolated from terrestrial bacteria

In the past the pharmaceutical industry has thoroughly investigated a large number of terrestrial microbes (bacteria and fungi), making it more difficult to isolate novel microorganisms and hence innovative chemistry. [10] However, different approaches are being investigated for the isolation of rarely isolated strains from soil samples that have proven to be successful. [14]

In contrast, the marine environment remains an underexplored source of natural products for drug discovery.[15] A variety of organisms found in marine habitats such as sponges, algae, coral, and other invertebrate species have provided a rich diversity of secondary metabolites that belong to different structural classes such as polyketides, alkaloids, terpenoids, non-ribosomal peptides and molecules of mixed biosynthetic pathways.[1, 16] Although, it has been shown that in many cases the natural products isolated from macroorganisms such as sponges and tunicates are not the actual producers, but the molecules are actually produced by associated microorganism. [17] Beginning with groundbreaking work by Fenical and co-workers in the early 2000s,[18] special interest has been placed on marine-derived bacteria due to the structurally diverse and biological active natural products that have been isolated from these bacterial strains. It has been demonstrated that the chemical diversity found in marine-derived bacteria is different from that of their terrestrial counterparts, opening a new avenue for drug discovery. [1, 16] One of these differences is a dramatic increase in halogenation, as can be observed in the natural products marinopyrrole[19] and ammmosamide [20].

As of 2012, the Food and Drug Administration (FDA) has approved 6 marine natural products or derivatives thereof as therapeutic agents and 14 others are currently in clinical

trials. [17b] Some of these natural products include ET-743 (molecular target minor groove of DNA) [21], salinosporamide A (molecular target 20S proteasome) [22], E7389 (molecular target microtubules)[23] and bryostatin 1 (molecular target protein kinase C) [24] shown in **Figure 1.2**.

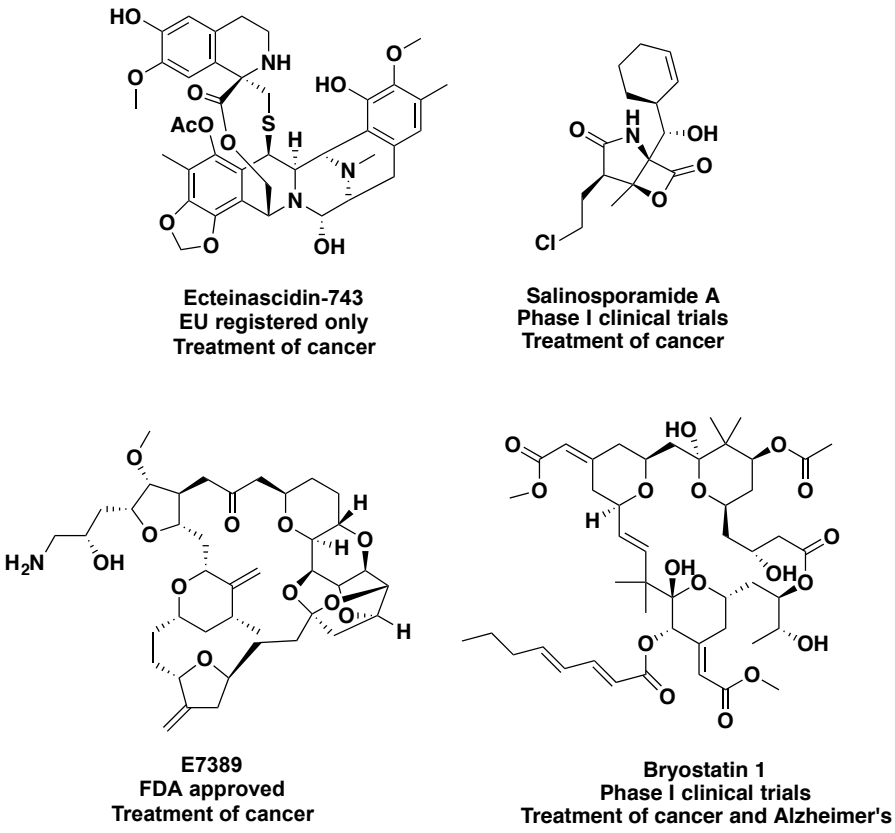

Figure 1.2 Marine natural products in clinical trials in the U.S.

Over the past decade many studies have looked at the microbial diversity in the ocean, showing that the ocean contains high concentrations of microbial diversity ranging from 10^6 bacteria per mL in seawater to 10^9 bacteria per mL in ocean-bottom sediments.[25] Metagenomics studies of the world's oceans reveal that not only is the ocean rich in total bacteria but also that there is high microbial diversity, with 85% of sequence data obtained unique at a 98% sequence homology limit.[26] The enormous microbial diversity found in the ocean reveals the great potential for natural product discovery.

1.1.2.2 Appropriate screening approaches for natural products

Often times screening of natural products was done using crude extracts leading to time-consuming dereplication efforts and lag times in lead selection. However, due to numerous innovations in HTS large number of samples can be analyzed, which allows for the pre-fractionation of crude extracts. Pre-fractionation can be achieved using automated purification systems that allow the access of semi-pure fractions of natural products. In one study Ireland and co-workers, demonstrated the impact of using semi-purified fractions in screening efforts. [27] This allows minor components to be detected in screens and at the same time can remove nuisance compounds that show positive results in every assay format. [27] For example, using a library of 15,360 fractions it was possible to identify breast cancer selective metabolites despite the presence of general cytotoxins in the crude extracts that would normally mask this selectivity.[27]

This example illustrates the advantages of pre-fractionation by obtaining semi-pure fractions, for example de-replication efforts were made easier and quicker. It also allowed for the identification of selective compounds that otherwise would have been masked by the general cytotoxins present in the crude. And most importantly, compounds found in small quantities can be detected that would have been overlooked in crude extracts.

An additional challenge is that in some cases compounds in fractions can have inherent characteristics that can interfere with the assay affecting its readout. For example, compounds that auto-fluoresce or that have UV absorption can interfere with the screen.[6] This is an inherent problem with small molecule screening and requires the use of orthogonal screening approaches.

1.1.2.3 Structure elucidation of the key compound

Advances in the fields of NMR spectroscopy and mass spectroscopy have had an impact on structure elucidation of small quantities of materials. Before, milligram quantities of material were needed for structure elucidation efforts, followed by funneling of the remainder of the compound for biological studies. [17b] Nowadays, with NMR instruments containing microcryoprobes, structures can be solved at the nanomole scale. [28] In addition, powerful mass spectrometry techniques coupled with algorithms has allowed for the high-throughput dereplication of non-ribosomal peptides saving time in dereplication efforts during hit selection. [29] Consequently, these technological advances have shortened the time of structure elucidation efforts allowing you to focus on the next stage of the drug discovery process, resupply of the natural product of interest and generation of analogs. However, stereochemical challenges still remain a limitation and need to be addressed on a molecule-by-molecule basis.

1.1.2.4 Resupply of natural product and generation of analogs

One of the major challenges in the drug discovery process involving natural products is constant supply, which can have an enormous effect on the development timeline. Additionally, there are instances where structural modifications of lead natural products are necessary for the development of analogs with greater potency or for improvement on their pharmacokinetic properties. Fortunately, there are some avenues that can be taken to ensure the resupply of natural product leads as well as the generation of analogs, which will be discussed in the section below.

Semisynthesis

Natural product leads are the starting point of medicinal chemistry efforts aimed at improving their biological properties. Thus, one necessity for semisynthesis is the constant resupply of compound for structural changes. An example of using semisynthesis for the generation of analogs with improved physicochemical properties was utilized for the production of rapamycin analogs shown in **Figure 1.3**. [7]

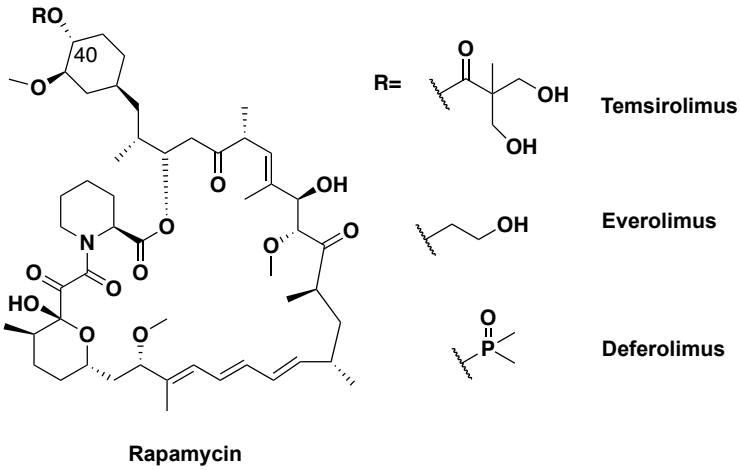

Figure 1.3. Analogs of rapamycin [7]

These analogs were created to improve their solubility for IV administration. All of the analogs were modified at position C-40 due to recognized tolerance for substitution at the cyclohexyl moiety. [7] This example highlights the use of semisynthesis as a technique to improve the pharmacokinetic properties of a natural product by generating analogues.

Total synthesis

Additionally, great effort has been place on formulating ways of synthesizing natural products with biological relevance in a manner that is economical and feasible for large-scale production, as well as to provide routes for the generation of structurally similar analogs with improved potency or properties. An exquisite example of this approach is the story of halichondrin B. [30] The total synthesis of this complex natural product by Kishi and co-workers led to the identification of the molecule's simpler pharmacophore. [23b, 23c, 31] The right hand side of the molecule (E7389) retained the biological activity of the parent compound but it is structurally simpler than the parent compound, resulting in the FDA approval of this analog in 2010 (**Figure 1.4**). [1, 32]

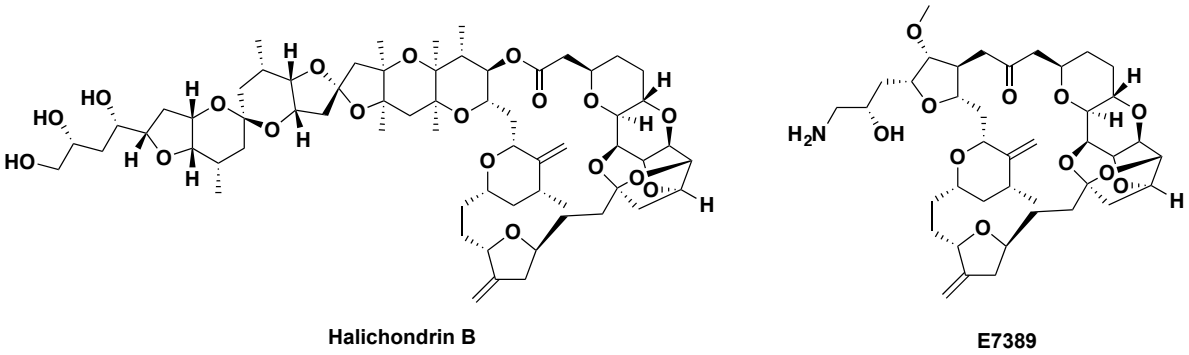

Figure 1.4. Halichondrin B and E7389

Total synthesis of halichondrin B and the identification of E7389 is a successful example of translation research. This example also highlights the important role of total synthesis of natural products in drug discovery for the generation of analogs as well as tackling the problem of supply of natural products.

Genomics

Developments in the area of genomics have allowed for the rapid sequencing of entire bacterial genomes and hence the discovery of the machinery responsible for production of natural products. Consequently, manipulation of biosynthetic gene clusters can be done more readily to produce analogs of lead natural product compounds (**Scheme 1.1**).

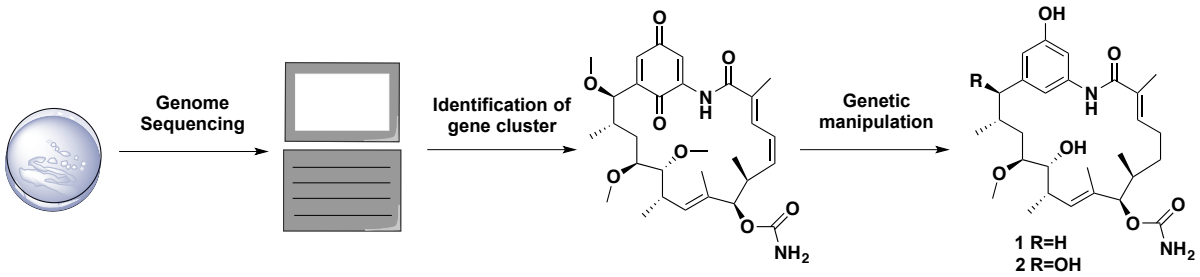

Scheme 1.1. Workflow of generation of analogues through genetic manipulation

An example of biosynthetic medicinal chemistry is shown in **figure 1.5** for macbecin, an Hsp90 inhibitor. [7] Genetic engineering mutants (deletion of tailoring genes, oxidases, etc.) of macbecin producing strain led to the generation of analogs with decreased toxicity due to its quinone moiety that was implicated in off-target effects.[33]

Knowledge of the biosynthetic gene cluster of macbecin allowed researchers at Biotica technologies to mutate the gene responsible for oxidation of carbon-21. Removing this oxidation step led to the production of compounds **1** and **2** without the redox reactive quinone moiety.

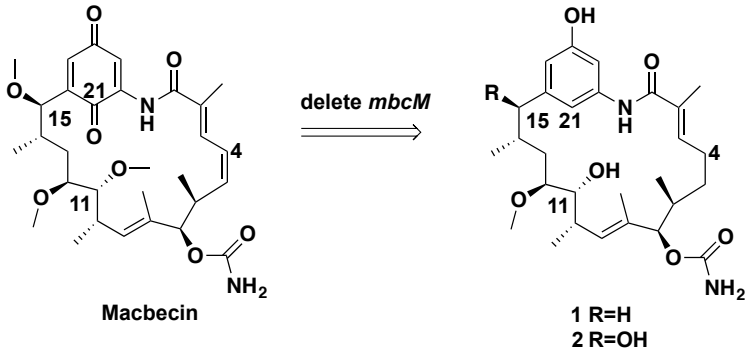

Figure 1.5 Macbecin and two analogs generated by genetic engineering. Removal of the *mbcM* gene results in compound **8** and **9**.[7]

Additionally, elimination of this oxygenation step caused an inhibition of downstream tailoring enzymes responsible for hydroxylation of C-15, dehydrogenation of C-4 and C-5, and methylation of C-11 and C-15. Compound **1** retained the same biological activity as the parent compound while decreasing its toxicity. In addition, to enhance the production of **1** the downstream tailoring enzyme responsible for oxidation of C-15 was deleted resulting in the sole production of **1**.[33] By biosynthetically engineering the producing strain of macbecin the group at Biotica Technologies was able to generate analogs with potent activity and reduced toxicity, as well as to obtain the desired product in good titers by removing unnecessary tailoring genes demonstrating the importance of this approach.

The field of genomics will play an important role in the rise of natural products as commercially available drugs. For secondary metabolites to be used as drugs, often times they need to be produced in the range of 1-10 g/L.[7] These yields have been previously observed from intense cycles of fermentation, enhancement of media and strain improvement. [7] The latter is achieved through a "mutate-and-screen" approach, which consists on randomly mutagenizing a strain and screen for mutants with improved production

of compound. [34] Using this approach the optimized strain of *Penicillium chrysogenum* is able to produce penicillin at a titer of 70 g/L, an increase of 1000-fold. [34] Even though these processes have had remarkable success they are long and resource-intensive. [35] Consequently, having knowledge on gene regulation of the biosynthetic pathway permits the manipulation of specific genes for strain improvement more rapidly. [36] Ben Shen and coworkers utilized this approach to engineer a *Streptomyces platensis* strain that had increased production of platensimycin, an antibiotic (**Figure 1.6**). [37] A bioinformatic analysis of the biosynthetic gene cluster of platensimycin identified the gene *ptmR1* as a negative regulator of the natural product's biosynthetic pathway. The inactivation of *ptmR1* in *S. platensis* resulted in overproduction of platensimycin by 100-fold compared to the wild type strain. [37]

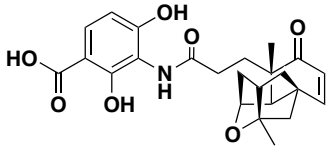

platensimycin

Figure 1.6. Structure of platensimycin

In natural products chemistry usually the compound of interest is found as a complex mixture of compounds that requires the use of chromatographic techniques for its purification that in cases can be a labor-intensive task. Ideally, one could modify the fermentation conditions and manipulate the strain for the production of a single product. [7] Once again, knowledge of the biosynthetic machinery can aid in the determination of unwanted steps that led to undesired products so that they can be genetically modified. In the case of the natural product doramectin, it is co-produced with a related compound CHC-B2 by *Streptomyces*

avermitilis (**Figure 1.7**). It is still unclear how the bacteria convert doramectin to CHC-B2 but it was believed that it involved the gene *aveC.* [34]

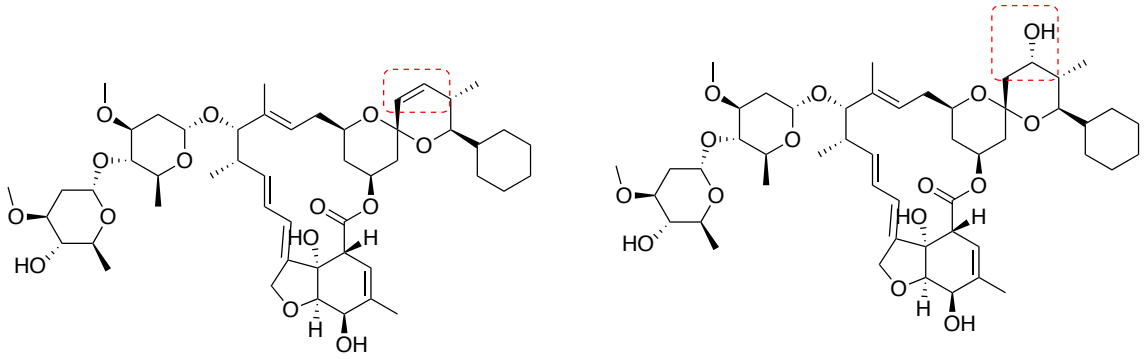

Figure 1.7 Doramectin and CHC-B2. Red rectangle = Structural differences between both compounds [7]

With this knowledge in hand, a knock out of *aveC* was generated that resulted in the elimination of doramectin and overexpression had no effect on production, consequently more refined changes were made. [7] Instead, DNA shuffling of the *aveC* gene produced a 10 amino acid long mutant that generated doramectin preferentially with overall improvement in production by 20-fold.[3, 38]This works highlights the power of genomics in natural products research.

In conclusion, natural products represent a great tool for the discovery of drugs due their evolutionarily diverse structural characteristics that make them amenable to interact with macromolecules, resulting in remarkable biological properties against a variety of diseases. Some of the challenges previously mentioned, such as constant supply of compound, access to new chemical diversity, or generation of analogs, have been and are currently under exploration for new and better ways to tackle these perceived limitations.

Nonetheless incorporation of phenotypic screens in drug discovery greatly enhances the potential of natural products, which is explained in the following section.

1.2 Phenotypic and target-based screens in drug discovery

1.2.1 Types of screens for drug discovery

There are two broad types of screens that have been utilized for drug discovery: 1) target-based and 2) phenotypic screens. In target-based screens, the drug discovery process is based on the selection of a target established by previous knowledge of the biology and evaluates the effects of a small molecule on the purified protein target. In contrast, phenotypic screens typically involve the use of whole cells, tissue or organism and rather than looking for activity against a specific target you are looking for a specific phenotypic response.

In the drug discovery process, in the pharmaceutical industry the target-based approach has been the method of choice. [39] This is due to important advances in the fields of genomics and molecular biology that have led to the discovery of important drug targets that are relevant to human disease. [40] For example, RNAi has been used as a powerful tool to identify drug targets, as well as advancements in high-throughput screening have allowed the rapid identification of compounds that interact with these targets. Also, structure-based tools have had an impact on target-based approaches since modifications to lead compounds can more readily be determined by computational modeling. [41] Furthermore, having a protein target allows for the development of a specific hypothesis and a starting point in the identification of a drug that targets the protein of interest (**Figure 1.8**). However, even with

the combination of all these tools, reduced success is still observed in discovering new drugs with unique therapeutic targets (first-in-class therapeutics). [41]

The pharmaceutical industry before relying on target-based screens for drug discovery focused on phenotypic screens, which led to the discovery of innovative drugs. [42] This observation suggests that perhaps replacing phenotypic screens with target-based screens contributed to a decrease in the discovery of innovative drugs. [41]

1.2.2 Phenotypic screens versus target-based screens

There are advantages and disadvantages to both types of screens. An advantage in target-based screens is that early on in the process you can apply molecular and chemical knowledge to gain specifics on the hypothesis being tested. [41] For example, having structural knowledge of the target protein allows the possibility for directed modification of the lead compound.

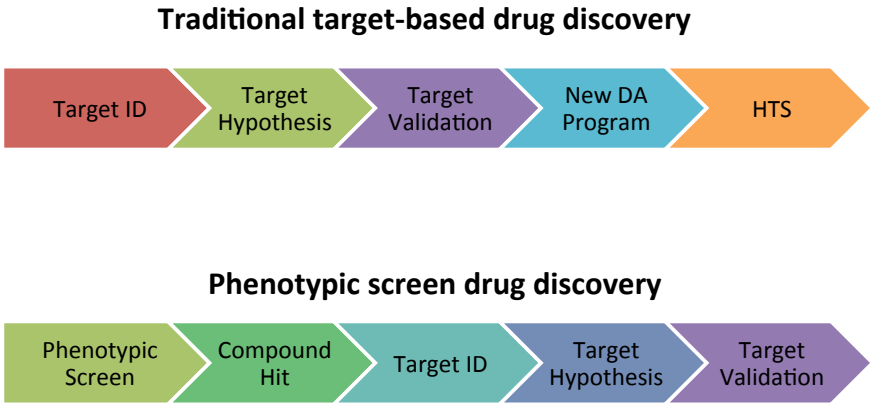

Figure 1.8 Target-based versus phenotypic screen. [43] Abbreviations: DA. Disease Area.

Contrary, one limitation in target-based screens is that it mainly focuses on measuring the activity of a specific protein or complex of proteins, for example measuring kinase activity or an interaction of a protein between other protein(s). [44] This may be oversimplifying a disease state and might lead to the drug not having a relevant therapeutic value. Additionally, if a drug is potent and selective *in vitro* it doesn't necessarily mean that this activity will translate *in vivo.* For example, access of the compound to the target protein maybe limited due to low cell permeability. [41, 44] Also, an important aspect that can be overlooked in target-based assays is the off-target effects that may result in the interaction of your compound with other proteins, that can lead to toxicity. [44]

An advantage of phenotypic screens is that instead of focusing on a specific molecular target, a small molecule can probe an entire pathway involved in a disease state for the best target (**Figure 1.8**). [43a] Also, since you are using whole cells you can target any protein, without any prior knowledge of the target. Additionally, any off-target effects will be evaluated early on, translating to a more efficient drug discovery process. [43a] Furthermore, the activity observed in phenotypic screens may translate to a therapeutic value more readily than at a target-based approach. Consistent with these observations, Swinney and Anthony reported that phenotypic screens were more successful at discovering first-in-class therapeutics than target-based screens. Between 1999 and 2008 a total of 75 first-in-class medicines were approved, 28 were discovered in phenotypic screens compared to 17 from target-based approaches, even with the current focus of target-based driven approach to drug discovery. [41] Nonetheless, a clear disadvantage in the phenotypic approach is the identification of the target resulting in the bottleneck of the drug discovery process.

Fortunately, important advances have been made in the area of target identification that this challenging task is now more tractable.

1.2.3 Workflow of the phenotypic screening approach

The first step in a phenotypic screen approach for drug discovery is to generate a cell-based assay to identify molecules that cause a specific phenotype (**Scheme 1.2**). After hit identification several secondary screens are performed to eliminate non-specific inhibitors. For example, compounds that perturb general cellular processes can affect expression of the reporter gene in the assay. [43a] Similarly, in a chemical genetics screen looking for nuclear export inhibitors of FOXO1a, a large number of compounds found in the screen were instead inhibitors of the general nuclear export machinery, such as CMR1, a nuclear export receptor. [45] Consequently, special attention has to be put on removing non-specific inhibitors from secondary screens to avoid complications later on in the discovery process. Since target identification is a time-consuming task you want to assure that you are carrying the best possible hit forward for mechanistic studies.

After removal of non-specific inhibitors, the focus is on prioritization of the biologically active compounds. There are different tools that can be utilized to aid in this aspect such as: gene expression profiling and data mining can aid in providing a potential mechanism of action, the use of in silico target prediction tools[46] for the generation of an early hypothesis or evaluation of the physicochemical properties of the compound. [43a] The latter is of great importance since it can affect future optimization studies of the lead compound. For example, having a hit compound with low solubility and low permeability

can give false-negatives delaying the optimization studies. Hence, the selection of hits with good physicochemical properties is desired since it allows for structure-activity relationship (SAR) studies to focus on improving the potency of the lead compound. Additionally, in silico scaffold- hopping can aid in the generation of SAR data that can be utilized to understand the pharmacophore in the molecule (**Scheme 1.2**).[43a] The combination of all these tools allows for the prioritization of hit compounds for subsequent studies on target identification.

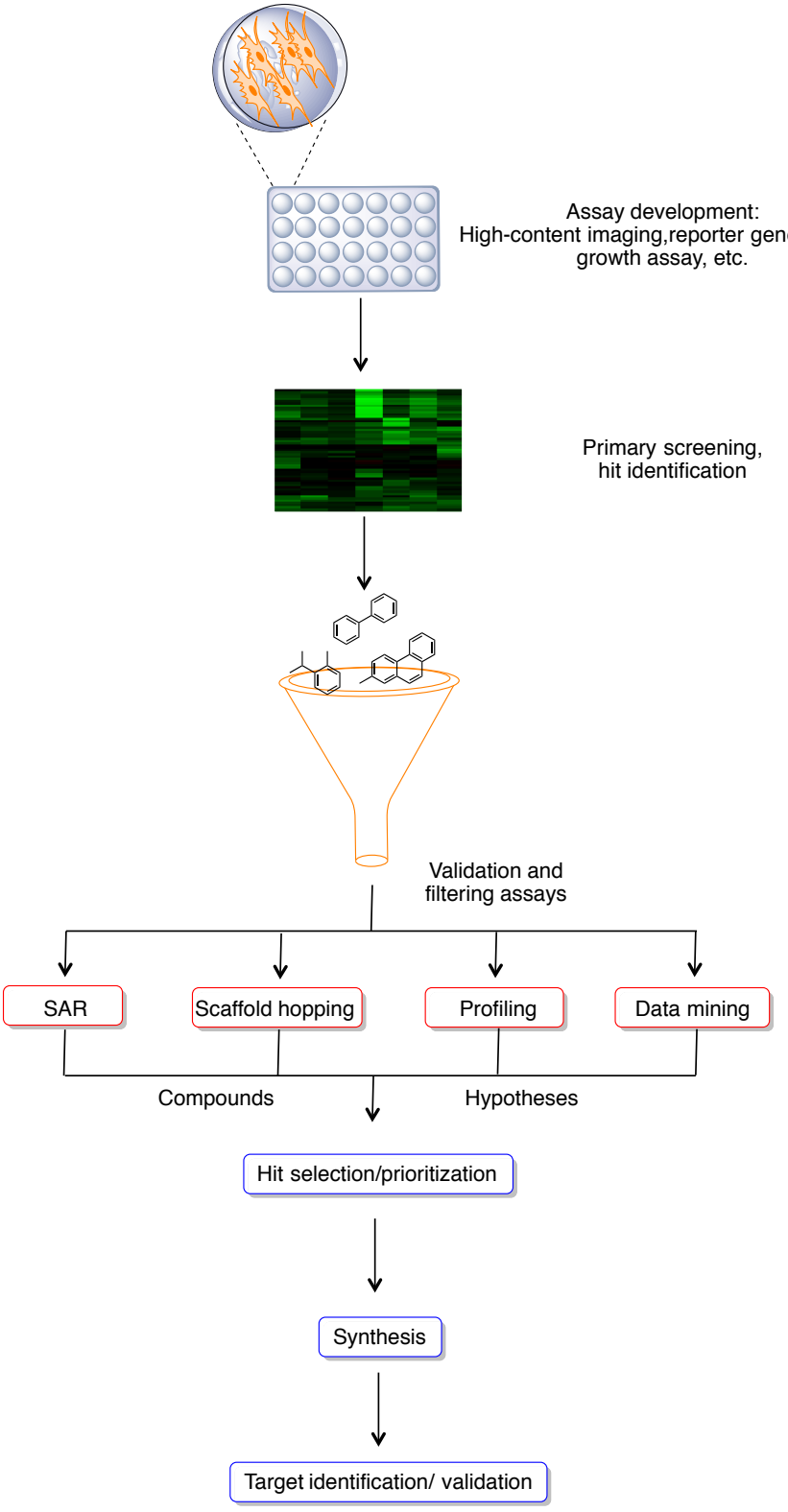

Scheme 1.2. Workflow of the phenotypic screening approach. [43a]

1.3 Target identification strategies

1.3.1 Chemical proteomics approach

The method of choice for determining the mode of action of biologically active small molecules has been chemical proteomics due in large part to its unbiased nature that enables the identification of the molecular target from a large number of proteins. [43a] This method requires the utilization of a "tagged" version of the active small molecule. It consists on the utilization of a matrix (e.g. streptavidin beads) for the immobilization of a pull down probe (e.g. biotin tagged compound) that is exposed to a protein mixture from cellular lysates. Exposure to the protein extracts leads to binding of the target to the probe; stringent washing is followed to remove non-specific binders from the probe and matrix. The target protein is then released by addition of the active molecule or by heating. Eluates are separated by SDS-PAGE and are digested with trypsin for analysis by MS/MS for the identification of the resulting peptides (**Scheme 1.3A**). [43b]

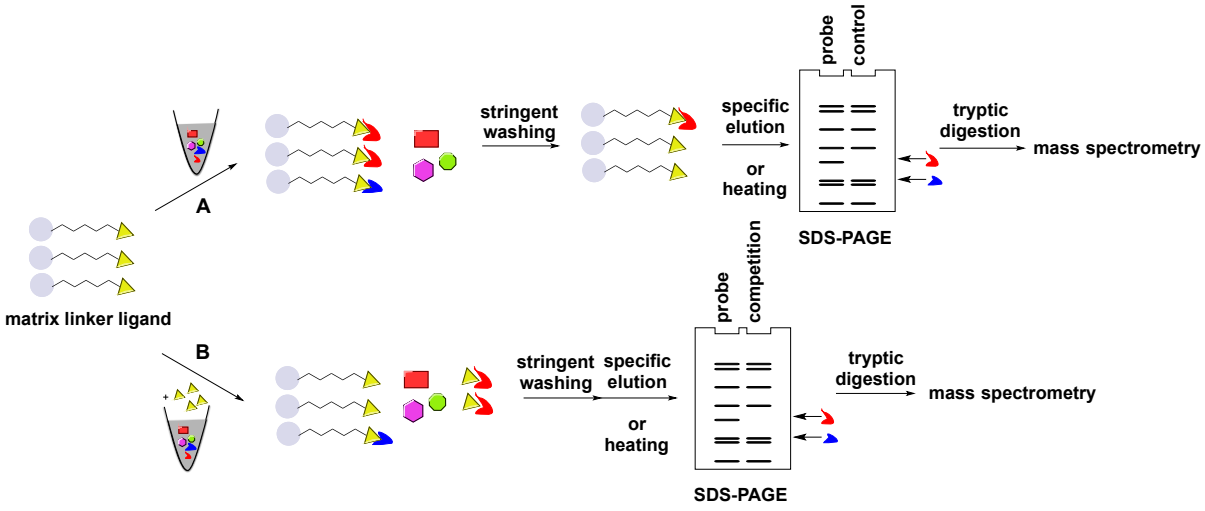

Scheme 1.3. Workflow of the chemical proteomics approach for targert identification. **A**. Process of affinity chromatography using control beads. **B**. Process of affinity chromatography using competition experiment with unmodified compound. [43b]

The probe needs to be equipped with a functional group (e.g. amines for covalent conjugation to an activated matrix such as N-hydroxysuccinimide) or affinity tag (e.g biotin strongly interacts with streptavidin) for immobilization of the active compound to the solid support. Extensive SAR-studies are performed on the lead compound as to improve its potency or pharmacokinetics properties, but also to delineate a site on the molecule that allows for substitution at that position without loss of activity. Once this tolerable site for modification has been identified a linker with a functional group or affinity tag is attached to this position for immobilization of the probe (**Scheme 1.4**). [43b]

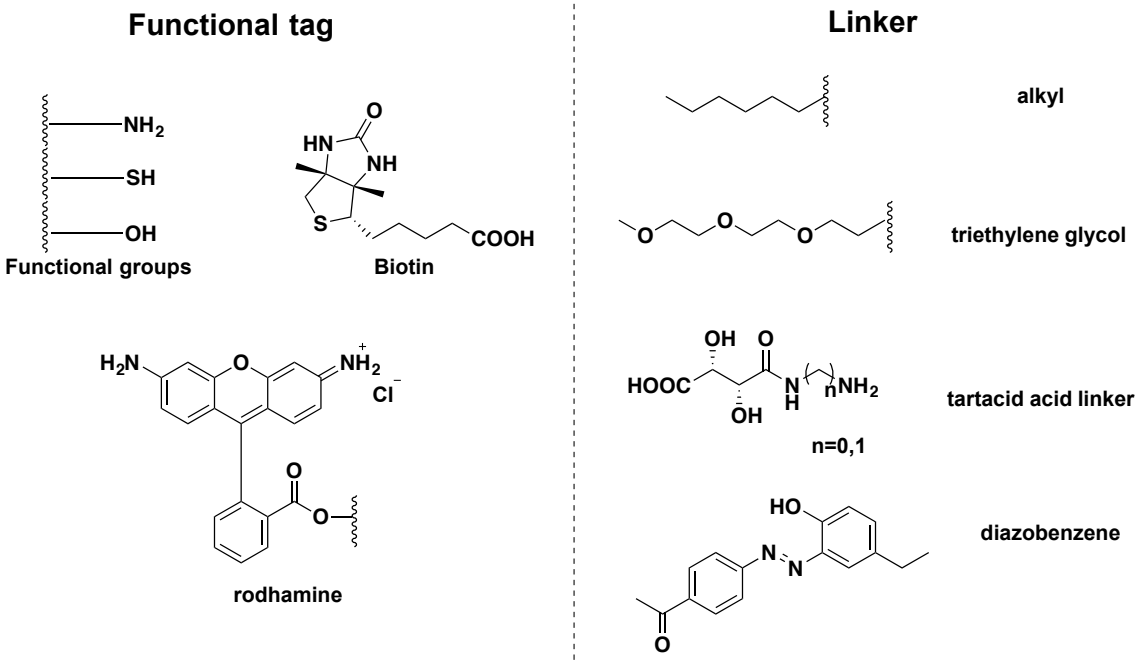

Scheme 1.4. Functional tags and linkers for affinity probe-based target identification

In some cases the linker of the probe to the affinity tag or functional group is implicated in background binding of proteins. It has been recognized that hydrophobic linkers (alkyl groups) tend to have more background binding.[43a] As a consequence,

hydrophilic linkers have been created such as tartaric acid derivatives [47] and polyethylene glycol [48] that decrease non-specific binding of proteins. Additionally, linkers that are cleaved under specialized conditions have been designed so that selective cleavage of the protein attached to the probe-linker complex occurs under these conditions leaving non-specific binders behind. [43b] An example is the use of diazobenzene-based linkers that are cleaved under mild reducing conditions (Sodium dithionite) for selective cleavage of the proteins bound to the probe (**Scheme 1.4**). [49]

One of the greatest limitations in chemical proteomics is the elimination of non-specific binders. In a phenotypic screen small molecules are exposed to a large number of cellular proteins. When the compound enters the cell it is in close proximity to many proteins and it can interact with a range of proteins at different degrees. [43a] Nonetheless, the high affinity interaction between the compound and its target is responsible for the phenotype observed and the biologically relevant interaction. [43a] However, due to the low affinity interactions of the active compound with abundant proteins, background noise is observed during purification of the target from cellular lysates. It is often recommended that affinity chromatography be utilized in the cases where the compound has high affinity for the target; otherwise the target would be washed away during purification.[43a] Since at this stage the target is not known, a good readout for affinity of the compound to its target is measurement of LC_{50} or EC_{50} of cellular assays. Ideal candidates for affinity chromatography are those in the low micromolar or nanomolar range. [43a]

An approach to reduce background binding is by cellular pre-fractionation, thus reducing the number of proteins that the probe and matrix are exposed to and enrichment of

the target protein. [43] A requirement for this approach is determining where the cell internalizes the compound. Consequently, the small molecule can be fluorescently tagged to detect in what compartments of the cell the compound is internalized. Kotake and co-workers utilized this approach for target identification of the natural product pladienolide B. The authors observed that fluorescence-tagged pladienolide B was localized in the nucleus and focused on nuclear extracts for target identification of the natural product. [50]

An additional strategy to minimize background binding is the use of serial-affinity chromatography. [51] This strategy consists on exposing cellular extracts to probe-derivatized beads. These beads are removed and the resulting lysate is then exposed to new probe-derivatized beads. The idea is that the first resin will be enriched with the specific target protein while the other resins would have the same amount of non-specific binders. This strategy was utilized to identify clathrin as the target of the natural product bolinaquinone. [52]

A popular approach to discriminate between non-specific binders from specific binders is the use of competition experiments with unmodified active compound and the affinity probe (**Scheme 1.3B**).[43b] In this approach cell lysates are first treated with active compound and then incubated with the probe. The target protein will bind to the unmodified compound preventing its binding to the immobilized probe. Consequently, the proteins that are found in a standard pull-down and are absent in the competition experiment will reveal the target. [43b] The target of the cytotoxic compound CB30865 was identified using this approach. [53] The compound was immobilized on beads and treated with cellular lysates in the presence and absence of unmodified compound. The only protein that was absent in the competition experiment was nicotinamide phosphoribosyltransferase (Nampt), an enzyme

involved in the biosynthesis of nicotinamide adenine dinucleotide (NAD). CB30865 was shown to inhibit Nampt at low nanomolar *in vitro* and *in vivo*.

Additionally, parallel pull-down experiments can be performed on the active compound as well as a close analogue that lacks biological activity *in vivo* to distinguish non-specific from specific binders. The proteins that are identified with the active compound but are not present in the inactive compound are considered the protein targets. [43]A drawback to this approach is that in some cases the inactive compound may not bind to the cellular target due to the inability to permeate the cell membrane and it never comes in contact with the target protein. [43] However, the inactive compound may still bind to the target protein in cell lysates. Consequently, the use of what appears to be an inactive compound in cell-based assays may still interact with the target protein in cell lysates leading to false negatives.[43a] This limitation can be overcomed by quantitative proteomics. This strategy allows for the quantification of proteins from different populations based on isotopic labeling (**Scheme 1.5**). [43b]

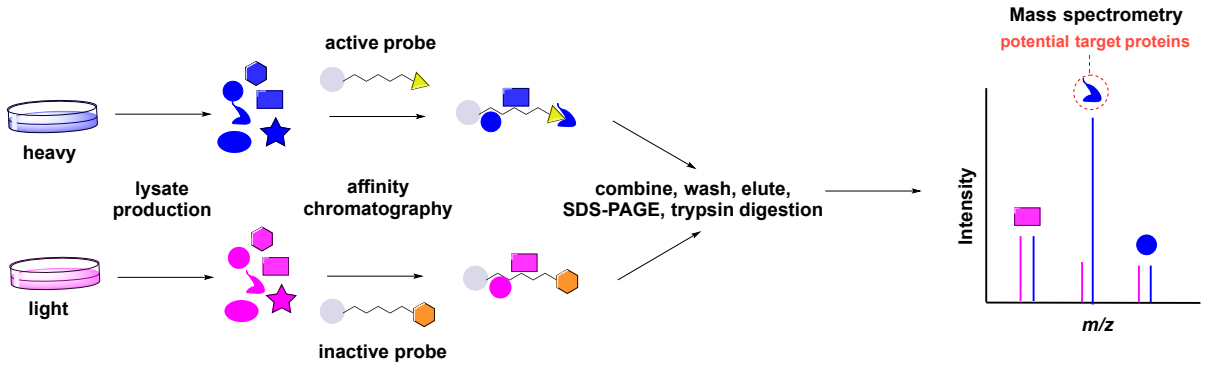

Scheme 1.5. Quantitative proteomics approach. Employing the SILAC method for the differentiation of non-specific and specific binders.[43b]

An example is the use of SILAC (stable isotope labeling by amino acids in cell culture), a technique that takes advantage of the metabolic need of mammalian cells for amino acids.[54] A set of cells are grown with normal or "light" amino acids and a different set of cells are grown with "heavy" amino acids (e.g. ^{13}C labeled $_L$-arginine[55]) which are incorporated into proteins after passaging cells several times. [43b] The two sets of cell lysates are incubated with the active probe ("heavy" lysate) and the inactive probe ("light" lysate) for affinity chromatography. The eluates from the two experiments are combined, washed, digested with trypsin and analyzed by mass spectrometry for quantitation of the resulting peptides. The "heavy" amino acids have a 6Da mass difference compared to the "light" amino acids, the change in mass can be distinguished by mass spectrometry and relatively quantified based on the "heavy" and "light" peptides ion intensities (**Scheme 1.5**). [43b] Similar approaches are available for protein quantification (iTRAQ[56] and ICAT[57]).

The field of chemical proteomics continues to evolve to overcome some of the challenges that are observed from this approach. For example, the development of a new method for target deconvolution named DARTS (Drug affinity responsive target stability) that is based on protein-drug interactions but does not require chemical modification of the active compound for attachment of the affinity label. [58] This approach is based on the fact that compound binding to the target protein increases the stability of the protein conformation and/or prevents access to the proteolytic site for degradation. [43a]

1.3.2 Genetics-based approach

Yeast has been utilized as an eukariotic model organism for the understanding of disease related pathways in mammalian systems due to the homology in protein expression (31%) to humans. [43b]Additionally, an estimated of 50% of human heritable disease genes are found in yeasts.[43b] Coupled with the ease of maintenance, their genetic tractability, the stability of its haploid and diploid states and access to *Saccharomyces cerevisiae* genome have made yeast a valuable model organism for the understanding of disease and basic cellular processes.[59] The precise deletion of genes using homologous recombination led to the development of the yeast deletion collection that consists on deletion mutants of all of the 6000 genes found in *S. cerevisiae* (homozygous for non-essential genes and heterozygous for essential genes).[60] An important feature is that each gene deletion mutant is equipped with two distinct bar codes that consist of 20-base-pair oligonucleotides for identification of the strain, enabling the study of all the yeast deletion mutants in a single culture. The development of this important technique has allowed genome wide screens to be completed in different conditions in order to provide functional information about the deleted genes and as a tool for target identification of biologically active compounds. [61]

The drug-induced haploinsufficiency profiling (HIP) assay takes advantage of the yeast deletion collection for target identification by relying on the fact that lowering the dosage of a drug target gene in a heterozygote mutant will have an increase sensitivity upon exposure to a drug (**Scheme 1.6**).[62] The increased sensitivity to drug can be reasoned based on the fact that having one less copy of a gene leads to less protein being produced. If the heterozygote mutant has decrease levels of the target protein then less amount of drug is

needed to deplete protein function. [61] This genomics approach is unbiased and does not require prior knowledge on the mode action of the active compound, but it does require cell growth inhibition by the compound. [43a] The HIP assay can recognize both the direct target protein and other members in the same signaling pathway that the compound is affecting. [43a] This assay has validated previously characterized targets and has also identified unknown drug targets. [63] Due to the unbiased nature of the assay surprising results have risen from this assay. For example, in the case of 5-fluorouracil it was believed that its target was thymidylate synthase, however HIP profiling suggests that the cytotoxic activity of this compound is due to inhibition of rRNA-processing exosomes.[63a, 63b]

An analogous approach to HIP is homozygous deletion profiling (HOP) that consists on deletion of both copies of non-essential genes.[43b] Screening of homozygous mutants can provide functional information on the removed gene and can aid in determining the mode of action. For example, if gene A has been removed from a strain and an increased sensitivity to a DNA-damaging agent is observed, then most likely gene A is involved in protecting the cell from DNA damage. [61] On the other hand, if a compound with unknown mechanism of action is added and sensitive strains are those with depletion in genes involved in responding to DNA damage, it suggests that the compound is a DNA-damaging agent. [61] An example of utilizing this technique was recently published by Wilmes and co-workers, looking to acquire further information on the primary and secondary targets in yeast of the natural product peloruside A. The initial HIP assay did not generate hits that could be validated; however HOP provided a number of validated genes that have an interaction with peloruside A.[64] The

previous example illustrates how the HIP and HOP assays are complementary techniques to each other in target identification.

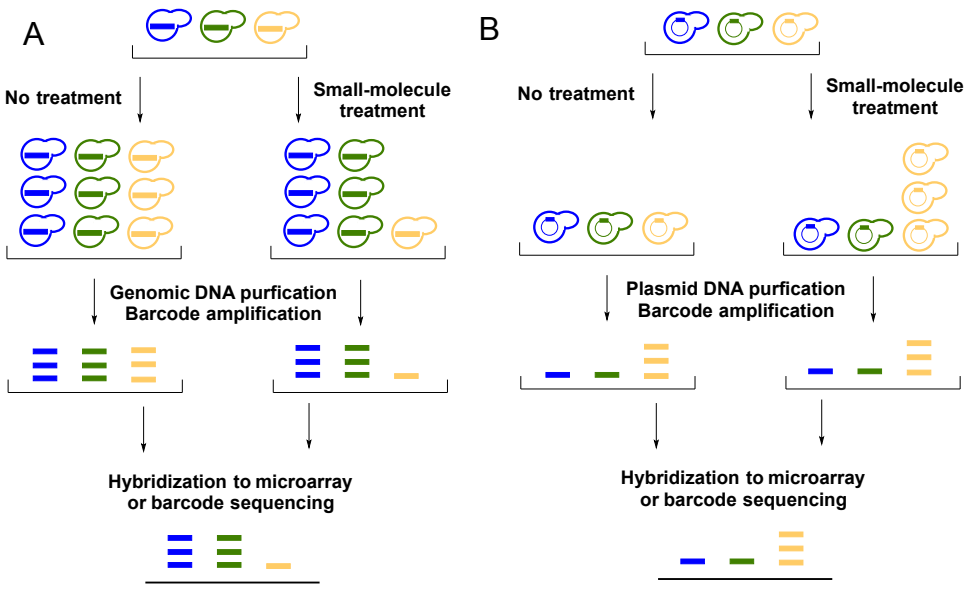

Scheme 1.6. Genomic-based approaches for target identification**. A**. HIP/HOP profiling techniques. **B**. MSP profiling assay. [43]

A similar strategy to HIP and HOP is multicopy suppression profiling (MSP), which is based on the notion that increasing the dosage of a small molecule target results in resistance to the drug (**Scheme 1.6**). [43] By overexpressing the compound's target a greater excess of the protein is present requiring an increase amount of compound to observe a loss in protein function. Butcher and co-workers developed a yeast collection of 3900 strains each harboring an overexpressed protein. As a proof of principle the authors utilized rapamycin as the active compound and monitored resistant strains by microarray. The technique confirmed TOR as the target of the natural product rapamycin. [65]

The genetic based approaches HIP, HOP and MSP are complementary to each other. For example, the HIP assay can help identify a target even when it is part of a multiple subunit, whereas the MSP assay would fail to recognize the target. [43a]Additionally, a target that has a functional paralog (gene that has the same function as a different gene but is found in a different part of the genome) would not be identified using HIP, however MSP would be able to detect the target. [43a] Furthermore, in the case where a yeast strain would be sensitive in HIP due to a gene involved in a drug detoxification process and resistant in the MSP assay the data would indicate the identification of the target. However if sensitivity is observed in the HOP assay, most likely this is not a direct target of the compound allowing you to remove false positives from the data. [43a]The combination of all the data obtained from the three assays provides a more complete understanding of the drug-protein interaction allowing the successful identification of targets. [43a]

Some of the molecular targets identified by this approach include ibandronate (molecular targets tubulin co-factor B and activator of S-phase kinase), [66] cladosporin (molecular target lysyl-tRNA synthase) [67] and phenylaminopyrimidine (molecular target PKC1). [68]

1.3.3 Transcriptional profiling-based approach

This approach is based on the generation of a database of transcriptional signatures of a cell line exposed to chemical perturbations with the end point of producing hypothesis on the possible mode of action of novel small molecules. [43] Perturbations targeting the same signaling pathway or gene will have the same transcriptional signature as other agents having

the same effect on the cell. A direct comparison can be carried out between compounds with unknown mechanism of action that cluster closely together on the database to compounds with known targets. [43a] Following this idea Hughes and co-workers generated a reference database of expression profiles containing a total of 300 different mutations in *S. cerevisiae* together with expression profiles of cells expose to compounds with known molecular targets. Using this methodology the group identified the target of dyclonine, a topical anesthetic, to be ERG2. [69] This approach allows for the study of compounds that have no effect on cell growth and viability as opposed to fitness-based approaches that require cell viability as readout. [43a]

Transcriptional profiling has also been utilized in mammalian cells for the identification of molecular targets of small molecules. Lamb et.al introduced the connectivity map as a tool for the discovery of connections between compounds with unknown mechanism of action to compounds with known targets, as well as connections between drugs and diseases, and connections with compounds and physiological process. The screen was done with 164 different small molecules that were selected to represent a large spectrum of biological activities. [70] Including compounds that have the same molecular target (e.g. histone deacetylase inhibitors), as well as compounds with the same clinical indication (e.g. antidiabetics). The MCF-7 cancer cell line was utilized to measure the mRNA expression profile of the different chemical perturbagens. The method starts by comparing a "query signature" to the reference expression profiles in the data set. This approach was utilized to determine the mode of action of the natural product gedunin. The natural product was identified from a separate screen looking for inhibitors of androgen receptor (AR) activation

in prostate cancer cells.[71] Gedunin had high connectivity to three other compounds known to inhibit the heat shock protein 90 (Hsp90) based on this result the group generate a hypothesis using the connectivity map and was able to confirm the participation of Hsp90 in the regulation of AR stability. [70] This example illustrates the power of transcriptional profiling for target identification.

These approaches allow the generation of mechanism of action hypothesis for compounds that their molecular targets remain elusive based on direct comparison to the expression profiles of compounds with known targets. Nonetheless, this approach is limited by target identification of only known targets. [43b]

1.4 Target Confirmation

The techniques for target identification described previously served as means to provide a mechanism of action hypothesis but confirmation studies are required to validate the proposed hypothesis. If a number of proteins are identified as potential targets they need to be prioritized based on their function in relation to the observed compound-induced phenotype. [43b] In order to prioritize targets proper control experiments are needed to discard non-specific interactions. Generally, confirmation of the target protein is done by immuno-blotting experiments with a specific antibody after its isolation by affinity chromatography. To determine which protein from the immunoblot analysis is the true target of the compound, pull-down assays of the purified recombinant protein with the active and inactive compounds are performed. In addition, competition experiments of unmodified compound can be done to corroborate the compound-target interaction. [43b]

Additionally, another avenue for target confirmation is determining the binding affinity of the compound to its target. Two methodologies widely used for this purpose are isothermal calorimetry (ITC) and surface plasmon resonance. [43b]

An additionally alternative is the use of RNAi to knockdown the target protein to observe if this will give a similar phenotype as compound treated cells. [43b] Target overexpression with cDNA can also provide evidence for target confirmation, since overexpression of the protein may eliminate the compounds phenotype. [43b]

Ding and colleagues take advantage of some of the techniques previously described to confirm the protein target of their active small molecule after affinity chromatography. The group set out to investigate small molecules that stimulate the differentiation of embryonic stem cells into neurons.[72] A high throughput phenotypic screen revealed a synthetic small molecule capable of inducing neurogenesis in murine embryonic stem cells. The active compound TSW119 was linked to an agarose affinity matrix as well as two other less active compounds, an inactive compound and an analogue with the affinity matrix attached to a nonpermissive position were also synthesized for affinity chromatography. The initial experiment revealed that the active compounds binds to GSK-3β. To confirm their initial observations the authors turned to western-blot analysis with a GSK-3β antibody that showed binding of the compound to the protein. Furthermore, the affinity matrix linked to the active compound selectively bound recombinant GSK-3β. The strong binding of the compound to GSK-3β (K_D =126 nM) was measured using surface plasmon resonance and further illustrated in a kinase inhibitory assay with an IC_{50} of 30nM.[72] This example illustrates that the combination of all these techniques for target confirmation allows a clearer picture of the

compound's cellular activity.

CONCLUSION

1.5 The importance of natural products in drug discovery

The impact of natural products in drug discovery is without question extraordinary. We have taken advantage of the chemical scaffolds found in natural products, which were evolutionarily perfected by nature to interact with macromolecules and we have utilized them not only to treat important diseases but also as chemical tools to understand important biological processes. Additionally, the perceived limitations in natural products research continue to be address by the scientific community developing different avenues to overcome these limitations. Last but not least, advancements in target identification technologies continue to impact the field of natural products making the process of target identification more manageable than before.

1.6 Aims of this study

This study mainly focuses on the identification of natural products that target a specific human cancer cell line of interest and using phenotypic screens as readout for biological activity. Using different methodologies we have interrogated what are the signaling pathways disrupted by our natural products and have been able to obtain a mechanistic understanding on the activity of the secondary metabolites (**Scheme 1.7**).

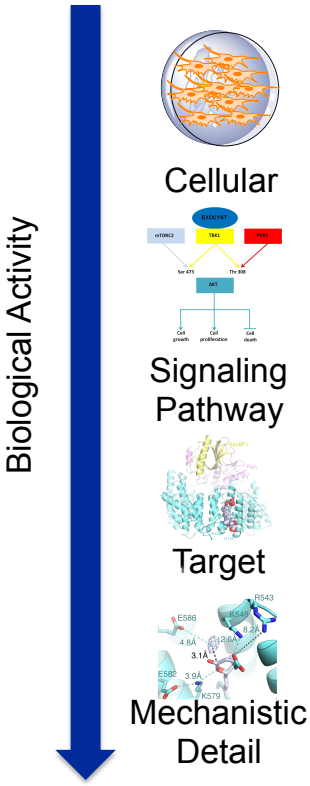

Scheme 1.7. Rationale followed by this study

The first aim discussed in this dissertation involves the identification and structure elucidation of a natural product with selective activity against a human gliobastoma cell line, as well as our efforts to determine its mode of action through the use of a novel platform called FUSION. This work was done in collaboration with Dr. Michael White at UTSW.

Additionally, I will discuss the isolation and structure determination of rifsaliniketal, a novel polyketide that is believed to be an intermediate in the biosynthesis of saliniketal.

Finally, the last aim involves the study of the natural product leptomycin B (LMB) and its inhibition of CRM1, a nuclear export protein. With the idea that by utilizing LMB as chemical probe, a better mechanistic understanding would be obtain of its inhibition of

CRM1. Furthermore, information obtained from these studies could aid in the design of a better inhibitor that targets this nuclear export receptor but without the toxicity that is associated with LMB. This work was done in collaboration with Dr. Yuh Min Chook at UTSW.

References

1. Cragg, G. M.; Newman, D. J., Natural products: a continuing source of novel drug leads. *Biochimica et biophysica acta* **2013,** *1830* (6), 3670-95.
2. Hamilton, G. R.; Baskett, T. F., In the arms of Morpheus the development of morphine for postoperative pain relief. *Canadian journal of anaesthesia = Journal canadien d'anesthesie* **2000,** *47* (4), 367-74.
3. Li, J. W.; Vederas, J. C., Drug discovery and natural products: end of an era or an endless frontier? *Science* **2009,** *325* (5937), 161-5.
4. Harvey, A. L., Natural products in drug discovery. *Drug discovery today* **2008,** *13* (19-20), 894-901.
5. McChesney, J. D.; Venkataraman, S. K.; Henri, J. T., Plant natural products: back to the future or into extinction? *Phytochemistry* **2007,** *68* (14), 2015-22.
6. Butler, M. S., The role of natural product chemistry in drug discovery. *Journal of natural products* **2004,** *67* (12), 2141-2153.
7. Carter, G. T., Natural products and Pharma 2011: strategic changes spur new opportunities. *Natural product reports* **2011,** *28* (11), 1783-9.
8. Newman, D. J.; Cragg, G. M., Natural products as sources of new drugs over the 30 years from 1981 to 2010. *Journal of natural products* **2012,** *75* (3), 311-35.
9. Borman, S., Organic lab sparks drug discovery. *Chem Eng News* **2002,** *80* (2), 23-24.
10. Lam, K. S., New aspects of natural products in drug discovery. *Trends in microbiology* **2007,** *15* (6), 279-89.
11. (a) Sabatini, D. M.; Erdjument-Bromage, H.; Lui, M.; Tempst, P.; Snyder, S. H., RAFT1: a mammalian protein that binds to FKBP12 in a rapamycin-dependent fashion and is homologous to yeast TORs. *Cell* **1994,** *78* (1), 35-43; (b) Sehgal, S. N.; Baker, H.; Vezina, C., Rapamycin (AY-22,989), a new antifungal antibiotic. II. Fermentation, isolation and characterization. *The Journal of antibiotics* **1975,** *28* (10), 727-32; (c) Vezina, C.; Kudelski, A.; Sehgal, S. N., Rapamycin (AY-22,989), a new antifungal antibiotic. I. Taxonomy of the producing streptomycete and isolation of the active principle. *The Journal of antibiotics* **1975,** *28* (10), 721-6.
12. (a) Alberts, A. W.; Chen, J.; Kuron, G.; Hunt, V.; Huff, J.; Hoffman, C.; Rothrock, J.; Lopez, M.; Joshua, H.; Harris, E.; Patchett, A.; Monaghan, R.; Currie, S.; Stapley, E.; Albers-Schonberg, G.; Hensens, O.; Hirshfield, J.; Hoogsteen, K.; Liesch, J.; Springer, J., Mevinolin: a highly potent competitive inhibitor of hydroxymethylglutaryl-coenzyme A reductase and a cholesterol-lowering agent. *Proceedings of the National Academy of Sciences of the United States of America* **1980,** *77* (7), 3957-61; (b) Brown, M. S.; Faust, J. R.; Goldstein, J. L.; Kaneko, I.; Endo, A., Induction of 3-hydroxy-3-methylglutaryl coenzyme A reductase activity in human fibroblasts incubated with compactin (ML-236B), a competitive inhibitor of the reductase. *J Biol Chem* **1978,** *253* (4), 1121-8; (c) Endo, A., Monacolin-K, a New Hypocholesterolemic Agent That Specifically Inhibits 3-Hydroxy-3-Methylglutaryl Coenzyme a Reductase. *J Antibiot* **1980,** *33* (3), 334-336; (d) Alberts, A. W.; Chen, J.; Kuron, G.; Hunt, V.; Huff, J.; Hoffman, C.; Rothrock, J.; Lopez, M.; Joshua, H.; Harris, E.; Patchett, A.; Monaghan, R.;

Currie, S.; Stapley, E.; Albersschonberg, G.; Hensens, O.; Hirshfield, J.; Hoogsteen, K.; Liesch, J.; Springer, J., Mevinolin - a Highly Potent Competitive Inhibitor of Hydroxymethylglutaryl-Coenzyme-a Reductase and a Cholesterol-Lowering Agent. *P Natl Acad Sci-Biol* **1980,** *77* (7), 3957-3961.
13. (a) Brodersen, D. E.; Clemons, W. M., Jr.; Carter, A. P.; Morgan-Warren, R. J.; Wimberly, B. T.; Ramakrishnan, V., The structural basis for the action of the antibiotics tetracycline, pactamycin, and hygromycin B on the 30S ribosomal subunit. *Cell* **2000,** *103* (7), 1143-54; (b) Finlay, A. C.; Hobby, G. L.; Pan, S. Y.; Regna, P. P.; Routien, J. B.; Seeley, D. B.; Shull, G. M.; Sobin, B. A.; Solomons, I. A.; Vinson, J. W.; Kane, J. H., Terramycin, a New Antibiotic. *Science* **1950,** *111* (2874), 85-85; (c) Hochstein, F. A.; Stephens, C. R.; Conover, L. H.; Regna, P. P.; Pasternack, R.; Gordon, P. N.; Pilgrim, F. J.; Brunings, K. J.; Woodward, R. B., The Structure of Terramycin. *Journal of the American Chemical Society* **1953,** *75* (22), 5455-5475.
14. (a) Davis, K. E.; Joseph, S. J.; Janssen, P. H., Effects of growth medium, inoculum size, and incubation time on culturability and isolation of soil bacteria. *Appl Environ Microbiol* **2005,** *71* (2), 826-34; (b) Busti, E.; Monciardini, P.; Cavaletti, L.; Bamonte, R.; Lazzarini, A.; Sosio, M.; Donadio, S., Antibiotic-producing ability by representatives of a newly discovered lineage of actinomycetes. *Microbiology* **2006,** *152* (Pt 3), 675-83.
15. Fenical, W.; Jensen, P. R., Developing a new resource for drug discovery: marine actinomycete bacteria. *Nature chemical biology* **2006,** *2* (12), 666-73.
16. (a) Faulkner, D. J., Marine natural products. *Natural product reports* **2000,** *17* (1), 7-55; (b) Blunt, J. W.; Copp, B. R.; Keyzers, R. A.; Munro, M. H. G.; Prinsep, M. R., Marine natural products. *Natural product reports* **2012,** *29* (2), 144-222.
17. (a) Piel, J., Bacterial symbionts: prospects for the sustainable production of invertebrate-derived pharmaceuticals. *Current medicinal chemistry* **2006,** *13* (1), 39-50; (b) Gerwick, W. H.; Moore, B. S., Lessons from the past and charting the future of marine natural products drug discovery and chemical biology. *Chemistry & biology* **2012,** *19* (1), 85-98.
18. Mincer, T. J.; Jensen, P. R.; Kauffman, C. A.; Fenical, W., Widespread and persistent populations of a major new marine actinomycete taxon in ocean sediments. *Appl Environ Microbiol* **2002,** *68* (10), 5005-11.
19. Hughes, C. C.; Prieto-Davo, A.; Jensen, P. R.; Fenical, W., The marinopyrroles, antibiotics of an unprecedented structure class from a marine Streptomyces sp. *Organic letters* **2008,** *10* (4), 629-31.
20. Hughes, C. C.; MacMillan, J. B.; Gaudencio, S. P.; Jensen, P. R.; Fenical, W., The ammosamides: structures of cell cycle modulators from a marine-derived Streptomyces species. *Angewandte Chemie* **2009,** *48* (4), 725-7.
21. (a) Rinehart, K. L.; Holt, T. G.; Fregeau, N. L.; Keifer, P. A.; Wilson, G. R.; Perun, T. J., Jr.; Sakai, R.; Thompson, A. G.; Stroh, J. G.; Shield, L. S.; et al., Bioactive compounds from aquatic and terrestrial sources. *Journal of natural products* **1990,** *53* (4), 771-92; (b) Rinehart, K. L.; Holt, T. G.; Fregeau, N. L.; Stroh, J. G.; Keifer, P. A.; Sun, F.; Li, L. H.; Martin, D. G., Isolation and Characterization of the Ecteinascidins, Potent Antitumor Compounds from the Caribbean Tunicate Ecteinascidia-Turbinata. *Abstr Pap*

Am Chem S **1990,** *200*, 141-ORGN; (c) Rinehart, K. L.; Holt, T. G.; Fregeau, N. L.; Stroh, J. G.; Keifer, P. A.; Sun, F.; Li, L. H.; Martin, D. G., Ecteinascidin-729, Ecteinascidin-743, Ecteinascidin-745, Ecteinascidin-759a, Ecteinascidin-759b, and Ecteinascidin-770 - Potent Antitumor Agents from the Caribbean Tunicate Ecteinascidia-Turbinata. *Journal of Organic Chemistry* **1990,** *55* (15), 4512-4515; (d) Sakai, R.; Rinehart, K. L.; Guan, Y.; Wang, A. H., Additional antitumor ecteinascidins from a Caribbean tunicate: crystal structures and activities in vivo. *Proceedings of the National Academy of Sciences of the United States of America* **1992,** *89* (23), 11456-60; (e) D'Incalci, M.; Galmarini, C. M., A review of trabectedin (ET-743): a unique mechanism of action. *Molecular cancer therapeutics* **2010,** *9* (8), 2157-63.

22. (a) Feling, R. H.; Buchanan, G. O.; Mincer, T. J.; Kauffman, C. A.; Jensen, P. R.; Fenical, W., Salinosporamide A: A highly cytotoxic proteasome inhibitor from a novel microbial source, a marine bacterium of the new genus Salinospora. *Angew Chem Int Edit* **2003,** *42* (3), 355-+; (b) Fenical, W.; Jensen, P. R.; Palladino, M. A.; Lam, K. S.; Lloyd, G. K.; Potts, B. C., Discovery and development of the anticancer agent salinosporamide A (NPI-0052). *Bioorganic & medicinal chemistry* **2009,** *17* (6), 2175-80.

23. (a) Jordan, M. A.; Kamath, K.; Manna, T.; Okouneva, T.; Miller, H. P.; Davis, C.; Littlefield, B. A.; Wilson, L., The primary antimitotic mechanism of action of the synthetic halichondrin E7389 is suppression of microtubule growth. *Molecular cancer therapeutics* **2005,** *4* (7), 1086-95; (b) Zheng, W. J.; Seletsky, B. M.; Palme, M. H.; Lydon, P. J.; Singer, L. A.; Chase, C. E.; Lemelin, C. A.; Shen, Y. C.; Davis, H.; Tremblay, L.; Towle, M. J.; Salvato, K. A.; Wels, B. F.; Aalfs, K. K.; Kishi, Y.; Littlefield, B. A.; Yu, M. J., Macrocyclic ketone analogues of halichondrin B. *Bioorganic & medicinal chemistry letters* **2004,** *14* (22), 5551-5554; (c) Aicher, T. D.; Buszek, K. R.; Fang, F. G.; Forsyth, C. J.; Jung, S. H.; Kishi, Y.; Matelich, M. C.; Scola, P. M.; Spero, D. M.; Yoon, S. K., Total Synthesis of Halichondrin-B and Norhalichondrin-B. *Journal of the American Chemical Society* **1992,** *114* (8), 3162-3164.

24. (a) Pettit, G. R.; Herald, C. L.; Doubek, D. L.; Herald, D. L.; Arnold, E.; Clardy, J., Anti-Neoplastic Agents .86. Isolation and Structure of Bryostatin-1. *Journal of the American Chemical Society* **1982,** *104* (24), 6846-6848; (b) Kraft, A. S.; Smith, J. B.; Berkow, R. L., Bryostatin, an Activator of the Calcium Phospholipid-Dependent Protein-Kinase, Blocks Phorbol Ester-Induced Differentiation of Human Promyelocytic Leukemia-Cells Hl-60. *Proceedings of the National Academy of Sciences of the United States of America* **1986,** *83* (5), 1334-1338.

25. Fenical, W.; Jensen, P. R., Developing a new resource for drug discovery: marine actinomycete bacteria. *Nat Chem Biol* **2006,** *2* (12), 666-673.

26. (a) Rusch, D. B.; Halpern, A. L.; Sutton, G.; Heidelberg, K. B.; Williamson, S.; Yooseph, S.; Wu, D.; Eisen, J. A.; Hoffman, J. M.; Remington, K.; Beeson, K.; Tran, B.; Smith, H.; Baden-Tillson, H.; Stewart, C.; Thorpe, J.; Freeman, J.; Andrews-Pfannkoch, C.; Venter, J. E.; Li, K.; Kravitz, S.; Heidelberg, J. F.; Utterback, T.; Rogers, Y. H.; Falcon, L. I.; Souza, V.; Bonilla-Rosso, G.; Eguiarte, L. E.; Karl, D. M.; Sathyendranath, S.; Platt, T.; Bermingham, E.; Gallardo, V.; Tamayo-Castillo, G.; Ferrari, M. R.; Strausberg, R. L.; Nealson, K.; Friedman, R.; Frazier, M.; Venter, J. C., The Sorcerer II Global Ocean Sampling expedition: northwest Atlantic through eastern tropical Pacific.

PLoS biology **2007,** *5* (3), e77; (b) Yooseph, S.; Sutton, G.; Rusch, D. B.; Halpern, A. L.; Williamson, S. J.; Remington, K.; Eisen, J. A.; Heidelberg, K. B.; Manning, G.; Li, W.; Jaroszewski, L.; Cieplak, P.; Miller, C. S.; Li, H.; Mashiyama, S. T.; Joachimiak, M. P.; van Belle, C.; Chandonia, J. M.; Soergel, D. A.; Zhai, Y.; Natarajan, K.; Lee, S.; Raphael, B. J.; Bafna, V.; Friedman, R.; Brenner, S. E.; Godzik, A.; Eisenberg, D.; Dixon, J. E.; Taylor, S. S.; Strausberg, R. L.; Frazier, M.; Venter, J. C., The Sorcerer II Global Ocean Sampling expedition: expanding the universe of protein families. *PLoS biology* **2007,** *5* (3), e16; (c) Kannan, N.; Taylor, S. S.; Zhai, Y.; Venter, J. C.; Manning, G., Structural and functional diversity of the microbial kinome. *PLoS biology* **2007,** *5* (3), e17.

27. Bugni, T. S.; Richards, B.; Bhoite, L.; Cimbora, D.; Harper, M. K.; Ireland, C. M., Marine natural product libraries for high-throughput screening and rapid drug discovery. *Journal of natural products* **2008,** *71* (6), 1095-8.

28. (a) Dalisay, D. S.; Molinski, T. F., Structure elucidation at the nanomole scale. 2. Hemi-phorboxazole A from Phorbas sp. *Organic letters* **2009,** *11* (9), 1967-70; (b) Dalisay, D. S.; Morinaka, B. I.; Skepper, C. K.; Molinski, T. F., A tetrachloro polyketide hexahydro-1H-isoindolone, muironolide A, from the marine sponge Phorbas sp. natural products at the nanomole scale. *Journal of the American Chemical Society* **2009,** *131* (22), 7552-3.

29. Ng, J.; Bandeira, N.; Liu, W. T.; Ghassemian, M.; Simmons, T. L.; Gerwick, W. H.; Linington, R.; Dorrestein, P. C.; Pevzner, P. A., Dereplication and de novo sequencing of nonribosomal peptides. *Nature methods* **2009,** *6* (8), 596-9.

30. Hirata, Y.; Uemura, D., Halichondrins - Antitumor Polyether Macrolides from a Marine Sponge. *Pure Appl Chem* **1986,** *58* (5), 701-710.

31. Stamos, D. P.; Chen, S. S.; Kishi, Y., New synthetic route to the C.14-C.38 segment of halichondrins. *Journal of Organic Chemistry* **1997,** *62* (22), 7552-7553.

32. Towle, M. J.; Salvato, K. A.; Budrow, J.; Wels, B. F.; Kuznetsov, G.; Aalfs, K. K.; Welsh, S.; Zheng, W. J.; Seletsky, B. M.; Palme, M. H.; Habgood, G. J.; Singer, L. A.; DiPietro, L. V.; Wang, Y.; Chen, J. J.; Quincy, D. A.; Davis, A.; Yoshimatsu, K.; Kishi, Y.; Yu, M. J.; Littlefield, B. A., In vitro and in vivo anticancer activities of synthetic macrocyclic ketone analogues of halichondrin B. *Cancer research* **2001,** *61* (3), 1013-1021.

33. Zhang, M. Q.; Gaisser, S.; Nur, E. A. M.; Sheehan, L. S.; Vousden, W. A.; Gaitatzis, N.; Peck, G.; Coates, N. J.; Moss, S. J.; Radzom, M.; Foster, T. A.; Sheridan, R. M.; Gregory, M. A.; Roe, S. M.; Prodromou, C.; Pearl, L.; Boyd, S. M.; Wilkinson, B.; Martin, C. J., Optimizing natural products by biosynthetic engineering: discovery of nonquinone Hsp90 inhibitors. *J Med Chem* **2008,** *51* (18), 5494-7.

34. Olano, C.; Lombo, F.; Mendez, C.; Salas, J. A., Improving production of bioactive secondary metabolites in actinomycetes by metabolic engineering. *Metabolic engineering* **2008,** *10* (5), 281-92.

35. Demain, A. L., From natural products discovery to commercialization: a success story. *Journal of industrial microbiology & biotechnology* **2006,** *33* (7), 486-95.

36. Chen, Y.; Smanski, M. J.; Shen, B., Improvement of secondary metabolite production in Streptomyces by manipulating pathway regulation. *Applied microbiology and biotechnology* **2010,** *86* (1), 19-25.

37. Smanski, M. J.; Peterson, R. M.; Rajski, S. R.; Shen, B., Engineered Streptomyces platensis strains that overproduce antibiotics platensimycin and platencin. *Antimicrobial agents and chemotherapy* **2009,** *53* (4), 1299-304.
38. Stutzman-Engwall, K.; Conlon, S.; Fedechko, R.; McArthur, H.; Pekrun, K.; Chen, Y.; Jenne, S.; La, C.; Trinh, N.; Kim, S.; Zhang, Y. X.; Fox, R.; Gustafsson, C.; Krebber, A., Semi-synthetic DNA shuffling of aveC leads to improved industrial scale production of doramectin by Streptomyces avermitilis. *Metabolic engineering* **2005,** *7* (1), 27-37.
39. Eggert, U. S., The why and how of phenotypic small-molecule screens. *Nature chemical biology* **2013,** *9* (4), 206-9.
40. (a) Lindsay, M. A., Target discovery. *Nature reviews. Drug discovery* **2003,** *2* (10), 831-8; (b) Imming, P.; Sinning, C.; Meyer, A., Drugs, their targets and the nature and number of drug targets. *Nature reviews. Drug discovery* **2006,** *5* (10), 821-34.
41. Swinney, D. C.; Anthony, J., How were new medicines discovered? *Nature Reviews Drug Discovery* **2011,** *10* (7), 507-519.
42. Kotz, J., Phenotypic Screening, take two. *Science-Business eXchange* **2012,** *5* (15), 1-3.
43. (a) Cong, F.; Cheung, A. K.; Huang, S. M., Chemical genetics-based target identification in drug discovery. *Annual review of pharmacology and toxicology* **2012,** *52*, 57-78; (b) Ziegler, S.; Pries, V.; Hedberg, C.; Waldmann, H., Target identification for small bioactive molecules: finding the needle in the haystack. *Angewandte Chemie* **2013,** *52* (10), 2744-92.
44. Castoreno, A. B.; Eggert, U. S., Small molecule probes of cellular pathways and networks. *ACS chemical biology* **2011,** *6* (1), 86-94.
45. Kau, T. R.; Schroeder, F.; Ramaswamy, S.; Wojciechowski, C. L.; Zhao, J. J.; Roberts, T. M.; Clardy, J.; Sellers, W. R.; Silver, P. A., A chemical genetic screen identifies inhibitors of regulated nuclear export of a Forkhead transcription factor in PTEN-deficient tumor cells. *Cancer cell* **2003,** *4* (6), 463-76.
46. Bender, A.; Mikhailov, D.; Glick, M.; Scheiber, J.; Davies, J. W.; Cleaver, S.; Marshall, S.; Tallarico, J. A.; Harrington, E.; Cornella-Taracido, I.; Jenkins, J. L., Use of ligand based models for protein domains to predict novel molecular targets and applications to triage affinity chromatography data. *Journal of proteome research* **2009,** *8* (5), 2575-85.
47. Shiyama, T.; Furuya, M.; Yamazaki, A.; Terada, T.; Tanaka, A., Design and synthesis of novel hydrophilic spacers for the reduction of nonspecific binding proteins on affinity resins. *Bioorganic & medicinal chemistry* **2004,** *12* (11), 2831-41.
48. Bach, S.; Knockaert, M.; Reinhardt, J.; Lozach, O.; Schmitt, S.; Baratte, B.; Koken, M.; Coburn, S. P.; Tang, L.; Jiang, T.; Liang, D. C.; Galons, H.; Dierick, J. F.; Pinna, L. A.; Meggio, F.; Totzke, F.; Schachtele, C.; Lerman, A. S.; Carnero, A.; Wan, Y.; Gray, N.; Meijer, L., Roscovitine targets, protein kinases and pyridoxal kinase. *J Biol Chem* **2005,** *280* (35), 31208-19.
49. Verhelst, S. H.; Fonovic, M.; Bogyo, M., A mild chemically cleavable linker system for functional proteomic applications. *Angewandte Chemie* **2007,** *46* (8), 1284-6.

50. Kotake, Y.; Sagane, K.; Owa, T.; Mimori-Kiyosue, Y.; Shimizu, H.; Uesugi, M.; Ishihama, Y.; Iwata, M.; Mizui, Y., Splicing factor SF3b as a target of the antitumor natural product pladienolide. *Nature chemical biology* **2007,** *3* (9), 570-5.
51. Yamamoto, K.; Yamazaki, A.; Takeuchi, M.; Tanaka, A., A versatile method of identifying specific binding proteins on affinity resins. *Anal Biochem* **2006,** *352* (1), 15-23.
52. Margarucci, L.; Monti, M. C.; Fontanella, B.; Riccio, R.; Casapullo, A., Chemical proteomics reveals bolinaquinone as a clathrin-mediated endocytosis inhibitor. *Molecular bioSystems* **2011,** *7* (2), 480-5.
53. Fleischer, T. C.; Murphy, B. R.; Flick, J. S.; Terry-Lorenzo, R. T.; Gao, Z. H.; Davis, T.; McKinnon, R.; Ostanin, K.; Willardsen, J. A.; Boniface, J. J., Chemical proteomics identifies Nampt as the target of CB30865, an orphan cytotoxic compound. *Chemistry & biology* **2010,** *17* (6), 659-64.
54. Ong, S. E.; Blagoev, B.; Kratchmarova, I.; Kristensen, D. B.; Steen, H.; Pandey, A.; Mann, M., Stable isotope labeling by amino acids in cell culture, SILAC, as a simple and accurate approach to expression proteomics. *Molecular & cellular proteomics : MCP* **2002,** *1* (5), 376-86.
55. Ong, S. E.; Kratchmarova, I.; Mann, M., Properties of 13C-substituted arginine in stable isotope labeling by amino acids in cell culture (SILAC). *Journal of proteome research* **2003,** *2* (2), 173-81.
56. Ross, P. L.; Huang, Y. N.; Marchese, J. N.; Williamson, B.; Parker, K.; Hattan, S.; Khainovski, N.; Pillai, S.; Dey, S.; Daniels, S.; Purkayastha, S.; Juhasz, P.; Martin, S.; Bartlet-Jones, M.; He, F.; Jacobson, A.; Pappin, D. J., Multiplexed protein quantitation in Saccharomyces cerevisiae using amine-reactive isobaric tagging reagents. *Molecular & cellular proteomics : MCP* **2004,** *3* (12), 1154-69.
57. Gygi, S. P.; Rist, B.; Gerber, S. A.; Turecek, F.; Gelb, M. H.; Aebersold, R., Quantitative analysis of complex protein mixtures using isotope-coded affinity tags. *Nature biotechnology* **1999,** *17* (10), 994-9.
58. Lomenick, B.; Hao, R.; Jonai, N.; Chin, R. M.; Aghajan, M.; Warburton, S.; Wang, J.; Wu, R. P.; Gomez, F.; Loo, J. A.; Wohlschlegel, J. A.; Vondriska, T. M.; Pelletier, J.; Herschman, H. R.; Clardy, J.; Clarke, C. F.; Huang, J., Target identification using drug affinity responsive target stability (DARTS). *Proceedings of the National Academy of Sciences of the United States of America* **2009,** *106* (51), 21984-9.
59. Suter, B.; Auerbach, D.; Stagljar, I., Yeast-based functional genomics and proteomics technologies: the first 15 years and beyond. *Biotechniques* **2006,** *40* (5), 625-644.
60. (a) Giaever, G.; Chu, A. M.; Ni, L.; Connelly, C.; Riles, L.; Veronneau, S.; Dow, S.; Lucau-Danila, A.; Anderson, K.; Andre, B.; Arkin, A. P.; Astromoff, A.; El-Bakkoury, M.; Bangham, R.; Benito, R.; Brachat, S.; Campanaro, S.; Curtiss, M.; Davis, K.; Deutschbauer, A.; Entian, K. D.; Flaherty, P.; Foury, F.; Garfinkel, D. J.; Gerstein, M.; Gotte, D.; Guldener, U.; Hegemann, J. H.; Hempel, S.; Herman, Z.; Jaramillo, D. F.; Kelly, D. E.; Kelly, S. L.; Kotter, P.; LaBonte, D.; Lamb, D. C.; Lan, N.; Liang, H.; Liao, H.; Liu, L.; Luo, C.; Lussier, M.; Mao, R.; Menard, P.; Ooi, S. L.; Revuelta, J. L.; Roberts, C. J.; Rose, M.; Ross-Macdonald, P.; Scherens, B.; Schimmack, G.; Shafer, B.;

Shoemaker, D. D.; Sookhai-Mahadeo, S.; Storms, R. K.; Strathern, J. N.; Valle, G.; Voet, M.; Volckaert, G.; Wang, C. Y.; Ward, T. R.; Wilhelmy, J.; Winzeler, E. A.; Yang, Y.; Yen, G.; Youngman, E.; Yu, K.; Bussey, H.; Boeke, J. D.; Snyder, M.; Philippsen, P.; Davis, R. W.; Johnston, M., Functional profiling of the Saccharomyces cerevisiae genome. *Nature* **2002,** *418* (6896), 387-91; (b) Winzeler, E. A.; Shoemaker, D. D.; Astromoff, A.; Liang, H.; Anderson, K.; Andre, B.; Bangham, R.; Benito, R.; Boeke, J. D.; Bussey, H.; Chu, A. M.; Connelly, C.; Davis, K.; Dietrich, F.; Dow, S. W.; El Bakkoury, M.; Foury, F.; Friend, S. H.; Gentalen, E.; Giaever, G.; Hegemann, J. H.; Jones, T.; Laub, M.; Liao, H.; Liebundguth, N.; Lockhart, D. J.; Lucau-Danila, A.; Lussier, M.; M'Rabet, N.; Menard, P.; Mittmann, M.; Pai, C.; Rebischung, C.; Revuelta, J. L.; Riles, L.; Roberts, C. J.; Ross-MacDonald, P.; Scherens, B.; Snyder, M.; Sookhai-Mahadeo, S.; Storms, R. K.; Veronneau, S.; Voet, M.; Volckaert, G.; Ward, T. R.; Wysocki, R.; Yen, G. S.; Yu, K.; Zimmermann, K.; Philippsen, P.; Johnston, M.; Davis, R. W., Functional characterization of the S. cerevisiae genome by gene deletion and parallel analysis. *Science* **1999,** *285* (5429), 901-6.

61. Pierce, S. E.; Davis, R. W.; Nislow, C.; Giaever, G., Genome-wide analysis of barcoded Saccharomyces cerevisiae gene-deletion mutants in pooled cultures. *Nature protocols* **2007,** *2* (11), 2958-74.

62. Giaever, G.; Shoemaker, D. D.; Jones, T. W.; Liang, H.; Winzeler, E. A.; Astromoff, A.; Davis, R. W., Genomic profiling of drug sensitivities via induced haploinsufficiency. *Nature genetics* **1999,** *21* (3), 278-83.

63. (a) Lum, P. Y.; Armour, C. D.; Stepaniants, S. B.; Cavet, G.; Wolf, M. K.; Butler, J. S.; Hinshaw, J. C.; Garnier, P.; Prestwich, G. D.; Leonardson, A.; Garrett-Engele, P.; Rush, C. M.; Bard, M.; Schimmack, G.; Phillips, J. W.; Roberts, C. J.; Shoemaker, D. D., Discovering modes of action for therapeutic compounds using a genome-wide screen of yeast heterozygotes. *Cell* **2004,** *116* (1), 121-37; (b) Giaever, G.; Flaherty, P.; Kumm, J.; Proctor, M.; Nislow, C.; Jaramillo, D. F.; Chu, A. M.; Jordan, M. I.; Arkin, A. P.; Davis, R. W., Chemogenomic profiling: identifying the functional interactions of small molecules in yeast. *Proceedings of the National Academy of Sciences of the United States of America* **2004,** *101* (3), 793-8; (c) Yan, Z.; Costanzo, M.; Heisler, L. E.; Paw, J.; Kaper, F.; Andrews, B. J.; Boone, C.; Giaever, G.; Nislow, C., Yeast Barcoders: a chemogenomic application of a universal donor-strain collection carrying bar-code identifiers. *Nature methods* **2008,** *5* (8), 719-25.

64. Wilmes, A.; Hanna, R.; Heathcott, R. W.; Northcote, P. T.; Atkinson, P. H.; Bellows, D. S.; Miller, J. H., Chemical genetic profiling of the microtubule-targeting agent peloruside A in budding yeast Saccharomyces cerevisiae. *Gene* **2012,** *497* (2), 140-6.

65. Butcher, R. A.; Bhullar, B. S.; Perlstein, E. O.; Marsischky, G.; LaBaer, J.; Schreiber, S. L., Microarray-based method for monitoring yeast overexpression strains reveals small-molecule targets in TOR pathway. *Nature chemical biology* **2006,** *2* (2), 103-9.

66. Bivi, N.; Romanello, M.; Harrison, R.; Clarke, I.; Hoyle, D. C.; Moro, L.; Ortolani, F.; Bonetti, A.; Quadrifoglio, F.; Tell, G.; Delneri, D., Identification of secondary targets of N-containing bisphosphonates in mammalian cells via parallel

competition analysis of the barcoded yeast deletion collection. *Genome biology* **2009,** *10* (9), R93.
67. Hoepfner, D.; McNamara, C. W.; Lim, C. S.; Studer, C.; Riedl, R.; Aust, T.; McCormack, S. L.; Plouffe, D. M.; Meister, S.; Schuierer, S.; Plikat, U.; Hartmann, N.; Staedtler, F.; Cotesta, S.; Schmitt, E. K.; Petersen, F.; Supek, F.; Glynne, R. J.; Tallarico, J. A.; Porter, J. A.; Fishman, M. C.; Bodenreider, C.; Diagana, T. T.; Movva, N. R.; Winzeler, E. A., Selective and specific inhibition of the plasmodium falciparum lysyl-tRNA synthetase by the fungal secondary metabolite cladosporin. *Cell host & microbe* **2012,** *11* (6), 654-63.
68. Luesch, H.; Wu, T. Y.; Ren, P.; Gray, N. S.; Schultz, P. G.; Supek, F., A genome-wide overexpression screen in yeast for small-molecule target identification. *Chemistry & biology* **2005,** *12* (1), 55-63.
69. Hughes, T. R.; Marton, M. J.; Jones, A. R.; Roberts, C. J.; Stoughton, R.; Armour, C. D.; Bennett, H. A.; Coffey, E.; Dai, H.; He, Y. D.; Kidd, M. J.; King, A. M.; Meyer, M. R.; Slade, D.; Lum, P. Y.; Stepaniants, S. B.; Shoemaker, D. D.; Gachotte, D.; Chakraburtty, K.; Simon, J.; Bard, M.; Friend, S. H., Functional discovery via a compendium of expression profiles. *Cell* **2000,** *102* (1), 109-26.
70. Lamb, J.; Crawford, E. D.; Peck, D.; Modell, J. W.; Blat, I. C.; Wrobel, M. J.; Lerner, J.; Brunet, J. P.; Subramanian, A.; Ross, K. N.; Reich, M.; Hieronymus, H.; Wei, G.; Armstrong, S. A.; Haggarty, S. J.; Clemons, P. A.; Wei, R.; Carr, S. A.; Lander, E. S.; Golub, T. R., The Connectivity Map: using gene-expression signatures to connect small molecules, genes, and disease. *Science* **2006,** *313* (5795), 1929-35.
71. Hieronymus, H.; Lamb, J.; Ross, K. N.; Peng, X. P.; Clement, C.; Rodina, A.; Nieto, M.; Du, J.; Stegmaier, K.; Raj, S. M.; Maloney, K. N.; Clardy, J.; Hahn, W. C.; Chiosis, G.; Golub, T. R., Gene expression signature-based chemical genomic prediction identifies a novel class of HSP90 pathway modulators. *Cancer cell* **2006,** *10* (4), 321-30.
72. Ding, S.; Wu, T. Y.; Brinker, A.; Peters, E. C.; Hur, W.; Gray, N. S.; Schultz, P. G., Synthetic small molecules that control stem cell fate. *Proceedings of the National Academy of Sciences of the United States of America* **2003,** *100* (13), 7632-7.

CHAPTER TWO
Introduction

NATURAL PRODUCT WITH SELECTIVE THERAPEUTIC PROPERTIES AND OUR EFFORTS TO DETERMINE ITS MODE OF ACTION

2.1 Cancer mortality: A desperate need for cancer therapies

In the United States alone it is estimated that in 2013 an approximate of 1.6 million new cases of cancer will be reported and approximately 580,000 cancer-related deaths.[1] It is with great necessity that new therapeutics be developed for the treatment of cancer.

2.1.1 Targeted cancer therapies

Different avenues can be taken for the treatment of cancer such as: chemotherapy, radiotherapy, transplantation and targeted therapies among others. [2] However, for this chapter focus will only be given to targeted cancer therapies. Targeted cancer therapies are drugs or biological substances (e.g. monoclonal antibodies) that target aberrant cells specifically by blocking their cell growth and stop cancer progression. [3] By concentrating on molecular and cellular cues that are specific to cancerous cells targeted therapies can be more effective and less toxic to normal cells. [3] It is believed that in the future cancer treatment may be individualized based on what molecular targets are produced by the tumor. The promise is that targeted therapies have greater selectivity towards cancer cells than their normal counterparts resulting in reduce toxicity, side effects and improve quality of life. [3]

With this idea in mind we have focused on the isolation of natural products that have selective cytotoxicity against a panel of tumor derived cell lines that will be discussed in more detail below.

Results and Discussion

2.2 Natural product with selective therapeutic properties against a glioblastoma cell line

Aware of the important role that terrestrial microbial natural products play in the discovery of therapeutics and the decrease in rate of discovery of new natural products in the pharmaceutical industry,[4] there is an immediate need to explore novel sources of microbial natural products with biological relevance. [5] Marine bacteria have proven to be an excellent source of bioactive metabolites,[6] however, a small amount of the marine environment has been studied. [5] There is a vast number of unique marine habitats to be explored. Therefore, with the idea that novel bacterial species will yield novel chemistry, the MacMillan lab has isolated >600 unique species of marine actinomycetes from marine sediments collected in a variety of microbial habitats such as mangroves, hypersaline lakes and estuaries. My research efforts have focused on using a library of natural product fractions created from these bacterial strains to screen for molecules that exhibit selective cytotoxicity against a panel of tumor derived cell lines (**Table 2.1**, more details on cancer cell line panel in section 2.2.2).

This approach to screen for active natural products against a panel of tumor-derived cell lines is similar to the National Cancer Institute 60 cell-line panel (NCI-60), which has been a key resource for drug discovery for the past 30 years as a means of evaluating pure compounds. [7] Because of the long historical data and biological evaluation of 1000s of

cytotoxic compounds the NCI-60 data can be used to predict the mechanism of action of compounds; based on similarity in cytotoxic profiles using the 'COMPARE' algorithm. [7-8] The 'COMPARE' algorithm allows for an automated method of comparing the sensitivity and resistance of the cancer cell lines against a compound by looking at three effects: 50% growth inhibition, total growth inhibition and 50% lethal concentration. [7] Obtaining inspiration from the NCI-60 screen we set out to test our fraction library against a panel of cancer cells (**Table 2.1**).

Table 2.1. Panel of tumor derived cell lines

Cell Line	Tissue Type	Known Mutations
MCF-7	breast tumor	PIK3CA E543K, CDKN2A
H2347	lung tumor	NRAS mutation Q61R
A549	lung tumor	STK11 Q37*, KRAS G12S
H1437	lung tumor	MET R998C, TP53 R267P
KM12	colon tumor	APC N1818fs, TP53 R72fs
T98G	glioblastoma	TP53 M273I, PTEN L42R
SKMEL-5	melanoma	BRAF V600E, STK11
MIA PaCa-2	pancreatic tumor	KRAS G12D

The ultimate goal of these screening efforts is to use natural products to identify vulnerabilities in cancer cells that can be exploited therapeutically. Here, I describe our work on identifying a natural product that targets a cell line derived from glioblastoma (T98G) and our efforts in understanding its mechanism of action**.**

2.2.1 Generation of natural product library

The creation of our natural product fraction library initiates by the collection of sediment samples from the environment that are subsequently treated with a variety of

conditions (desiccation, heat shock, spore isolation) and ultimately added to agar plates on different media.[9] Unique bacterial colonies are selected and re-plated until pure cultures are obtained and the strains are added to the MacMillan lab collection. With a pure culture in hand 5L fermentations are carried out in a defined medium for 7 days, followed by a resin-based extraction (XAD-7, polymeric adsorbent resin) to yield a crude extract composed of 10 to 100 metabolites. This crude extract is then purified using an automated system (ISCO) into 20 semi-pure fractions containing an approximate of 5-10 compounds each. These semi-pure fractions are introduced to the high-throughput screening (HTS) facility at UT Southwestern for biological testing. Based on the biological data obtained from HTS facility the laboratory follows the chemistry from these biologically active natural products (**Scheme 2.1**).

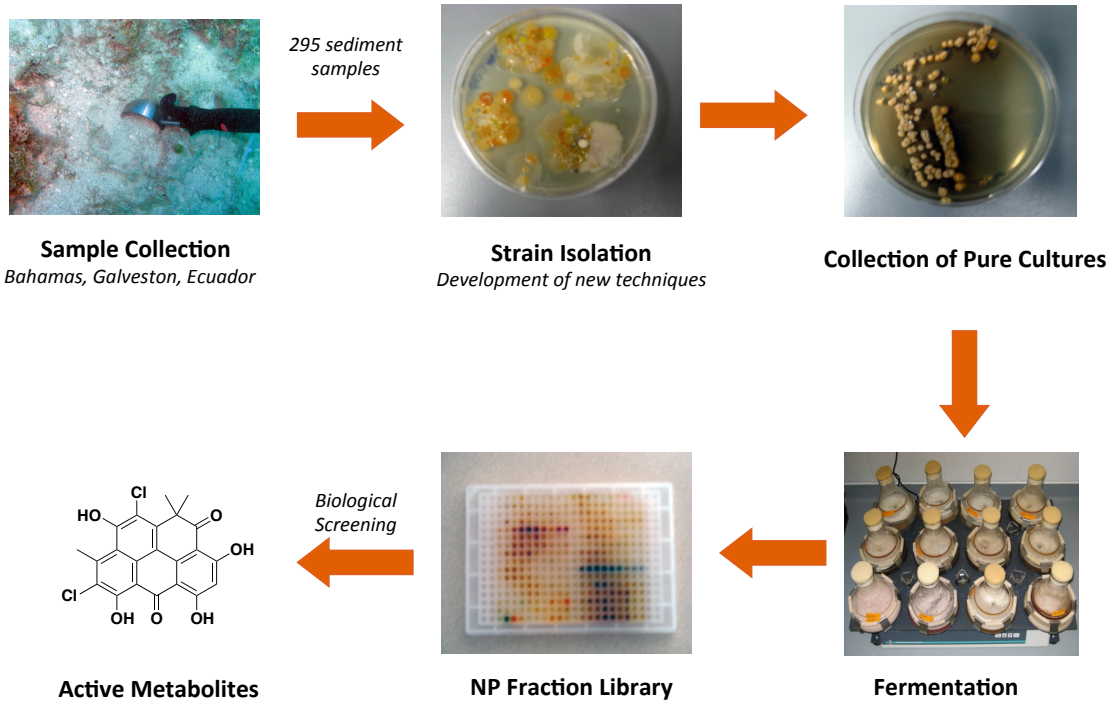

Scheme 2.1. Workflow for the generation of our natural product fraction library.

2.2.2 Tumor-derived cell lines

The cell lines tested against our library of natural products represent 6 different tumor types that include colon, lung, breast, melanoma, glioblastoma, and pancreatic cancer (**Table 2.1**). Each cell line was selected for their sensitive against cytotoxins. For example, H1437 a lung cancer derived cell line is more sensitive than the T98G glioblastoma cell line that exhibits higher resistance when exposed to cytotoxins. In addition, our panel of cancer cells can also be evaluated based on genetic mutations, for example the Mia PaCa-2 cell line that has a *KRAS* mutation can exhibit resistance towards inhibitors of epidermal growth factor receptors (EGFR), providing clues on a possible mechanism of action. This approach takes advantage of the successful strategy of the past in conjunction with advances in both high-throughput screening and genomics to identify natural products with specific therapeutic potential.

2.2.3 Screening of our library of natural product fractions against a panel of tumor derived cell lines

The primary focus was to screen our natural product fraction library in search for novel cytotoxic agents capable of being selective against a single cell line. As previously mentioned, testing our library against multiple cell lines will give an insight on the mechanism of action as well as selectivity of the secondary metabolite. The use of UT Southwestern's HTS core facility has proven to be an invaluable asset for this project since one can screen up to twelve 384-well plates against our panel of eight cancer cell lines in a single week. The standard CellTiter-Glo® assay (Promega), which measures intracellular

ATP levels was utilized by the HTS facility to screen all the fractions at a single concentration of 6 μg/ml, using robotic liquid handlers that dispensed the fractions from the library plates to the experimental plates. The MacMillan's fraction library (~ 1200) was screened against our previously described eight cell lines (**Table 2.1**). The raw data was manually analyzed looking for specific patterns of cytotoxicity, more specifically, selectivity against one or two cell lines and not to the rest. As estimated, a large number of fractions (~ 140) exhibit a general profile of activity. However, another set of fractions (~70) show selective cytotoxicity against one or two cell lines in the assay.

Furthermore, a hierarchical clustering map was completed in collaboration with Dr. Michael White (Cell Biology, UTSW) using the data obtained from the cell-based assay confirming our initial findings (**Figure 2.1**). The use of clustering analysis allowed us to identify natural product fractions that have similar activity profiles as well as visually recognize interesting activity patterns. The clustering analysis was obtained by calculating the Log2 normalized viability ratios as percent cells remaining (as assessed by ATP concentration) upon compound exposure as compared to the global mean. A Euclidean distance matrix of compound/toxicity relationships among all cell lines was constructed and used for unsupervised hierarchical clustering of compounds and cell lines. As shown in **figure 2.1**, while there is a set of compounds that are broadly toxic, there are also a large number of compounds with very diverse toxicity profiles within the cell line panel. This later observation gives great confidence that different biochemical pathways are being selectively perturbed by distinct compounds in this collection.

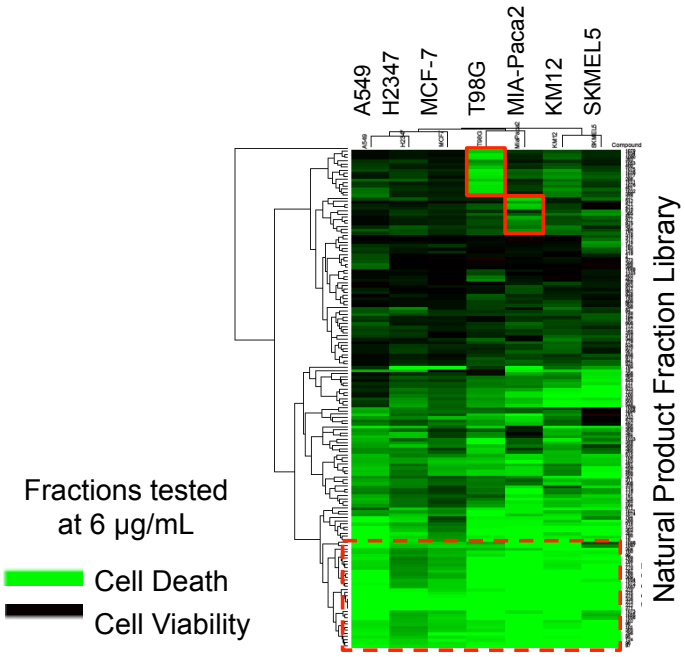

Figure 2.1. Natural products affecting cancer cell proliferation. The green color represents cell death and black represents cell viability. The solid square represent natural product fractions that have selective cytotoxicity against the T98G and MIA-PaCa2 cell lines. The dashed square represents natural product fractions that are broadly cytotoxic

Furthermore, the active hits that exhibited potent selectivity towards the T98G glioblastoma cell line in the initial screen were retested for their cytotoxicity using the library's mother plates, to confirm our initial results (**Figure 2.2**). The fractions from the library's mother plate retained their observed biological activity against the T98G cell line. Strain SNB-003 was selected for chemical examination due to its remarkable cytotoxic activity observed *in vivo* at a concentration of 6µg/mL. We began our chemical analysis of strain SNB-003, a member of the genus *Salinispora*.

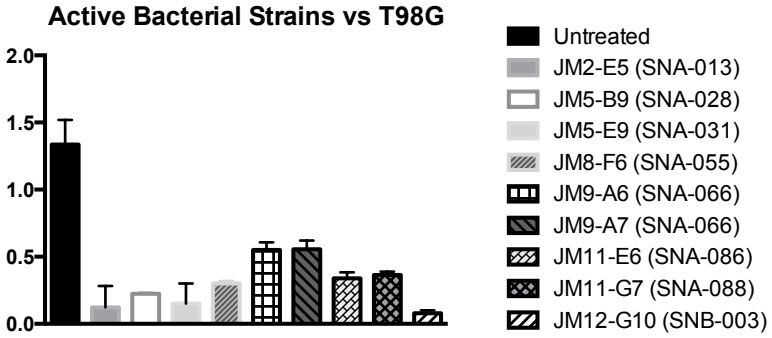

Figure 2.2. Cytotoxic fractions that exhibit selectivity towards glioblastoma cell line retested for activity using the library's mother plates. Each fraction was tested at a concentration of 6 μg/mL. The JM# represents the location of the fraction in the library's mother plate and SNA# is the strain identifier.

Glioblastoma multiforme (GBM) is the most abundant and aggressive type of brain tumor involving glial cells. [10] GBM has the capacity of diffusing through out the brain preventing the complete surgical removal of cancerous cells due to their migration to essential parts of the brain for survival. [10] Due to the nature of the disease most patients diagnosed with GBM die after one year and essentially have no long-term survival. [10] The current treatment for GMB includes: surgery, radiation and chemotherapy. Even under the best treatment circumstances, the survival for patients is only prolonged 2-3 months to a year. [10] Consequently, there is a need for the development of novel therapeutics that treat this disease.

2.2.4 Chemical examination of strain SNB-003

The crude extract from *Salinispora arenicola* was purified through the use of bioassay-guided fractionation as shown in **figure 2.3**. The crude extract was purified using an automated purification system (ISCO), 7 total fractions were collected and tested for

biological activity against the T98G cell line (**Figure 2.4A**). Based on the proton NMR, the active fraction 6 was selected for further fractionation.

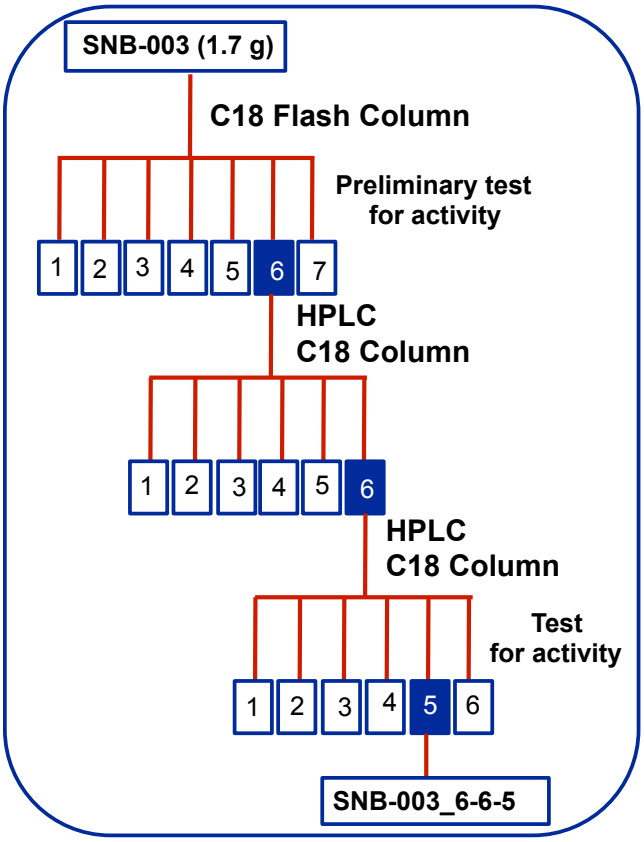

Figure 2.3. Bioassay-guided fractionation of crude extract from strain SNB-003

Fraction 6 was further purified by reversed-phase HPLC giving a total of 6 fractions. A final purification step via HPLC and test for biological activity against the T98G cell line (**Figure 2.4B**) gave SNB-003-6-6-5 as a solid (~ 400µg) as shown in **figure 2.3**.

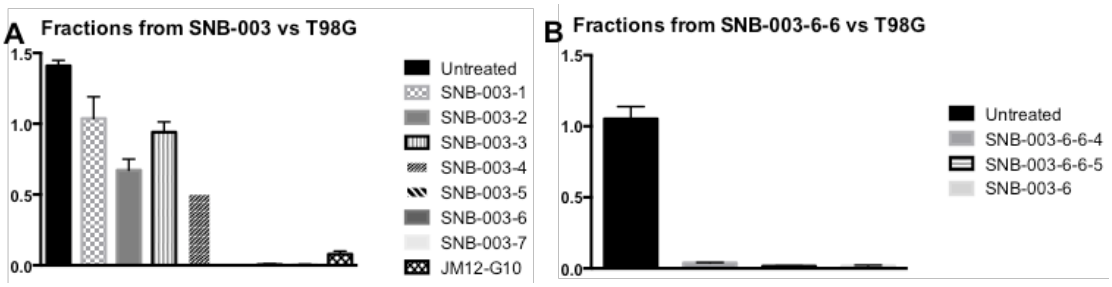

Figure 2.4. Fractions from SNB-003 tested for cytotoxic activity. **A.** Cytotoxicity from initial separation fractions 1-7 and fraction from the library's mother plate as positive control against gliobastoma cell line at a concentration of 6 µg/mL. **B.** Cytotoxicity of third round of purification of fractions 4 and 5 against gliobastoma cell line at a concentration of 6 µg/mL

With the pure natural product in hand a dose response curve of SNB-003-6-6-5 was done against T98G, SKMEL-5, MCF-7, HCC44, and MiaPaca tumor cell lines (*IC_{50} response curve by HTS-core facility, UTSW*). A two log difference in selectivity of SNB-003-6-6-5 was observed when comparing the activity of the following cell lines against T98G: MCF-7, HCC44, MiaPaca, while a log more potent than SKMEL-5 as shown in **figure 2.5**.

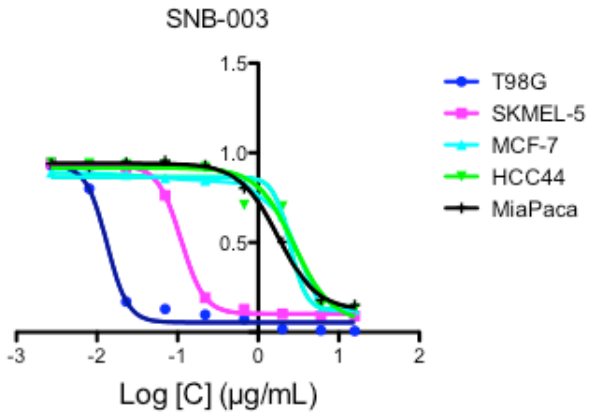

Figure 2.5. Log-dose response curve of SNB-003-6-6-5 against T98G, SKMEL-5, MCF-7, HCC44 and MiaPaca cancer cell lines.

Encouragingly, the observed selectivity of SNB-003-6-6-5 against the glioblastoma cell line motivated us to continue with structure elucidation efforts of the compound. However, due to the small amount of material initially isolated it was difficult to obtained quality data for structure elucidation. Consequently, the next strategy was to isolate more material using the compound's distinctive UV-spectrum, retention time and proton NMR for identification during crude extract purification.

2.3 Mechanism of action studies of natural product with selective therapeutic properties

In parallel to structure elucidation efforts of SNB-003-6-6-5, the White and MacMillan laboratories were working towards the design of a new platform for determining the mechanism of action of natural products. Through the use of a new screening tool called FUSION (**Fu**nctional **Si**gnature **On**tology) that utilizes RNAi perturbations and our natural product fraction library to measure the expression profile of dynamic, non-covariant reporter genes generating a functional signature. This functional signature is then compared to the expression profile of our natural product fraction library allowing us to make predictions into a possible mode of action. The pure compound from SNB-003 was one of the key proof-of-principle examples for validation of the FUSION platform.

2.3.1 FUSION

This novel platform was used to analyze the gene expression profile of one cell type exposed to 1124 genetic and 1186 chemical perturbations (**Scheme 2.2**). The chemical perturbations used in the assay are part of our natural product fraction library. Additionally,

344 human microRNA mimics and 780 siRNA perturbagens that target the human kinome and phosphatases are part of the genetic perturbations utilized in this platform. The idea is that a broad number of genetic relationships can be interrogated by specifically targeting genes that encode kinases and phosphatases, and genes whose expression is regulated by microRNAs.

The expression profile of six endogenous reporter genes is utilized to create a functional signature of chemical and genetic perturbations. In general, the expression profile of known genetic perturbations can be compared to that of a compound with unknown mechanism of action and based on this correlation generate a testable hypothesis on the possible pathway(s) that the natural product targets. In other words, if a compound has the same expression profile as an siRNA that targets a specific kinase then it means that both of these perturbations may have the same effect on the cell allowing for the prediction on the mode of action of the compound. This method won't reveal the direct target of the natural product, but rather provides information on a signaling pathway that is commonly affected between an RNAi perturbation and the compound of interest.

The endogenous reporter genes were selected based on a bioinformatic study of publicly available gene expression arrays (~3700) for genes that are dynamic and non-covariant to different genetic and pharmacological perturbations. The following genes met this criteria: ACSL5, BNIP3L, ALDOC, LOXL2, BNIP3 and NDRG1. Additionally, two other invariant genes (PPIB and HPRT) were selected as controls for the assay.

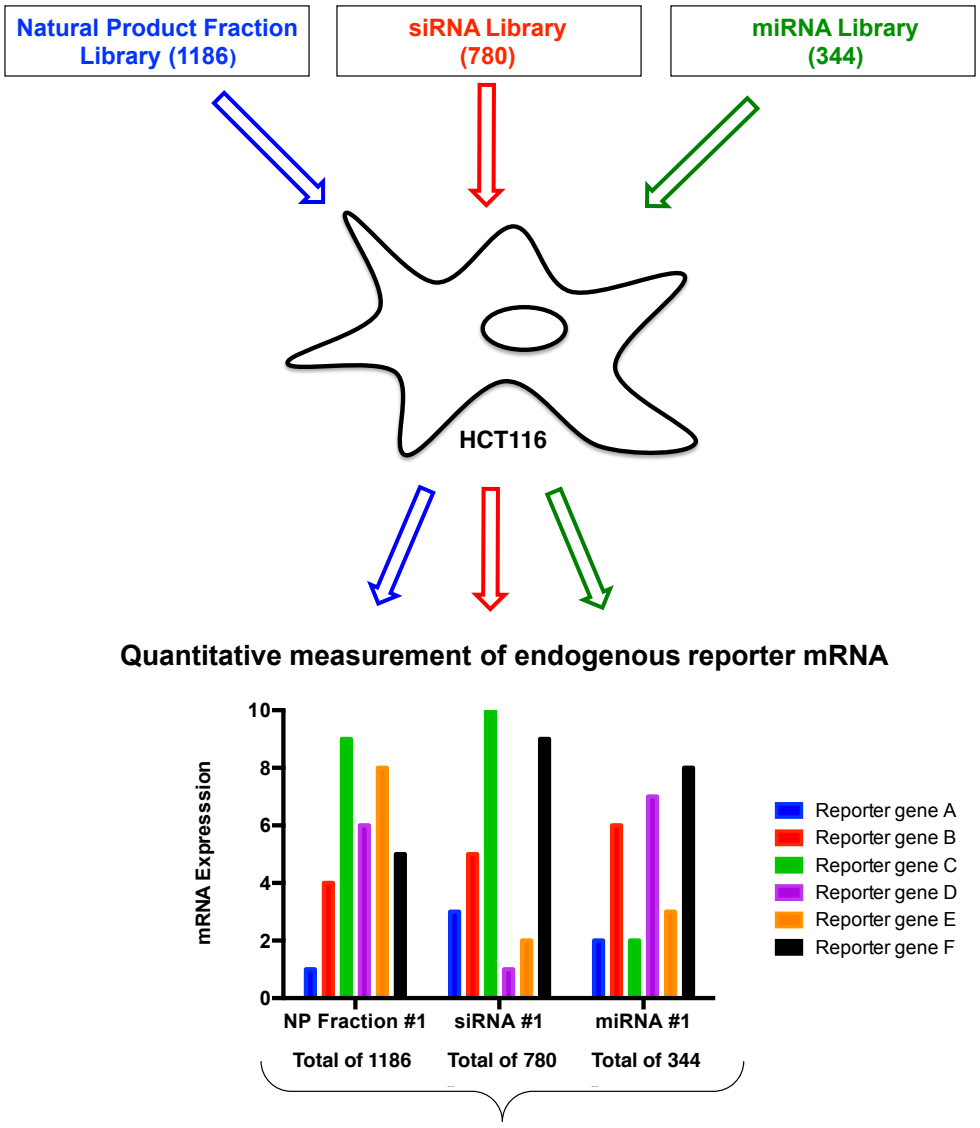

Scheme 2.2. Schematic representation of FUSION.

The high throughput readout of the reporter genes was done using a multiplex assay format and branched DNA technology, which allows the quantification of multiple mRNA levels in a single well using QuantiGene Plex 2.0 assay (Panomics) with a Luminex 200 machine (Luminex). The functional signature from the reporter genes was compiled using Euclidean distance distribution to connect compounds and RNAs that have similar effects on the cell. In this manner hierarchical clustering analysis allows the visualization of compounds that grouped close together to RNAs with similar phenotype.

2.3.2 FUSION and SNB-003-6-6-5

While working on the isolation of more material of SNB-003-6-6-5, with the aid of FUSION it was determined that a cluster of fractions from strain SNB-003 that shared a similar UV-pattern to SNB-003-6-6-5 had the same expression profile as an RNAi targeting TBK1. Additionally, the White laboratory had been working with a synthetic inhibitor of TBK1 (UTSW BX) [11] that also exhibited the same expression profile (**Figure 2.6**).

Figure 2.6. Natural product fractions that cluster with a synthetic inhibitor of TBK1

TBK1 (TANK- binding kinase 1) is a serine/threonine protein kinase that is a critical component of the host immune response to viral infection; activation of TBK1 triggers a signaling cascade resulting in the expression of a battery of cellular factors implicated in the inhibition of virus replication. [12] Under oncogenic stress conditions, TBK1 activation can overcome programmed cell death. [12]

Previous published data by the White lab has shown that upon a number of environmental stresses TBK1 activates AKT, a regulator of cell growth and proliferation, independently of mTORC2 and PDK1 (also known as PDPK1). [11] These environmental cues include triggering of the innate immune response, mitogen stimulation, re-exposure to glucose or oncogenic activation. In these occurrences TBK1 immediately associates with the exocyst to phosphorylate AKT as shown in **Figure 2.7**. [11]

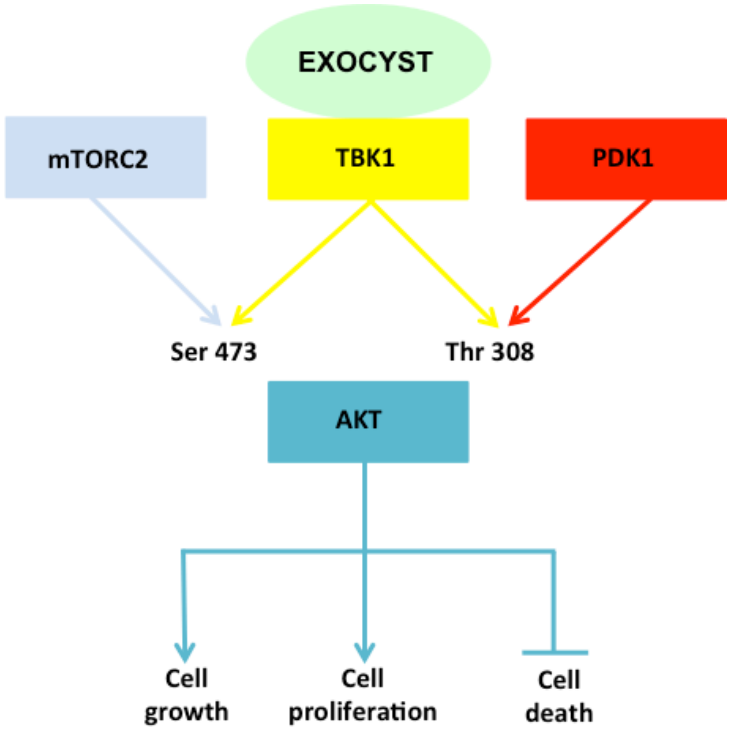

Figure 2.7 TBK1 activates AKT independently of PDK1 and mTORC2.[11]

As mentioned before within the SNB-003 fractions was a compound with a distinctive UV- chromatograph similar to that of SNB-003-6-6-5, which suggested that both were structurally related compounds. Consequently, we purified this compound from SNB-003 since it could provide the basis for the selectivity observed from SNB-003-6-6-5 against

the glioblastoma cell line and a prediction on the mechanism of action of these closely related compounds.

The crude extract from SNB-003 (7.2g) was separated using solvent/solvent partition (methanol, and ethyl acetate: water = 1:1). The ethyl acetate layer (1.3g) was dried down and purified via reversed phase flash column chromatography as shown in **figure 2.8**. One fraction containing the compound of interest was purified by HPLC.

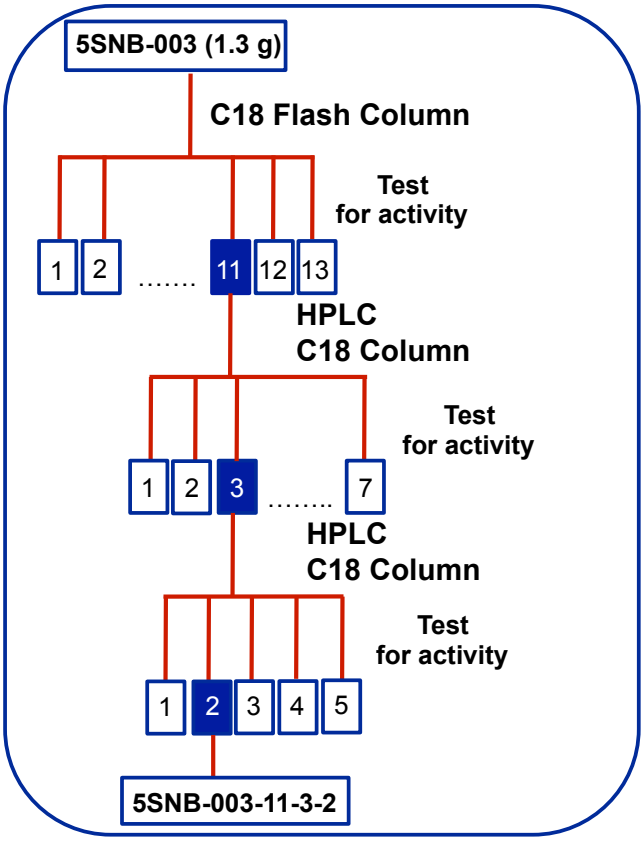

Figure 2.8. Bioassay-guided fractionation of crude extract from strain 5SNB-003

A final HPLC purification step gave the desired compound 5SNB-003-11-3-2 (7 mg). Furthermore, after each purification step in **figure 2.8** the compound was measured for its ability to inhibit TBK1 by looking at its downstream effectors AKT, GSK3b, TSC2 and S6K as shown in **figure 2.9** (*Immunoblot by Malia Potts, UTSW*)

In a dose dependent manner fractions purified from 5SNB-003 inhibited downstream targets of TBK1 at the phosphorylation level because total proteins levels remain unchanged in the presence or absence of compound.

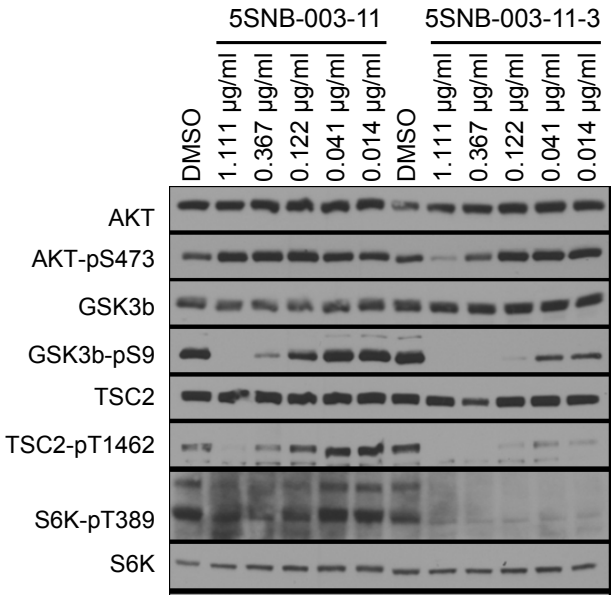

Figure 2.9 Natural product fractions from SNB-003 displayed inhibition of TBK1 by inhibiting phosphorylation of AKT, GSK3b, TSC2 and S6K

This led us to directly measure the ability of the pure compound 5SNB-003-11-3-2 to inhibit TBK1 by looking at its downstream targets, GSK3beta and S6 in a mammalian tissue culture system and *in vitro*. Our data shows that 5SNB-003-11-3-2 inhibits AKT signaling at low nanomolar activity as evidence by the inhibition of GSK3b (S9) and S6 (S235/6) phosphorylation (*Immunoblot by Malia Potts*, **Figure 2.10)**.

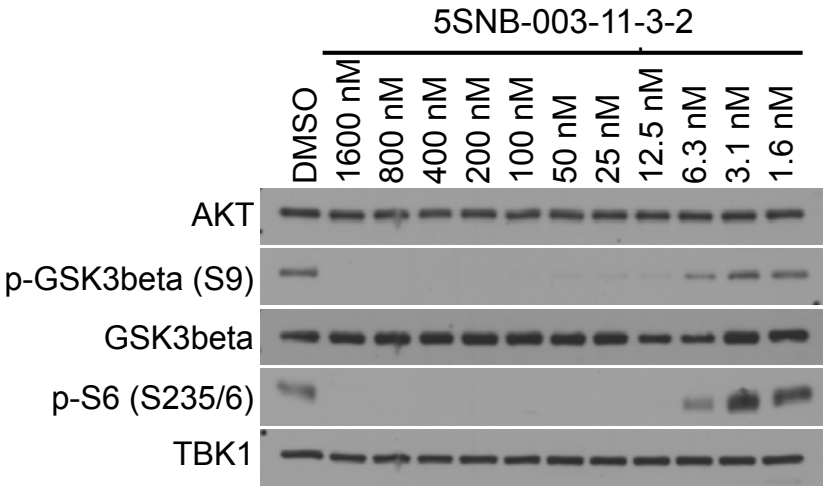

Figure 2.10. The natural product 5SNB-003-11-3-2 displays dose dependent inhibition of TBK1, as viewed by inhibiting the phosphorylation of GSK3b and S6

In addition, *in vitro* reconstitution assays of purified protein indicated that 5SNB-003-11-3-2 at subnanomolar concentrations selectively inhibit TBK1's (IC_{50} 300pM) kinase activity compared to PDK1 (IC_{50} 2nM) and AKT (IC_{50} 17nM) as shown in **figure 2.11**.

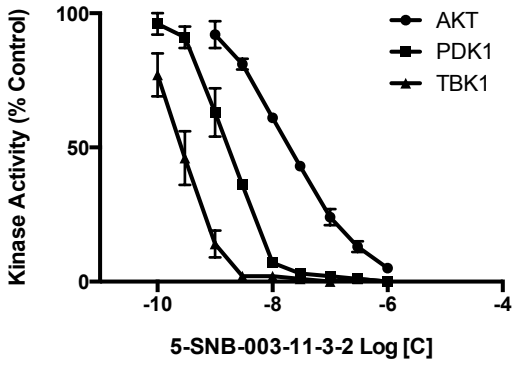

Figure 2.11. Millipore KinomeProfiler service was used to determine the IC_{50} of the natural product 5SNB-003-11-3-2 against AKT, PDK1 and TBK1.

Motivated by the initial selectivity observed within the three kinase panel in **figure 2.11** by 5SNB-003-11-3-2, we set out to investigate the selectivity of this compound against a larger panel of human kinases (253) at 1x and 10x the IC_{50} for TBK1 (**Table 2A.1**). At a

concentration of 300pM the compound activity was confined to only TBK1 and CAMKIIgamma kinases as shown in **Figure 2.12A**. However, at 3 nM the compound starts to behave more like a pan-kinase inhibitor by displaying activity towards TBK1, PDK1, TSSK1, PAR-1Bα, GCK, CaMKII, AMPKα and Rsk1-4 (**Figure 2.12B**).

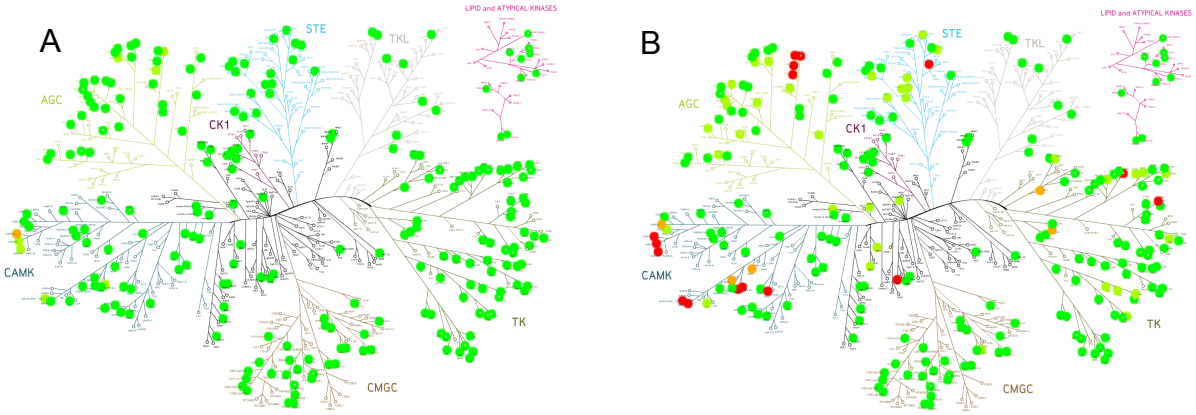

Figure 2.12. Inhibition of kinase activity of 5SNB-003-11-3-2 against 235 human kinases *in vitro*. Red circle indicate > 75% inhibition; orange indicates > 50% inhibition; yellow indicates > 25% inhibition and green indicats <25% inhibition. **A.** 0.3nM concentration of 5SNB-003-11-3-2 **B.** 3nM concentration of 5SNB-003-11-3-2

The structure of 5SNB-003-11-3-2 was determined using NMR and MS information. Based on a molecular ion of 511.2 $[M + Formic\ Acid - H]^-$ together with Antibase, a database containing descriptive information on natural products such UV-chromatogram, proton NMR, etc. we predicted that both of our compounds (SNB-003-6-6-5 and 5SNB-003-11-3-2) belonged to the family of staurosporines. It was not until a full set of 2D- NMR analysis was performed that we concluded our initial observations.

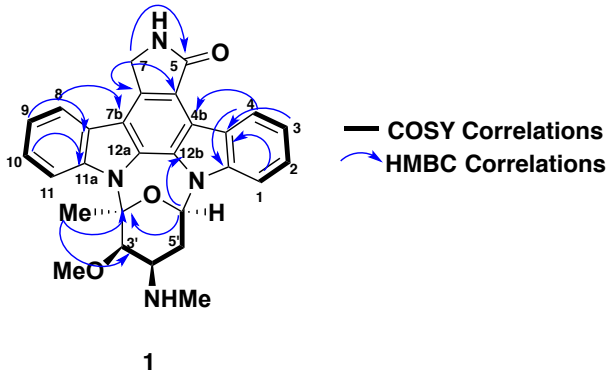

1

Figure 2.13. Key correlations used to assemble **1**.

The molecular formula of **1** was established as $C_{28}H_{26}N_4O_3$ based on a molecular ion peak at 467.2082 $[M + H]^+$ with 18 degrees of unsaturation. Utilizing COSY correlations both aromatic rings were assembled as shown in **figure 2.13**. Due to the high number of quaternary carbons present in the molecule HMBC was key to connect the structure together (**Table 2.2**).

The selective natural product SNB-003-6-6-5 is a structural analogue of **1**, based on the molecular ion of 527 that corresponds to the [M + Formic Acid – H], it is hypothesized that the compound is the hydroxyl derivative of **1**. Unfortunately, due to the lack of material for 2D-NMR analysis a definite placement of the alcohol was not possible. However based on the proton NMR hydroxylation of the aromatic ring is not possible since all aromatic protons are accounted for, possible alternatives for placement of the alcohol moiety include C7 and C5' (**Figure 2.13**). [13]

Table 2.2. 1D and 2D NMR data of staurosporine (**1)** in CD_3OD.

No.	δH, mult. (J in Hz)	δC	COSY	HMBC
1	7.33 dd (7.8,3.4)	107.9 CH	2	3, 4a
2	7.46 dt (7.8, 7.8, 3.3)	125.0 CH	1, 3	4, 13a
3	7.28 dt (7.8,7.8, 3.2)	119.3 CH	2, 4	1, 4a
4	9.24 d (7.8)	125.6 CH	3	2, 4b, 13a
4a		123.0 qC		1, 3
4b		115.3 qC		4
4c		118.6 qC		7
5		173.6 qC		7
7	7A 4.92 7B 4.81	45.8 CH_2		4c, 5, 7a
7a		132.4 qC		7
7b		114.2 qC		8
7c		124.4 qC		9, 11
8	7.94 d (7.9)	121.0 CH	9	7b, 10, 11a
9	7.37 t (7.9)	120.5 CH	8, 10	7c, 11
10	7.50 t (7.9)	124.8 CH	9, 11	8, 11a
11	7.99 dd (7.9, 4.5)	112.8 CH	10	7c, 9
11a		138.4 qC		8, 10
12a				
12b		126.6 qC		6’
13a		136.5 qC		4, 2
2’		92.9 qC		2-CH_3, 6’
3’	4.21 d (1.8)	81.2 CH	4’	2’-CH_3, 3’-OCH_3, 5’
4’	3.75 m	53.3 CH	3’, 5’	
5’	5’A 3.05 m 5’B 2.30 m	28.4 CH_2	4’, 6’	3’
6’	6.63 dd (8.7,1.9)	81.0 CH	5’	2’, 12b
2’-CH_3	2.45 s	30.9 CH_3		2’, 3’
3’- OCH_3	2.55 s	58.6 CH_3		3’
N-CH_3	2.49 s	41.6 CH_3		

At the time of structure elucidation efforts of 5SNB-003-11-3-2, in parallel the White laboratory was working towards the determination of its mode of action. Once it was determined that it was a known compound as a proof of principle it was decided to continue

on with the mechanism of action studies since we were interested in exploiting a new technique for determining the mode of action of natural products. Furthermore, very good selectivity was observed from an analogue (SNB-003-6-6-5) of this compound against the glioblastoma cell line (**Figure 2.5**) so determining the protein target of this structurally similar compound might help reveal an important therapeutic target for the treatment of GBM. It is important to point out that even though it is recognized that staurosporine is a pan-kinase inhibitor by utilizing FUSION it was observed that its highest activity is against TBK1. This technique afforded great discrimination for the determination of the signaling pathway that the compound was inhibiting. *In vitro* and immunoblot studies confirmed TBK1 as a direct target of our compound.

2.3.3 Selectivity of SNB-003-6-6-5 against T98G

The hydroxyl derivate of staurosporine (SNB-003-6-6-5) exhibited low nanomolar selectivity against the glioblastoma cell line in a panel of tumor derived cell lines. Furthermore, the mechanistic studies performed on the parent compound (staurosporine) through FUSION revealed the extraordinary selectivity of this compound against TBK1, which upon oncogenic activation regulates AKT, a controller of cell growth and proliferation. Based on these results it is hypothesized that the potent selectivity observed *in vivo* of SNB-003-6-6-5 might be due to a PTEN mutation found in the T98G cell line (**Table 2.1**). PTEN is a phosphatase that negatively regulates AKT activation, [14] suggesting that our compound mimics the effects of PTEN on AKT regulation. Thus, explaining the observed

selectivity of our compound against the glioblastoma cell line compared to the other cell lines present in the panel that may not have a PTEN mutation.

2.3.4 Staurosporine

Staurosporine was isolated over 30 years ago from *Streptomyces staurosporeus*.[15] Although staurosporine was initially found to have inhibitory activity against protein kinase C, later studies showed it's a pan-kinase inhibitor. [16] Additionally, a unique property of staurosporine is its ability to induce apoptosis of cells. [16] In a study done by Stepczynska and colleagues staurosporine induced apoptosis of cancer cells that were resistant to anti-cancer drugs. [16] Furthermore, in a follow up study it was observed that staurosporine induces apoptosis of tumor cells through different mechanisms, including the canonical and a novel intrinsic apoptotic pathway even when the apoptosis inhibitor Bcl-2 was overexpressed.[17] This represents an attractive strategy for the treatment of drug-resistant cancer cells by staurosporine and its analogues. [17] Currently there are different analogues of staurosporine that are at different stages of clinical trials for the treatment of cancer including a hydroxyl derivative (7-hydroxystaurosporine). [18]

Even to this date staurosporine continues to be a powerful chemical probe for the understanding of important biological processes. Additionally, our studies showed the potent and selective activity of staurosporine towards TBK1 at low nanomolar concentrations, providing additional information into staurosporine's activity profile. Even when this molecule has been extensively studied its biological activity continues to surprise us. Additionally, with technology continuing to impact biomedical research, where before we

were limited in the number of cell lines and natural products that could be tested we now have the ability of testing entire natural product fraction libraries against multiple cell lines, translating into access to broader activity profiles. Also, the current platforms for target identification of biologically active small molecules has allowed us to obtain an in depth mechanistic understanding of drug interactions. Natural products that were discarded due to wide spectrum cytotoxicity in the past might now reveal more specific targets with the advancement in drug-discovery platforms that can result in the utilization of these natural products as chemical probes to help unravel important biological questions.

Conclusion

2.4 FUSION: A novel approach for determining the mode of action of a natural product with selective activity against a panel of tumor derived cell lines

Our natural product fraction library revealed SNB-003-6-6-5 as a potent natural product against a panel of tumor derived cell lines with selective activity towards the glioblastoma cell line. The use of a novel technique for determining mechanism of action named FUSION, revealed the target of a closely related analogue 5SNB-003-11-3-2 to be TBK1. Inhibition of TBK1 by the compound was assessed by looking at its downstream targets: GSK3beta and S6 in a mammalian tissue culture system. Additionally, *in vitro* reconstitution studies with purified protein were consistent with inhibition of TBK1 by the compound at picomolar concentrations. However, increasing the concentration of the compound caused inhibition of multiple kinases.

Structure determination efforts revealed that 5SNB-003-11-3-2 is staurosporine and that SNB-003-6-6-5 is the hydroxyl derivative of staurosporine. Presumably, the selectivity observed *in vivo* of SNB-003-6-6-5 was due to a PTEN mutation in the glioblastoma cell line, a negative regulator of the AKT pathway.

FUSION demonstrated to be a technique capable of generating experimentally verifiable mode of action hypothesis. A FUSION database is available as an open-source web tool for the identification of natural product fractions that match genetic perturbations tested in the study (http;//whitelab.swmed.edu/fmap/fusion1.php).

Experimental Section

2.5 Materials and methods

2.5.1 General procedure

^{1}H and 2D experiments were recorded at a 600 MHZ using MeOH-d_4 in a Varian spectrometer and chemical shifts were recorded based on the corresponding solvent signal (δ_H 3.31ppm and δ_C 49.0 ppm for MeOH-d_4). High resolution ESI-TOF mass spectra were provided by The Scripps Research Institute, La Jolla, CA. Low-resolution LC/ESI-MS data were measured using an Agilent 1200 series LC/MS system with a reversed- phase C18 column (Phenomenex Luna, 150 mm × 4.6 mm, 5 μm) at a flow rate of 0.7 mL/min. Semi-preparative HPLC was performed on an Agilent 1200 series, using a C18 column (Phenomenex Luna, 250 ×10.0 mm, 5 μm).

2.5.2 Collection and phylogenetic analysis of strain SNB-003

The marine-derived bacterium strain SNB-003, was isolated from sediment sample collected from Trinity Bay, Galveston, TX (29° 42.419'N, 94° 49165' W). Bacterial spores were collected via stepwise centrifugation as follows: 2 g of sediment was dried over 24 h in an incubator at 35 °C and the resulting sediment added to 10 mL sH2O containing 0.05% Tween 20. After a vigorous vortex for 10 min, the sediment was centrifuged at 18000 rpm for 25 min (4 °C) and the resulting spore pellet collected. The resuspended spore pellet (4 mL sH2O) was plated on an acidified Gauze media, giving rise to individual colonies of SNB-003 after two weeks. Analysis of the 16S rRNA sequence of SNB-003 revealed 98% identity to *Salinospora arenicola.*

2.5.3 Cultivation and extraction

Bacterium SNB-003 was cultured in 120 × 2.8 L Fernbach flasks each containing 1 L of a seawater based medium (10 g starch, 4 g yeast extract, 2 g peptone, 1 g $CaCO_3$, 40 mg $Fe_2(SO_4)_3 \cdot 4H_2O$, 100 mg KBr) and shaken at 200 rpm at 27 °C. After seven days of cultivation, sterilized XAD-7-HP resin (20 g/L) was added to adsorb the organic products, and the culture and resin were shaken at 200 rpm for 2 h. The resin was filtered through cheesecloth, washed with deionized water, and eluted with acetone. The acetone soluble fraction was dried *in vacuo* to yield 7.2g of extract.

2.5.4 Isolation of 5SNB-003-11-3-2

The dried crude extract (SNB-003) obtained from the actinomycete *Salinispora arenicola* (7.2 g) was purified using solvent partition (MeOH) , the methanol soluble portion (4.6g) was further partitioned using EtOAc and H_2O (1:1 mixture). The ethyl acetate layer (1.3g) was purified via reversed phase flash column chromatography, eluting with a step gradient of H_2O and MeOH (90:10-100:0) collecting a total of 13 fractions. Fraction 11 (120mg) was purified by reversed phase HPLC (Phenomenex Luna, C18, 250×21.2 mm, 8.0 ml/min, 10µm, UV=254nm) using a gradient solvent system from 35% to 70% MeOH (0.1% formic acid) over 35 min, collecting 7 fractions. Fraction 3 (9.7mg) was further purified by reversed phase HPLC (Phenomenex Luna, C18, 250×10 mm, 2.5 ml/min, 5µm, UV=254nm), a gradient solvent system was utilized (60% to 100% MeOH + 0.1% formic acid over 28 min) to give 5SNB-003-11-3-2 (7.08mg).

Staurosporine (**1**, 7.08 mg) pale yellow solid; ^{1}H NMR, HMBC, HSQC and COSY (600 MHz, MeOH-d_4), see **Table 2.2**. ESI-MS *m*/*z* 467.2 $[M + H]^+$, 511.2 [M +Formic acid- H]$^-$. HRESIMS *m*/*z* 467.2082 $[M + H]^+$ ($C_{28}H_{27}N_4O_{11}$, calcd 467.2077).

2.5.5 Isolation of SNB-003-6-6-5

The dried crude extract (1.7 g) was purified using an automated purification system (ISCO) via reversed phase flash column chromatography, eluting with a gradient of H_2O: MeOH (90:10-0:100) collecting a total of 7 fractions. Fraction 6 (9.6mg) was purified by reversed phase HPLC (Phenomenex Luna, C18, 250×10 mm, 2.5 ml/min, 5µm, UV=254nm)

using isocratic conditions 70% CH_3CN (0.1% formic acid) over 35 min, collecting 6 fractions. Fraction 6 (0.86 mg) was further purified by reversed phase HPLC (Phenomenex Luna, PFP, 250×10 mm, 2.5 ml/min, 5µm, UV=254nm), isocratic conditions (30% CH_3CN + 0.1% formic acid) to give SNB-003-6-6-5 (~0.400 µg).

Hydroxystaurosporine; ^{1}H NMR (600 MHz, MeOH-d_4) δ 9.27 (d, *J*=8.0 Hz, 1H), 8.04 (d, *J*=8.4 Hz, 1H), 8.00 (d, *J*=8.4 Hz, 1H), 7.57 (d, *J*= 8.4 Hz, 1H), 7.52 (ddd, *J* = 8.0 Hz, 7.0 Hz, 1.1 Hz, 1H), 7.47 (ddd, *J* = 8.4 Hz, 7.2 Hz, 1.1 Hz, 1H), 7.35 (t, *J*=8.0 Hz, 1H), 7.32 (ddd, *J* = 8.0 Hz, 7.2 Hz, 0.77 Hz, 1H), 6.44 (d, *J*=1.0 Hz, 1H), 5.03 (d, *J*= 4.0 Hz, 2H), 4.39 (dd, *J*=5.4 Hz, 1.0Hz, 1H), 4.31 (d, *J*=3.3 Hz, 1H), 3.04 (s, 3H), 2.44 (s, 3H), 1.99 (s, 3H).

ESI-MS *m*/*z* 483.3 $[M + H]^+$, 527.2 $[M + \text{Formic acid}- H]^-$

2.5.6 Cytotoxicity assay

Cells were dispensed at 750 cells per well in 384-well plates. After ~2 hours fractions were added to a final concentration of 6 µg/ml. Control wells were treated with 1% DMSO. Plates were incubated with compound for 96 h at 37 °C in 5% CO_2, cells were treated with CellTiter-Glo (Promega) and incubated for 4 min, then luminescence was recorded.

References

1. NCI What is cancer? http://www.cancer.gov/cancertopics/cancerlibrary/what-is-cancer (accessed 2013, August 02).
2. NCI Types of treatment. http://www.cancer.gov/cancertopics/treatment/types-of-treatment (accessed Agust 05,2013).
3. NCI Targeted Cancer Therapies. http://www.cancer.gov/cancertopics/factsheet/Therapy/targeted (accessed 2013, August 05).
4. Li, J. W.; Vederas, J. C., Drug discovery and natural products: end of an era or an endless frontier? *Science* **2009,** *325* (5937), 161-5.
5. Fenical, W.; Jensen, P. R., Developing a new resource for drug discovery: marine actinomycete bacteria. *Nature chemical biology* **2006,** *2* (12), 666-73.
6. Gerwick, W. H.; Moore, B. S., Lessons from the past and charting the future of marine natural products drug discovery and chemical biology. *Chemistry & biology* **2012,** *19* (1), 85-98.
7. Shoemaker, R. H., The NCI60 human tumour cell line anticancer drug screen. *Nature reviews. Cancer* **2006,** *6* (10), 813-23.
8. Ziegler, S.; Pries, V.; Hedberg, C.; Waldmann, H., Target identification for small bioactive molecules: finding the needle in the haystack. *Angewandte Chemie* **2013,** *52* (10), 2744-92.
9. (a) Gontang, E. A.; Fenical, W.; Jensen, P. R., Phylogenetic diversity of gram-positive bacteria cultured from marine sediments. *Appl Environ Microb* **2007,** *73* (10), 3272-3282; (b) Koehn, F. E., New strategies and methods in the discovery of natural product anti-infective agents: The mannopeptimycins. *J Med Chem* **2008,** *51* (9), 2613-2617.
10. Holland, E. C., Glioblastoma multiforme: the terminator. *Proceedings of the National Academy of Sciences of the United States of America* **2000,** *97* (12), 6242-4.
11. Ou, Y. H.; Torres, M.; Ram, R.; Formstecher, E.; Roland, C.; Cheng, T.; Brekken, R.; Wurz, R.; Tasker, A.; Polverino, T.; Tan, S. L.; White, M. A., TBK1 directly engages Akt/PKB survival signaling to support oncogenic transformation. *Molecular cell* **2011,** *41* (4), 458-70.
12. Bodemann, B. O.; White, M. A., Ral GTPases and cancer: linchpin support of the tumorigenic platform. *Nature reviews. Cancer* **2008,** *8* (2), 133-40.
13. (a) Hernandez, L. M.; Blanco, J. A.; Baz, J. P.; Puentes, J. L.; Millan, F. R.; Vazquez, F. E.; Fernandez-Chimeno, R. I.; Gravalos, D. G., 4'-N-methyl-5'-hydroxystaurosporine and 5'-hydroxystaurosporine, new indolocarbazole alkaloids from a marine Micromonospora sp. strain. *The Journal of antibiotics* **2000,** *53* (9), 895-902; (b) Takahashi, I.; Saitoh, Y.; Yoshida, M.; Sano, H.; Nakano, H.; Morimoto, M.; Tamaoki, T., Ucn-01 and Ucn-02, New Selective Inhibitors of Protein Kinase-C .2. Purification, Physicochemical Properties, Structural Determination and Biological-Activities. *J Antibiot* **1989,** *42* (4), 571-576.
14. Moon, S. H.; Kim, D. K.; Cha, Y.; Jeon, I.; Song, J.; Park, K. S., PI3K/Akt and Stat3 signaling regulated by PTEN control of the cancer stem cell population,

proliferation and senescence in a glioblastoma cell line. *International journal of oncology* **2013,** *42* (3), 921-8.
15. Omura, S.; Iwai, Y.; Hirano, A.; Nakagawa, A.; Awaya, J.; Tsuchya, H.; Takahashi, Y.; Masuma, R., A new alkaloid AM-2282 OF Streptomyces origin. Taxonomy, fermentation, isolation and preliminary characterization. *The Journal of antibiotics* **1977,** *30* (4), 275-82.
16. Stepczynska, A.; Lauber, K.; Engels, I. H.; Janssen, O.; Kabelitz, D.; Wesselborg, S.; Schulze-Osthoff, K., Staurosporine and conventional anticancer drugs induce overlapping, yet distinct pathways of apoptosis and caspase activation. *Oncogene* **2001,** *20* (10), 1193-202.
17. Manns, J.; Daubrawa, M.; Driessen, S.; Paasch, F.; Hoffmann, N.; Loffler, A.; Lauber, K.; Dieterle, A.; Alers, S.; Iftner, T.; Schulze-Osthoff, K.; Stork, B.; Wesselborg, S., Triggering of a novel intrinsic apoptosis pathway by the kinase inhibitor staurosporine: activation of caspase-9 in the absence of Apaf-1. *FASEB journal : official publication of the Federation of American Societies for Experimental Biology* **2011,** *25* (9), 3250-61.
18. (a) Fischer, T.; Stone, R. M.; Deangelo, D. J.; Galinsky, I.; Estey, E.; Lanza, C.; Fox, E.; Ehninger, G.; Feldman, E. J.; Schiller, G. J.; Klimek, V. M.; Nimer, S. D.; Gilliland, D. G.; Dutreix, C.; Huntsman-Labed, A.; Virkus, J.; Giles, F. J., Phase IIB trial of oral Midostaurin (PKC412), the FMS-like tyrosine kinase 3 receptor (FLT3) and multi-targeted kinase inhibitor, in patients with acute myeloid leukemia and high-risk myelodysplastic syndrome with either wild-type or mutated FLT3. *Journal of clinical oncology : official journal of the American Society of Clinical Oncology* **2010,** *28* (28), 4339-45; (b) Kummar, S.; Gutierrez, M. E.; Gardner, E. R.; Figg, W. D.; Melillo, G.; Dancey, J.; Sausville, E. A.; Conley, B. A.; Murgo, A. J.; Doroshow, J. H., A phase I trial of UCN-01 and prednisone in patients with refractory solid tumors and lymphomas. *Cancer chemotherapy and pharmacology* **2010,** *65* (2), 383-9.

APPENDIX 2A

Table 2A.1 Millipore KinomeProfiler service was used to determine the inhibition of the natural product 5SNB-003-11-3-2 against a panel of kinases at a concentration of 0.3nM and 3nM.

Kinase	5SNB-003-11-3-2 @ 0.0003 µM	5SNB-003-11-3-2 @ 0.003 µM
Abl(h)	107	114
Abl(m)	114	106
Abl (H396P) (h)	106	107
Abl (M351T)(h)	107	100
Abl (Q252H) (h)	101	88
Abl(T315I)(h)	105	102
Abl(Y253F)(h)	105	97
ACK1(h)	95	43
ALK(h)	121	117
ALK4(h)	113	122
Arg(h)	112	102
AMPKα1(h)	93	10
AMPKα2(h)	58	5
Arg(m)	103	93
ARK5(h)	149	111
ASK1(h)	99	102
Aurora-A(h)	116	107
Aurora-B(h)	129	71
Aurora-C(h)	103	90
Axl(h)	130	99
Blk(h)	100	93
Blk(m)	101	85
Bmx(h)	106	84
BRK(h)	117	110
BrSK1(h)	82	30
BrSK2(h)	94	87
BTK(h)	102	93
BTK(R28H)(h)	89	104
CaMKI(h)	102	84
CaMKIIβ(h)	60	6
CaMKIIγ(h)	37	2
CaMKIδ(h)	90	39
CaMKIIδ(h)	51	4
CaMKIV(h)	105	86
CDK1/cyclinB(h)	107	83
CDK2/cyclinA(h)	106	80
CDK2/cyclinE(h)	99	79
CDK3/cyclinE(h)	101	93
CDK5/p25(h)	107	72
CDK5/p35(h)	100	84
CDK6/cyclinD3(h)	101	90

CDK7/cyclinH/MAT1(h)	113	101
CDK9/cyclin T1(h)	95	91
CHK1(h)	102	76
CHK2(h)	114	91
CHK2(I157T)(h)	111	96
CHK2(R145W)(h)	110	86
CK1γ1(h)	101	107
CK1γ2(h)	97	100
CK1γ3(h)	104	102
CK1δ(h)	114	103
CK1(y)	86	88
CK2(h)	109	108
CK2α2(h)	105	101
CLK2(h)	112	75
CLK3(h)	103	109
cKit(h)	116	112
cKit(D816V)(h)	100	99
cKit(D816H)(h)	80	17
cKit(V560G)(h)	118	59
cKit(V654A)(h)	97	69
CSK(h)	103	90
c-RAF(h)	107	95
cSRC(h)	99	100
DAPK1(h)	115	104
DAPK2(h)	109	92
DCAMKL2(h)	117	117
DDR2(h)	101	110
DMPK(h)	99	110
DRAK1(h)	99	105
DYRK2(h)	104	102
eEF-2K(h)	114	94
EGFR(h)	106	98
EGFR(L858R)(h)	95	94
EGFR(L861Q)(h)	101	98
EGFR(T790M)(h)	84	33
EGFR(T790M,L858R)(h)	84	27
EphA1(h)	119	98
EphA2(h)	94	105
EphA3(h)	98	103
EphA4(h)	112	114
EphA5(h)	123	117
EphA7(h)	113	114
EphA8(h)	96	106
EphB2(h)	91	101
EphB1(h)	110	93
EphB3(h)	105	104
EphB4(h)	103	107
ErbB4(h)	105	102
FAK(h)	107	111
Fer(h)	106	103
Fes(h)	97	87

FGFR1(h)	126	94
FGFR1(V561M)(h)	94	39
FGFR2(h)	92	74
FGFR2(N549H)(h)	107	92
FGFR3(h)	112	110
FGFR4(h)	88	82
Fgr(h)	148	67
Flt1(h)	83	67
Flt3(D835Y)(h)	109	67
Flt3(h)	91	71
Flt4(h)	104	70
Fms(h)	105	23
Fms(Y969C)(h)	109	78
Fyn(h)	85	53
GCK(h)	93	17
GRK5(h)	109	103
GRK6(h)	97	95
GRK7(h)	95	87
GSK3α(h)	102	77
GSK3β(h)	109	106
Haspin(h)	76	64
Hck(h)	110	86
Hck(h) activated	81	62
HIPK1(h)	111	104
HIPK2(h)	106	102
HIPK3(h)	100	103
IGF-1R(h)	109	109
IGF-1R(h), activated	102	100
IKKα(h)	106	93
IKKβ(h)	108	103
IR(h)	110	109
IR(h), activated	105	98
IRR(h)	105	102
IRAK1(h)	97	102
IRAK4(h)	97	85
Itk(h)	110	105
JAK2(h)	101	70
JAK3(h)	132	84
JNK1α1(h)	96	91
JNK2α2(h)	109	109
JNK3(h)	93	98
KDR(h)	96	99
Lck(h)	107	81
Lck(h) activated	96	86
LIMK1(h)	100	83
LKB1(h)	90	96
LOK(h)	104	54
Lyn(h)	96	56
Lyn(m)	100	65
MAPK1(h)	129	127
MAPK2(h)	101	102

MAPK2(m)	97	94
MAPKAP-K2(h)	97	93
MAPKAP-K3(h)	99	98
MEK1(h)	99	55
MARK1(h)	83	23
MELK(h)	86	37
Mer(h)	77	22
Met(h)	103	110
Met(D1246H)(h)	98	87
Met(D1246N)(h)	82	83
Met(M1268T)(h)	82	85
Met(Y1248C)(h)	88	86
Met(Y1248D)(h)	97	88
Met(Y1248H)(h)	88	80
MINK(h)	116	95
MKK4(m)	125	141
MKK6(h)	135	103
MKK7β(h)	118	147
MLCK(h)	117	98
MLK1(h)	100	88
Mnk2(h)	104	96
MRCKα(h)	106	103
MRCKβ(h)	106	90
MSK1(h)	109	94
MSK2(h)	103	88
MSSK1(h)	97	97
MST1(h)	110	68
MST2(h)	92	77
MST3(h)	79	65
mTOR(h)	96	83
mTOR/FKBP12(h)	92	101
MuSK(h)	106	86
NEK2(h)	113	111
NEK3(h)	89	89
NEK6(h)	89	96
NEK7(h)	101	86
NEK11(h)	107	97
NLK(h)	108	100
p70S6K(h)	109	72
PAK2(h)	120	94
PAK4(h)	105	95
PAK5(h)	91	83
PAK6(h)	101	63
PAR-1Bα(h)	63	5
PASK(h)	94	88
PEK(h)	97	104
PDGFRα(h)	96	105
PDGFRα(D842V)(h)	89	26
PDGFRα(V561D)(h)	91	26
PDGFRβ(h)	97	90
PDK1(h)	111	70

PhKγ2(h)	105	63
Pim-1(h)	97	100
Pim-2(h)	109	88
Pim-3(h)	104	86
PKA(h)	107	58
PKBα(h)	95	86
PKBβ(h)	93	87
PKBγ(h)	95	62
PKCα(h)	96	88
PKCβI(h)	91	60
PKCβII(h)	104	81
PKCγ(h)	105	73
PKCδ(h)	91	65
PKCε(h)	110	90
PKCη(h)	100	95
PKCι(h)	103	100
PKCμ(h)	100	95
PKCθ(h)	92	64
PKCζ(h)	109	103
PKD2(h)	93	89
PKG1α(h)	115	67
PKG1β(h)	77	63
Plk1(h)	102	95
Plk3(h)	106	110
PRAK(h)	133	141
PRK2(h)	115	69
PrKX(h)	118	98
PTK5(h)	106	86
Pyk2(h)	95	103
Ret(h)	108	76
Ret (V804L)(h)	98	82
Ret(V804M)(h)	100	85
RIPK2(h)	99	96
ROCK-I(h)	95	105
ROCK-II(h)	95	70
ROCK-II(r)	90	74
Ron(h)	110	114
Ros(h)	97	90
Rse(h)	111	107
Rsk1(h)	62	24
Rsk1(r)	68	16
Rsk2(h)	78	5
Rsk3(h)	68	10
Rsk4(h)	108	16
SAPK2a(h)	94	102
SAPK2a(T106M)(h)	107	108
SAPK2b(h)	99	96
SAPK3(h)	92	99
SAPK4(h)	100	108
SGK(h)	119	105
SGK2(h)	63	73

SGK3(h)	94	98
SIK(h)	111	60
Snk(h)	93	95
Src(1-530)(h)	103	80
Src(T341M)(h)	65	28
SRPK1(h)	113	111
SRPK2(h)	100	100
STK33(h)	104	110
Syk(h)	99	43
TAK1(h)	104	117
TAO1(h)	103	59
TAO2(h)	89	74
TAO3(h)	93	73
TBK1(h)	88	22
Tec(h) activated	112	111
TGFBR1(h)	107	101
Tie2 (h)	112	105
Tie2(R849W)(h)	102	110
Tie2(Y897S)(h)	101	93
TLK2(h)	96	65
TrkA(h)	82	72
TrkB(h)	135	127
TSSK1(h)	80	11
TSSK2(h)	104	80
Txk(h)	116	119
ULK2(h)	96	73
ULK3(h)	102	63
WNK2(h)	98	99
WNK3(h)	115	111
VRK2(h)	99	97
Yes(h)	94	51
ZAP-70(h)	104	116
ZIPK(h)	122	108

Figure 2A.1 ^{1}H- NMR of **1** in MeOH-d_4. 600 MHz

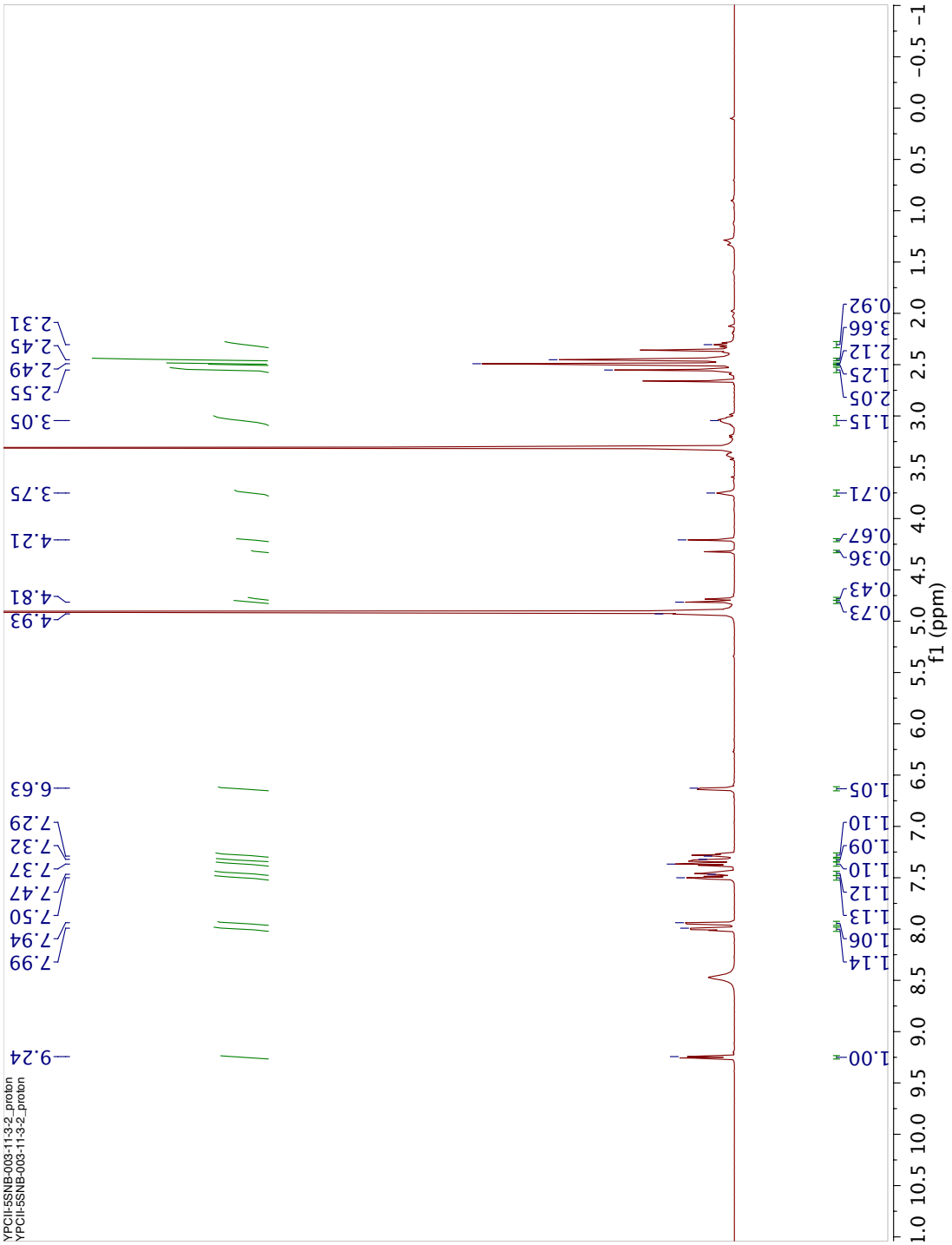

Figure 2A.2 gCOSY NMR of **1** in MeOH-d_4. 600 MHz

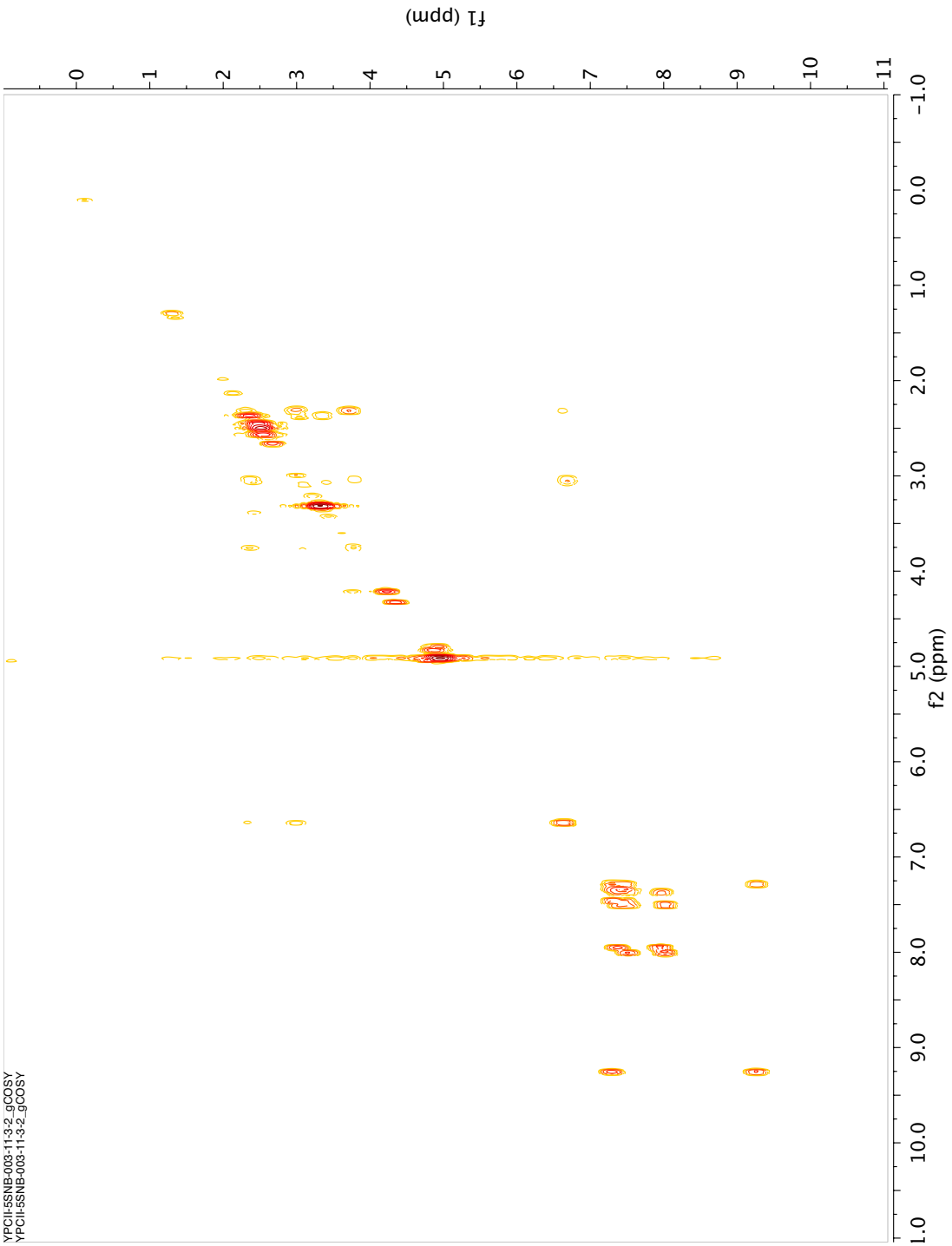

Figure 2A.3 gHSQC NMR of **1** in MeOH-d_4. 600 MHz

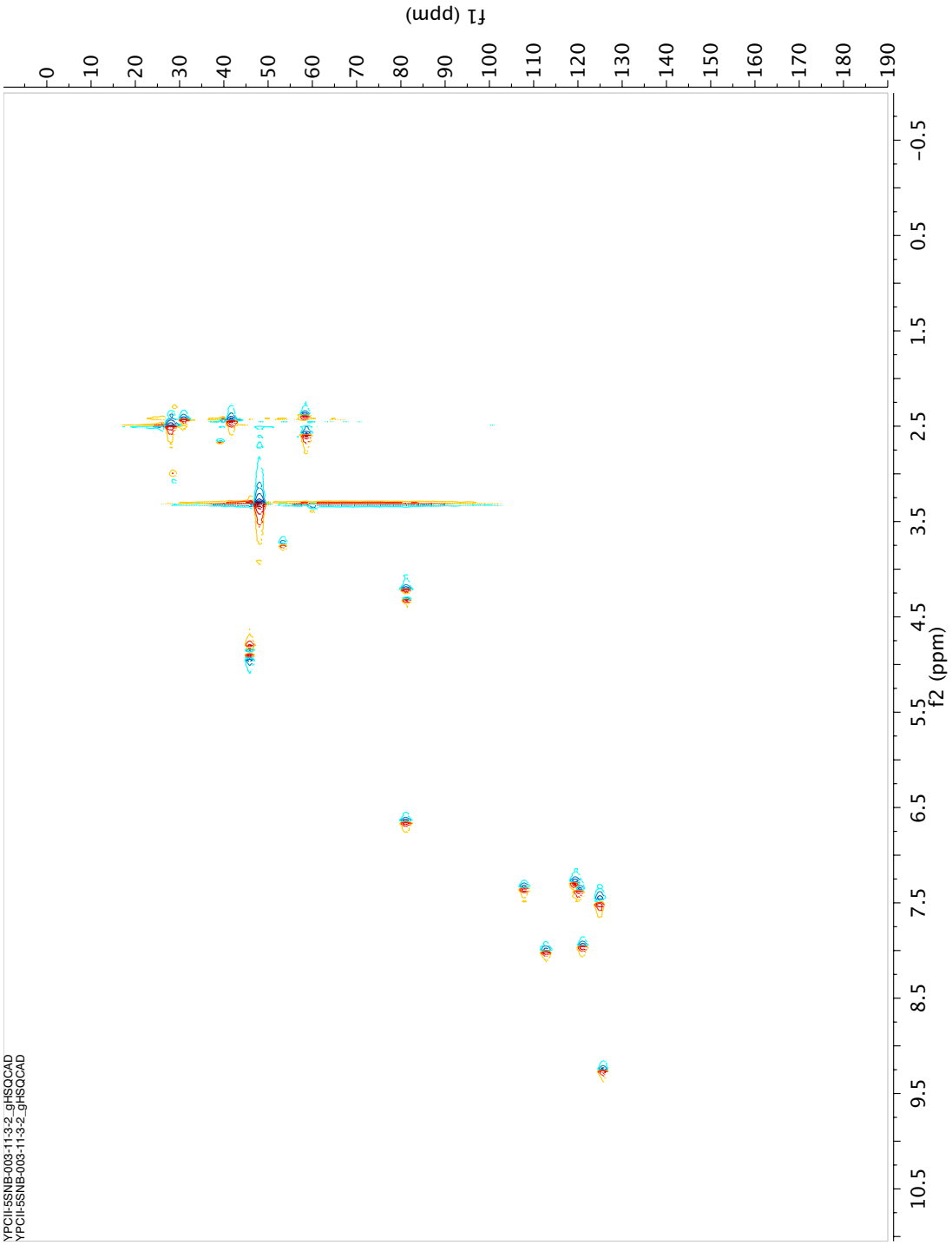

Figure 2A.4 gHMBC NMR of **1** in MeOH-d_4. 600 MHz

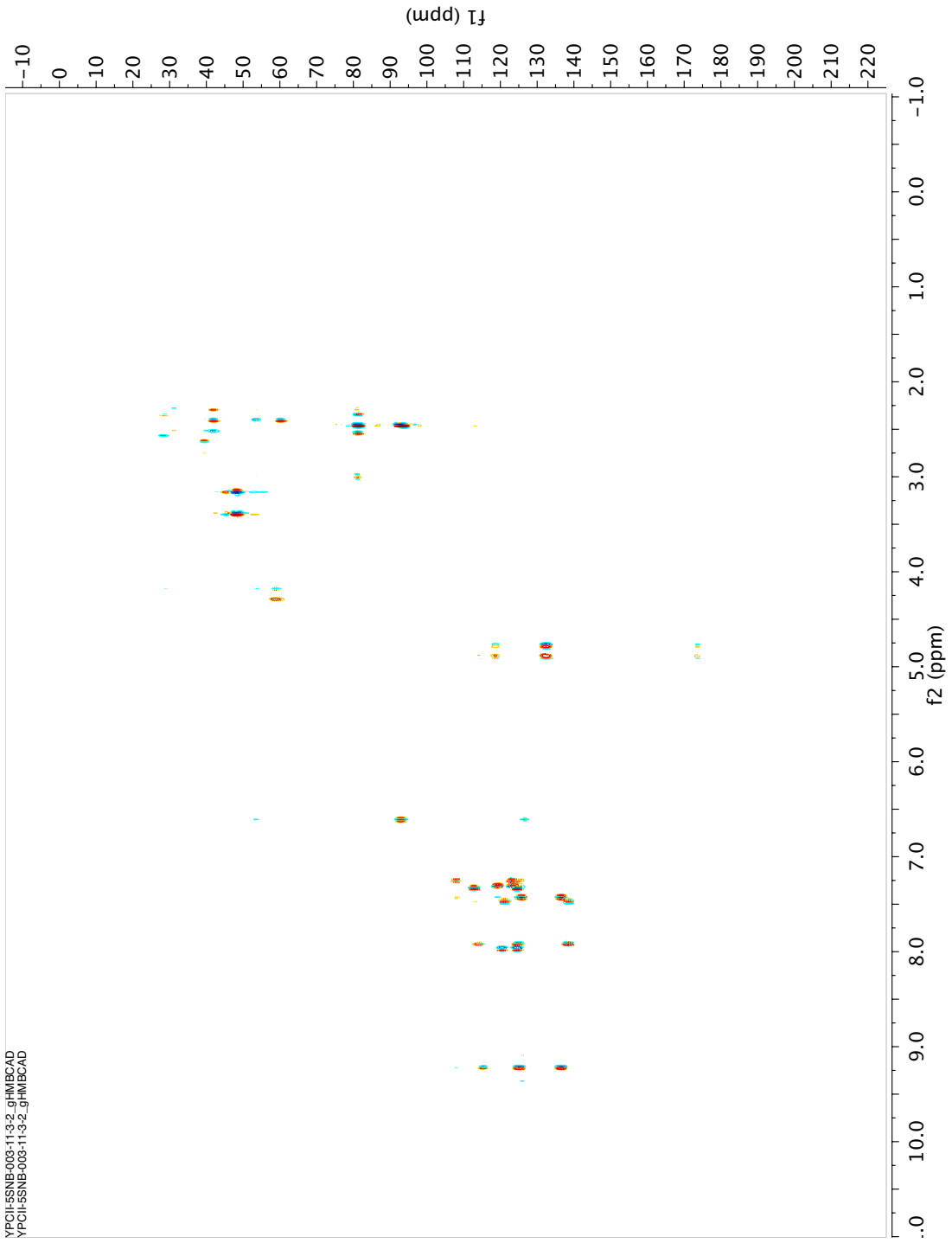

Figure 2A.5 ^{1}H NMR of SNB-003-6-6-5 in MeOH-d_4. 600 MHz

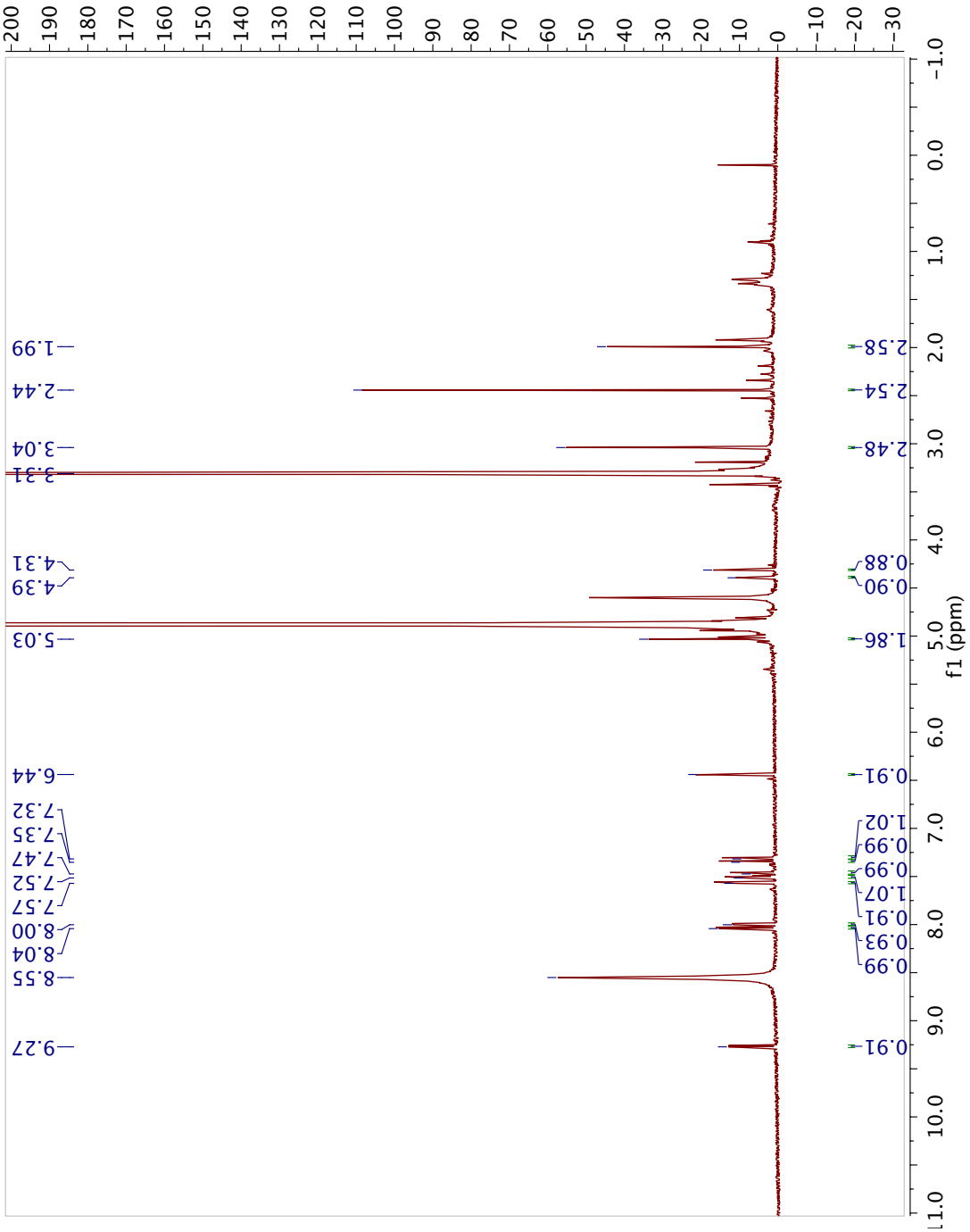

CHAPTER THREE
Introduction

RIFSALINIKETAL: NOVEL POLYKETIDE FROM *S. ARENICOLA*

3.1 The genus *Salinispora*: a productive source of natural products

The genus *Salinispora* has been a prolific source of secondary metabolites. Currently, there are three species that belong to this genus: *Salinispora tropica, Salinispora arenicola* and *Salinispora pacifica*.[1] The potent proteasome inhibitor salinosporamide A, the first natural product isolated from the obligate marine bacteria *S. tropica*,[2] is currently in clinical trials for the treatment of cancer.[3] Other examples of natural products from this genus include: sporolide[4], arenicolide[5], cyanosporaside[6], salinilactam,[7] saliniketal[8], straurosporine[9], and rifamycin [9] (**Figure 3.1**).

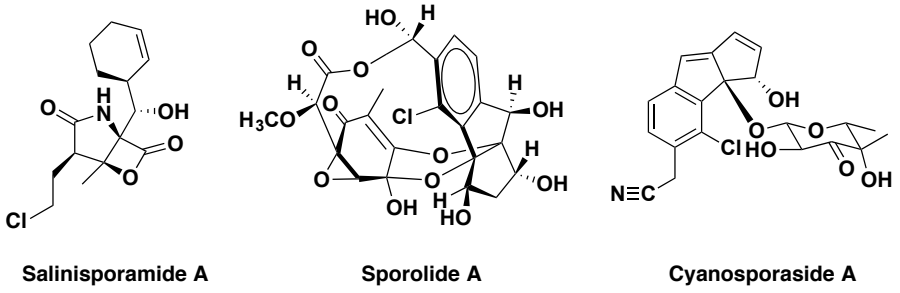

Figure 3.1. Examples of natural products isolated from the genus *Salinispora*

The genomes of *S.tropica* and *S. arenicola* were sequenced to provide insight into their biosynthetic potential.[7, 10] It was shown that a large percentage of their genome is devoted to the assembly of natural products, [7, 10] suggesting that there is still a large chemical diversity to explore within this genus.

3.1.1 Saliniketals

The polyketides salniketal A (**1**) and B (**2**) were isolated from the marine-derived bacteria *S. arenicola* by Williams and co-workers (**Figure 3.2**).[8] Saliniketals were found to be inhibitors of ornithine decarboxylase (ODC) induction,[8] which is a critical enzyme involved in polyamine synthesis. [11] Polyamines are cations derived from amino acids that have been shown to stabilize chromatin, prevent DNA damage by acting as reactive oxygen species (ROS) scavengers, and are required for mice development. [12] Polyamine pools are involved in normal cellular growth and in many adult tissues when cells become senescent polyamine synthesis is downregulated.[8, 13] In addition, ODC is a direct target of the *MYC* oncogene, and it has been shown to be overexpressed in different tumor cells.[11, 14] The inhibition of ODC leads to an imbalance in polyamine synthesis that can lead to DNA-damage and inhibition of cellular proliferation.[11-12] As a consequence, ODC may represent a chemopreventive target to avert the development of cancer, with the idea to reduce the levels of polyamine pools. [11, 15] Saliniketal A and B were found to inhibit ODC induction with IC_{50} values of 1.95 ±0.37 µg/ml and 7.83 ± 1.2 µg/mL, respectively. [8]

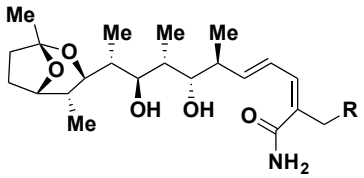

Figure 3.2. Saliniketal A and B

Some of the structural characteristic of these molecules includes its polyketide side chain terminating in a 1, 4- dimethyl-2, 8- dioxabicyclo [3.2.1] octane ring. The essential 2D NMR spectroscopic methods were obtained to solve the structure of **1** and **2**. The relative

stereochemistry of the compounds was solved utilizing proton-carbon coupling constants and 1D NOE experiments. The absolute stereochemistry of **1** and **2** was assigned by Mosher's analysis. The unique structural characteristics of the saliniketals along with its interesting biological activity have resulted in three total syntheses of these molecules. [16]

Surprisingly, the saliniketals share common structural characteristics to the *ansa* side chain of rifamycin (**3**), which co-occur in the fermentation media (**Figure 3.3**).[8]

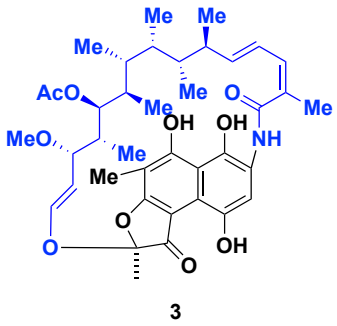

3

Figure 3.3. Rifamycin SV. The *ansa* side chain of rifamycin is highlighted in blue.[8]

3.1.2 Biosynthesis of the saliniketals

The elegant work done by Moore and co-workers provided evidence that saliniketals are byproducts of rifamycin biosynthesis. [17] Using PCR-directed mutagenesis, chemical complementation studies, and isotope feeding experiments they were able to demonstrate that the enzyme cytochrome P450 monoxygenase, encoded by the biosynthetic gene *sare1259* is involved in multiple oxidative rearrangement reactions of 34a-deoxyrifamycin W (**4**) to afford the saliniketals and rifamycin (**Scheme 3.1**). Along the biosynthetic pathway of rifamycin, 34a-deoxyrifamycin W undergoes multiple oxidation steps at position C34 that lead to the decarboxylation of the resulting carboxylic acid.[18] The group believes that the

timing of this decarboxylation step is crucial in determining what biosynthetic pathway the organism will undergo, that can either provide the rifamycins or the saliniketals as final products. [17] The conversion of **4** into rifamycin by the enzyme Sare1259 is achieved by oxidative bond cleavage of the double bond at C12 and C19.[18] Conversely, for the conversion of **4** into saliniketal the bond at C11 and C12 is cleaved in a similar fashion (**Scheme 3.1**). [17] This is followed by reduction of the double bond between C28 and C29 and subsequent nucleophilic attack of the secondary alcohol to the ketone moiety affords naphthoquinone derivative **8.** Moreover, loss of water affords rifsaliniketal (**9**), a key intermediate in the biosynthetic descriptions of saliniketal that is thought to undergo a decarboxylation step to give salinisporamycin (**10**), which was isolated by Matsuda and co-workers (**Scheme 3.1**).[17, 19] Sequential steps give rise to the saliniketals.[17] Isolation of **9** was not possible until now, which lends support to Moore's biosynthetic proposal. The isolation and structure elucidation of rifsaliniketal will be described in detail in this chapter.

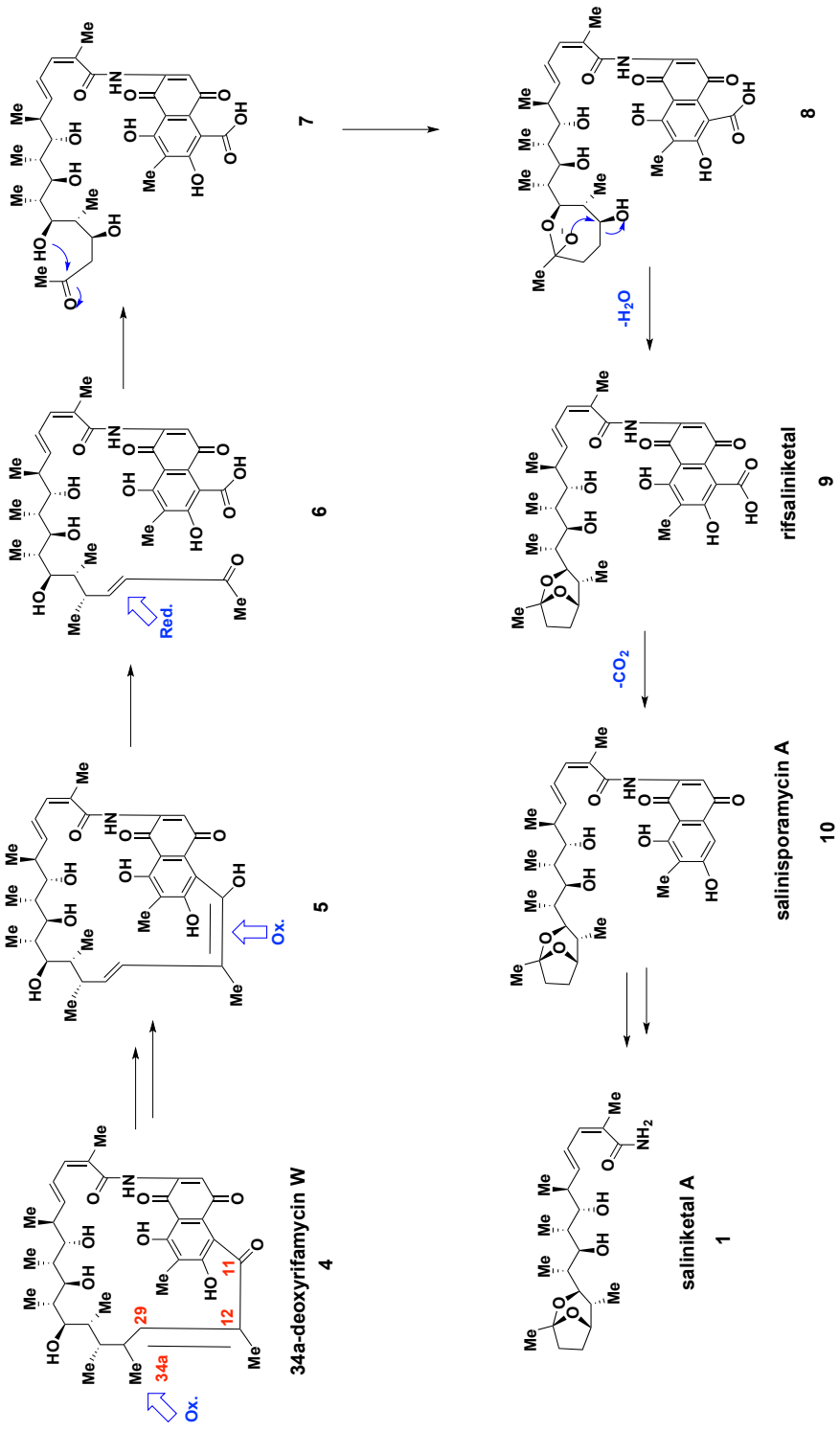

Scheme 3.1 Biosynthetic proposal of saliniketal.[17]

Results and Discussion

3.2 Rifsaliniketal

3.2.1 Isolation and structure elucidation of rifsaliniketal

In an effort to identify natural products with selective activity against a panel of tumor-derived cell lines we came across a fraction from SNB-003 with interesting chemical characteristics based on the proton NMR. The marine-derived bacteria SNB-003 was isolated from a marine sediment sample collected in Galveston, TX. Analysis of the strain by 16s rRNA revealed high sequence identity to *S. arenicola.* A twenty-liter scale fermentation of SNB-003 was carried out, and the secondary metabolites were extracted using XAD-7 resin. The crude extract was then purified using solvent/solvent partition (methanol, and ethyl acetate: water = 1:1). The organic layer was dried down and purified via reversed phase column chromatrography. A major fraction containing **9** was purified by HPLC to give an enriched fraction of rifsaliniketal. A final purification via reversed phase HPLC gave rifsaliniketal (**9**, 1.79mg).

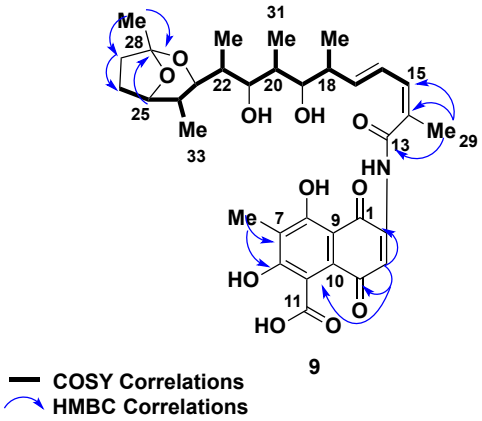

Figure 3.4. Key correlations used to assemble **9**.

Rifsaliniketal (**9**) was isolated as a yellow powder. The molecular formula of **9** was established as $C_{34}H_{43}NO_{11}$ based on a molecular ion peak at 642.2901 $[M + H]^+$ and 14 degrees of unsaturation were calculated. From COSY correlations the polyketide side chain of **9** was assembled (**Figure 3.4**). More specifically, fragment C13 to C18 was established by COSY correlation from H15/H16, H16/H17 and H17/H18 along with key HMBC correlations from H29 methyl (δ_H 2.08) to C13 (δ_C 169.7), C14 (δ_C 129.2) and C15 (δ_C 138.2; **Table 3.1**). The double bond configuration of the C16/C17 was assigned as *E* based on the H16/H17 proton-proton coupling constant of 15.2 Hz. The configuration of the double bond between C14/C15 was assigned as *Z* based on the chemical shift of C29 (δ_C 20.2). [20] COSY correlations from H18/H19 and H30, H19/H20, H20/H21 and H31, H21/H22, H22/ H23 and H32 established fragment C18- C23. To assign the bicyclic ketal found in **9** HMBC and COSY correlations were needed. Interpretation of HMBC correlations from H27 (δ_H 1.78-1.83) to C26 (δ_C 24.6); from H25 (δ_H 4.22) to C28 (δ_C 106.1); from methyl singlet at δ_H 1.39 to a quaternary carbon with an indicative chemical shift (δ_C 106.1) of a ketal functionality and to C27 (δ_C 34.8) allowed the assembly of the bicyclic system. COSY correlations from H23/H24, H24/H25 and H33, H25/H26 allowed the connection of the bicyclic system to the polyketide side chain of **9**.

Table 3.1 1D and 2D NMR data of rifsaliniketal (**9**) in CD_3OD

No.	δ_H, mult. (*J* in Hz)	δ_C	COSY	HMBC
1				
2		141.3 qC		3
3	7.66, s	117.6 CH		2, 4, 10
4		184.0 qC		3
5				
6		162.8 qC		12
7		117.6 qC		12
8				
9				
10		128.8 qC		3
11				
12	2.16, s	8.0 CH_3		6, 7
13		169.9 qC		15, 29
14		129.5 qC		29
15	6.46, d (11.2)	138.2 CH	16, 29	13, 17, 29
16	6.78, dd (11.2,15.2)	127.5 CH	15, 17	14, 15, 18
17	6.02, dd (8.0,15.2)	145.6 CH	16, 18	15, 18, 19, 30
18	2.42, ddq (9.1,8.0,6.9)	42.2 CH	17, 19, 30	16, 17, 19, 30
19	3.77,dd (9.1,1.4)	75.6 CH	18, 20	17, 18, 20, 21,30,31
20	1.86-1.89 m	36.0 CH	19, 21, 31	21, 31
21	3.51, dd (8.3,4.3)	78.1 CH	20, 22	19, 22
22	1.83-1.86 m	36.9 CH	21, 23, 32	21, 32
23	3.95, dd (10.6,1.1)	74.9 CH	22, 24	21, 22, 32, 33
24	1.97-2.01,m	35.2 CH	23, 25, 33	
25	4.22, dd (6.7,3.4)	81.5 CH	24, 26	23, 28
26a	1.89-1.93, m	24.8 CH_2	25	24, 25, 27
26b	1.93-1.97, m			
27a	1.78-1.83, m	35.1 CH_2		26
27b	2.01-2.05, m			
28		106.4 qC		25,34
29	2.08, s	20.5 CH_3	15	13,14,15
30	0.99, d (6.9)	16.9 CH_3	18	17,18,19
31	1.01, d (7.2)	11.1 CH_3	20	19,20,21
32	0.89, d (7.0)	10.3 CH_3	22	21,22,23
33	0.73, d (6.9)	12.8 CH_3	24	23,24,25
34	1.39, s	24.2 CH_3		27,28

In addition, by means of a powerful technique that allows the homonuclear decoupling of multiple neighboring protons simultaneously, we were able to obtain coupling constants on H18. [21] The proton on C18 is coupled to three distinct sets of protons giving rise to a ddq.

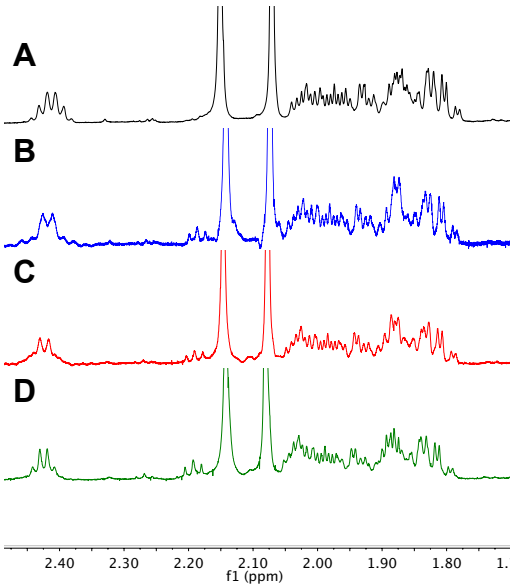

Figure 3.5. ^{1}H NMR of rifsaliniketal in CD_3OD. **A**. ^{1}H NMR of **9**. **B**. Decoupling of H17 and H30. **C.** Homonuclear decoupling of H19 and H30.**D.** Decoupling of H17 and H19.

Application of the homonuclear decoupling to H17 and H30 causes H18 to collapse to a doublet with coupling to H19 (9.1 Hz). Additional decoupling of H19 and H30 collapsed H18 to a doublet coupled to H17 (8.0 Hz). Finally, decoupling of H17 and H19 collapse it down to a quartet coupled to H30 (6.9 Hz; **Figure 3.5**). The technique was only utilized for H18 since it was not possible to obtain coupling constant information on other multiplets found in the molecule due to small coupling constants.

One of the challenges of solving the structure of **9** was the lack of protons in the naphthoquinone ring, making it difficult to confidently assess the functionality at position 11 (**Figure 3.4**). Based on the HIRESMS it was predicted that a carboxylic acid was present at this position. Initially, crystallization of **9** was attempted using different combinations of solvents (methanol and chloroform or acetone, methanol and chloroform or methanol and toluene), however in every case the crystals were too thin to diffract. Another alternative was to convert the carboxylic acid into its methyl ester derivative (**10**) using CH_2N_2; unfortunately the desired compound was not present possibly due to the decomposition of the reagent prior to using in the reaction. Changing to TMS-CHN_2 (**Scheme 3.2**) the reaction proceeded smoothly to afford the methyl ester derivative **10**, purified by HPLC. The presence of a methyl peak on the proton NMR (δ_H 3.87) and a mass indicative of the methyl ester derivative ($[M + Na]^+$: m/z 678.3) together with an HMBC correlation of the resulting methyl ester to the carbonyl carbon (δ_C 172.6) validated our suspicion that in fact there was a carboxylic acid present (**Figure 3A.9 and 3A.10**).

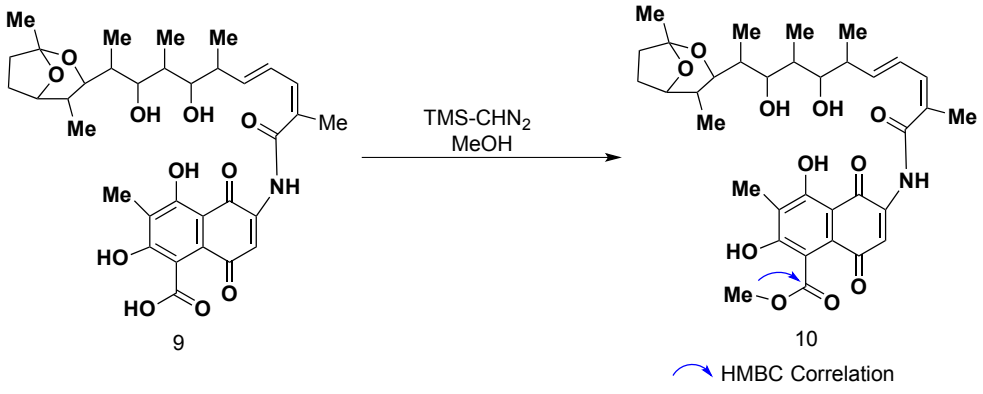

Scheme 3.2. Esterification of carboxylic acid found in rifsaliniketal using TMS-CHN_2.

Several 20-liter fermentations have been purified in an attempt to isolate more material of polyketide **9** for biological studies, however we have not been able to obtain more of the needed compound. This can be explained by the rapid conversion of rifsaliniketal into the saliniketals and why our group and others have had difficulty in isolating this natural product.[17] In agreement with this statement, one-liter fermentations were extracted using ethyl acetate: water at different time points (3, 5, 7 and 9 days) with the idea of observing whether rifsaliniketal would accumulate prior to its conversion to saliniketal and analyzed by LC-MS.

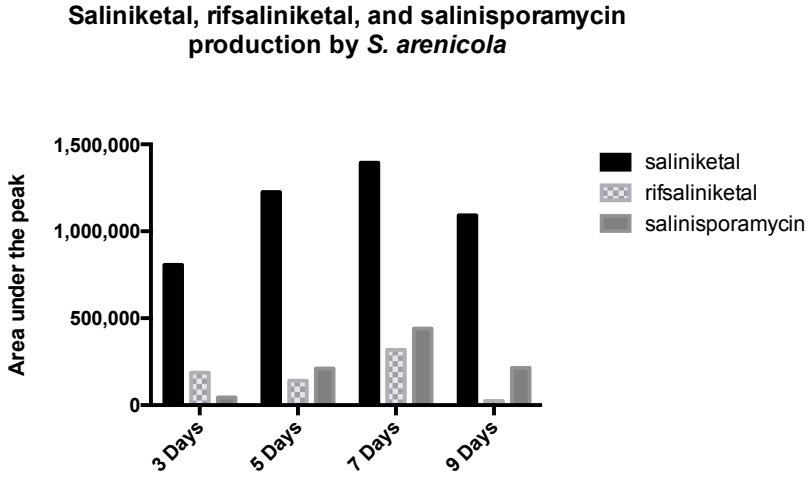

Figure 3.6. Saliniketal, rifsaliniketal and salinisporamycin production over 3, 5, 7 and 9 days

From the crude extract the corresponding mass for rifsaliniketal, salinisporamycin A and saliniketal A were all present at all time points assessed suggesting that rifsaliniketal is being rapidly converted to saliniketal (**Figure 3.6**). Additionally, the Moore group did not identify a gene associated with the conversion of rifsaliniketal to salinisporamycin in the biosynthetic gene cluster of rifamycin, suggesting that perhaps if this reaction is catalyzed by

an enzyme it is encoded outside the rifamycin biosynthetic pathway.[17] In accordance with the previous statement only trace amounts of salinisporamycin are present by LC-MS in our rifsaliniketal sample after several months of sitting in a flask, suggesting rifsaliniketal is highly stable (**Figure 3A.11**).

3.2.2 Biological activity of rifsaliniketal

The antimicrobial activity of **9** and **10** were investigated by disk diffusion assay against two strains of bacteria, *Pseudomonas aeruginosa* and *Bacillus subtilis,* gram-negative and gram-positive bacteria, respectively. Due to lack of availability of the compound, the highest concentration that could be tested was 2 mg ml^{-1}. Despite the similar structural characteristics with rifamycin, we were not able to detect antimicrobial activity neither of **9** nor of its methyl esther derivative (**10**) against these two bacterial strains (**Table 3A.1**). The lack of antimicrobial activity of **9** and **10** may be attributed to the absence of one of the four free hydroxyl groups (C1, C8, C21 and C23) found in rifamycin. These alcohols are involved in hydrogen bonding with the DNA-dependent RNA polymerase of prokaryotes; this interaction is responsible for rifamycin's activity. [22] Further biological studies are underway pending the total synthesis of rifsaliniketal, salinisporamycin and saliniketal by the group of Dr. Jef De Brabander.

Conclusion

3.3 Rifsaliniketal an important intermediate in the biosynthesis of saliniketal

In conclusion, we have isolated a novel polyketide with structural similarities to saliniketal and rifamycin. Structural elucidation was achieved by COSY, HMBC, and HSQC correlations. In addition, homonuclear decoupling experiments were performed for deconvolution of complex multiplets. Chemical derivatization of rifsaliniketal allowed the confirmation of its carboxylic acid moiety. The isolation of rifsaliniketal lends support to the proposed biosynthetic pathway of the saliniketals by the Moore group from a common starting unit diverging at 34a-deoxyrifamycin W to give the rifamycins or saliniketals. Biological activity was evaluated against two strains of bacteria and further biological testing is underway.

Experimental Section

3.4 Materials and methods

3.4.1 General procedure

^{1}H and 2D experiments were recorded at a 600 MHZ using MeOH-d_4 in a Varian spectrometer and chemical shifts were recorded based on the corresponding solvent signal (δ_H 3.31ppm and δ_C 49.0 ppm for MeOH-d_4). ^{13}C was acquired in a 125 MHz on a Varian spectrometer. UV spectra were recorded on a Shimadzu UV-1601 UV–VIS spectrophotometer. High resolution ESI-TOF mass spectra were provided by The Scripps Research Institute, La Jolla, CA. Low-resolution LC/ESI-MS data were measured using an

Agilent 1200 series LC/MS system with a reversed- phase C18 column (Phenomenex Luna, 150 mm × 4.6 mm, 5 μm) at a flow rate of 0.7 mL/min. Semi-preparative HPLC was performed on an Agilent 1200 series, using a Phenyl-Hexyl column (Phenomenex Luna, 250 ×10.0 mm, 5 μm).

3.4.2 Collection and phylogenetic analysis of strain SNB-003

The marine-derived bacterium strain SNB-003, was isolated from sediment sample collected from Trinity Bay, Galveston, TX (29° 42.419'N, 94° 49165' W). Bacterial spores were collected via stepwise centrifugation as follows: 2 g of sediment was dried over 24 h in an incubator at 35 °C and the resulting sediment added to 10 mL sH2O containing 0.05% Tween 20. After a vigorous vortex for 10 min, the sediment was centrifuged at 18000 rpm for 25 min (4 °C) and the resulting spore pellet collected. The resuspended spore pellet (4 mL sH2O) was plated on an acidified Gauze media, giving rise to individual colonies of SNB-003 after two weeks. Analysis of the 16S rRNA sequence of SNB-003 revealed 98% identity to *Salinospora arenicola.*

3.4.3 Cultivation and extraction

Bacterium SNB-003 was cultured in 120 × 2.8 L Fernbach flasks each containing 1 L of a seawater based medium (10 g starch, 4 g yeast extract, 2 g peptone, 1 g $CaCO_3$, 40 mg

$Fe_2(SO_4)_3 \cdot 4H_2O$, 100 mg KBr) and shaken at 200 rpm at 27 °C. After seven days of cultivation, sterilized XAD-7-HP resin (20 g/L) was added to adsorb the organic products, and the culture and resin were shaken at 200 rpm for 2 h. The resin was filtered through cheesecloth, washed with deionized water, and eluted with acetone. The acetone soluble fraction was dried in vacuo to yield 22.1g of extract.

3.4.4 Isolation

The dried crude extract (SNB-003) obtained from the actinomycete *Salinispora arenicola* (22.1 g) was purified using solvent partition (MeOH) , the methanol soluble portion (16.0 g) was further partitioned using EtOAc and H_2O (1:1 mixture). The ethyl acetate layer (2.2g) was purified via reversed phase flash column chromatography, eluting with a step gradient of H_2O and MeOH (90:10-100:0) collecting 12 fractions. Fraction 12 (89.5 mg) was purified by reversed phase HPLC (Phenomenex Luna, Phenyl-Hexyl, 250×10 mm, 2.5 ml/min, 5µm, UV=254nm) using a gradient solvent system from 20% to 100% CH_3CN (+ 0.1% formic acid) over 20 min, collecting 11 fractions. Fraction 4 (8.7 mg) was further purified by reversed phase HPLC (Phenomenex Luna, Phenyl-Hexyl, 250×10 mm, 2.5 ml/min, 5µm, UV=254nm), a gradient solvent system was utilized (10% to 100% CH_3CN + 0.1% formic acid over 26 min) to give 3SNB-003-12-4-4 (1.79mg).

Rifsaliniketal (**9**, 1.70 mg) yellow solid; UV (MeOH) λ_{max} (log ε) 216 (3.80), 281 (3.71), 338 (3.73), 433 (3.44) ; ^{1}H NMR (600 MHz, MeOH-d_4) and ^{13}C NMR (125 MHz, MeOH-d_4) see **Table 3.1**. ESI-MS *m*/*z* 664.2 $[M + Na]^+$, 640.2 $[M - H]^-$. HRESIMS *m*/*z*

642.2901 $[M + H]^+$ ($C_{34}H_{44}NO_{11}$, calcd 642.2908); 664.2713 $[M + Na]^+$ ($C_{34}H_{43}NO_{11}Na$, calcd 664.2728).

3.4.5 MDEC experiment

MDEC experiment was performed using the procedure found in Espindola et al. [21]

*3.4.6 Esterification of carboxylic acid from **9***

To a solution of **9** (0.37 mg, 0.57 μmol) dissolved in dry methanol (300 μL) was added TMS-CH_2N_2 (0.6 μL) and was let to stir for 15 mins the reaction was stopped due to the appearance of undesired products. Reaction mixture was dried under nitrogen and was purified by reverse phase HPLC (Phenomenex Luna, C18, 150 mm × 4.6 mm, 5 μm) isocratic conditions were utilized (58% CH_3CN + 0.1% formic acid over 15 min) followed by a gradient system from 58% to 100% CH_3CN + 0.1% formic acid over 8 min to give **10** (0.20mg, 53% yield). Rotamers were present in the sample in an approximate ratio of 0.6:0.4. Signals are of the major rotamer . ^{1}H NMR (600 MHz, MeOH-d_4) δ 7.44 (s, 1H), 6.78 (dd, *J*=11.2 Hz, 15.2 Hz, 1H), 6.48 (d, *J*=11.2, 1H), 6.04 (dd, *J*= 8.0 Hz, 15.2 Hz, 1H), 4.21 (dd, *J* = 6.7 Hz, 3.4 Hz, 1H), 3.94 (d, *J* = 10.5 Hz, 1H), 3.87 (s, 3H), 3.79 (d, *J* = 9.1 Hz, 1H), 3.51 (dd, 8.3 Hz, 4.3 Hz, 1H), 2.43 (m, 1H), 2.07(s, 3H), 2.01 (s, 3H), 1.78-1.83 (m, 1H), 1.83-1.86 (m, 1H), 1.86-1.89 (m, 1H), 1.89-1.93 (m, 1H), 1.93-1.97 (m, 1H), 1.97-2.01(m, 1H), 2.01-2.05 (m, 1H), 1.39 (s, 3H), 1.01 (d, 7.3 Hz, 3H), 0.99 (d, 7.3 Hz, 3H), 0.89 (d, 7.1 Hz,

3H), 0.71(d, 6.9 Hz, 3H). ESI-MS *m/z* 678.3 $[M + Na]^+$, 654.2 $[M - H]^-$

3.4.7 Quantification of production of saliniketal, rifsaliniketal and salinisporamycin

Bacterium SNB-003 was cultured in 2.8 L Fernbach flasks each containing 1 L of a seawater based medium (10 g starch, 4 g yeast extract, 2 g peptone, 1 g $CaCO_3$, 40 mg $Fe_2(SO_4)_3 \cdot 4H_2O$, 100 mg KBr) and shaken at 200 rpm at 27 °C. After each time point (3, 5, 7, and 9 days) of cultivation, sterilized XAD-7-HP resin (20 g/L) was added to adsorb the organic products, and the culture and resin were shaken at 200 rpm for 2 h. The resin was filtered through cheesecloth, washed with deionized water, and eluted with acetone. The acetone soluble fraction was dried *in vacuo*. The crude was extracted with ethyl acetate (4 x 50 ml) and the organic layer was concentrated *in vacuo*. A stock solution was prepared (50 mg/mL in methanol) and further diluted to 10 mg/mL for LC-MS analysis. Single –ion mode was utilized to analyze samples for ions of: saliniketal (*m/z* 418 $[M + Na]^+$, 440 [M + formic acid- H]$^-$), rifsaliniketal (*m/z* 664 $[M + Na]^+$, 640 $[M - H]^-$) and salinisporamycin (*m/z* 620 $[M + Na]^+$, 596 $[M - H]^-$) the negative ion peak was integrated.

3.4.8 Antibiotic disk diffusion assay

Freezer stocks of *Pseudomonas aeruginosa* and *Bacillus subtilis* were grown in LB

media. Once the culture reached an acceptable density a cotton tip was submerged into the culture and was spread out in the agar to create a lawn of bacteria. Disks were inoculated with 10μL of a 2mg ml^{-1} methanol solution of compounds **9** and **10**. After overnight incubation the zone of inhibition was measured.

References

1. Jensen, P. R.; Mafnas, C., Biogeography of the marine actinomycete Salinispora. *Environmental microbiology* **2006,** *8* (11), 1881-8.
2. Feling, R. H.; Buchanan, G. O.; Mincer, T. J.; Kauffman, C. A.; Jensen, P. R.; Fenical, W., Salinosporamide A: A highly cytotoxic proteasome inhibitor from a novel microbial source, a marine bacterium of the new genus Salinospora. *Angew Chem Int Edit* **2003,** *42* (3), 355-+.
3. Gerwick, W. H.; Moore, B. S., Lessons from the past and charting the future of marine natural products drug discovery and chemical biology. *Chemistry & biology* **2012,** *19* (1), 85-98.
4. Buchanan, G. O.; Williams, P. G.; Feling, R. H.; Kauffman, C. A.; Jensen, P. R.; Fenical, W., Sporolides A and B: structurally unprecedented halogenated macrolides from the marine actinomycete Salinispora tropica. *Organic letters* **2005,** *7* (13), 2731-4.
5. Williams, P. G.; Miller, E. D.; Asolkar, R. N.; Jensen, P. R.; Fenical, W., Arenicolides A-C, 26-membered ring macrolides from the marine actinomycete Salinispora arenicola. *The Journal of organic chemistry* **2007,** *72* (14), 5025-34.
6. Oh, D. C.; Williams, P. G.; Kauffman, C. A.; Jensen, P. R.; Fenical, W., Cyanosporasides A and B, chloro- and cyano-cyclopenta[a]indene glycosides from the marine actinomycete "Salinispora pacifica". *Organic letters* **2006,** *8* (6), 1021-1024.
7. Udwary, D. W.; Zeigler, L.; Asolkar, R. N.; Singan, V.; Lapidus, A.; Fenical, W.; Jensen, P. R.; Moore, B. S., Genome sequencing reveals complex secondary metabolome in the marine actinomycete Salinispora tropica. *Proc Natl Acad Sci U S A* **2007,** *104* (25), 10376-81.
8. Williams, P. G.; Asolkar, R. N.; Kondratyuk, T.; Pezzuto, J. M.; Jensen, P. R.; Fenical, W., Saliniketals A and B, bicyclic polyketides from the marine actinomycete Salinispora arenicola. *Journal of natural products* **2007,** *70* (1), 83-8.
9. Jensen, P. R.; Williams, P. G.; Oh, D. C.; Zeigler, L.; Fenical, W., Species-specific secondary metabolite production in marine actinomycetes of the genus Salinispora. *Appl Environ Microbiol* **2007,** *73* (4), 1146-52.
10. Penn, K.; Jenkins, C.; Nett, M.; Udwary, D. W.; Gontang, E. A.; McGlinchey, R. P.; Foster, B.; Lapidus, A.; Podell, S.; Allen, E. E.; Moore, B. S.; Jensen, P. R., Genomic islands link secondary metabolism to functional adaptation in marine Actinobacteria. *The ISME journal* **2009,** *3* (10), 1193-203.
11. Gerner, E. W.; Meyskens, F. L., Jr., Polyamines and cancer: old molecules, new understanding. *Nature reviews. Cancer* **2004,** *4* (10), 781-92.
12. Pendeville, H.; Carpino, N.; Marine, J. C.; Takahashi, Y.; Muller, M.; Martial, J. A.; Cleveland, J. L., The ornithine decarboxylase gene is essential for cell survival during early murine development. *Molecular and cellular biology* **2001,** *21* (19), 6549-58.
13. Chang, Z. F.; Chen, K. Y., Regulation of ornithine decarboxylase and other cell cycle-dependent genes during senescence of IMR-90 human diploid fibroblasts. *J Biol Chem* **1988,** *263* (23), 11431-5.

14. Bello-Fernandez, C.; Packham, G.; Cleveland, J. L., The ornithine decarboxylase gene is a transcriptional target of c-Myc. *Proceedings of the National Academy of Sciences of the United States of America* **1993,** *90* (16), 7804-8.
15. Kelloff, G. J.; Boone, C. W.; Crowell, J. A.; Steele, V. E.; Lubet, R.; Sigman, C. C., Chemopreventive drug development: perspectives and progress. *Cancer epidemiology, biomarkers & prevention : a publication of the American Association for Cancer Research, cosponsored by the American Society of Preventive Oncology* **1994,** *3* (1), 85-98.
16. (a) Liu, J.; De Brabander, J. K., A concise total synthesis of saliniketal B. *Journal of the American Chemical Society* **2009,** *131* (35), 12562-3; (b) Yadav, J. S.; Hossain, S. S.; Madhu, M.; Mohapatra, D. K., Formal total synthesis of (-)-saliniketals. *The Journal of organic chemistry* **2009,** *74* (22), 8822-5; (c) Paterson, I.; Razzak, M.; Anderson, E. A., Total synthesis of (-)-saliniketals A and B. *Organic letters* **2008,** *10* (15), 3295-8.
17. Wilson, M. C.; Gulder, T. A.; Mahmud, T.; Moore, B. S., Shared biosynthesis of the saliniketals and rifamycins in Salinispora arenicola is controlled by the sare1259-encoded cytochrome P450. *Journal of the American Chemical Society* **2010,** *132* (36), 12757-65.
18. Xu, J.; Wan, E.; Kim, C. J.; Floss, H. G.; Mahmud, T., Identification of tailoring genes involved in the modification of the polyketide backbone of rifamycin B by Amycolatopsis mediterranei S699. *Microbiology* **2005,** *151* (Pt 8), 2515-28.
19. Matsuda, S.; Adachi, K.; Matsuo, Y.; Nukina, M.; Shizuri, Y., Salinisporamycin, a novel metabolite from Salinispora arenicola. [corrected]. *The Journal of antibiotics* **2009,** *62* (9), 519-26.
20. Maxwell, A.; Rampersad, D., Novel Prenylated Hydroxybenzoic Acid-Derivatives from Piper-Saltuum. *Journal of natural products* **1989,** *52* (3), 614-618.
21. Espindola, A. P.; Crouch, R.; DeBergh, J. R.; Ready, J. M.; MacMillan, J. B., Deconvolution of complex NMR spectra in small molecules by multi frequency homonuclear decoupling (MDEC). *J Am Chem Soc* **2009,** *131* (44), 15994-5.
22. Floss, H. G.; Yu, T. W., Rifamycin-mode of action, resistance, and biosynthesis. *Chemical reviews* **2005,** *105* (2), 621-32.

APPENDIX 3A

Figure 3A.1 ^{1}H- NMR of **9** in MeOH-d_4. 600 MHz

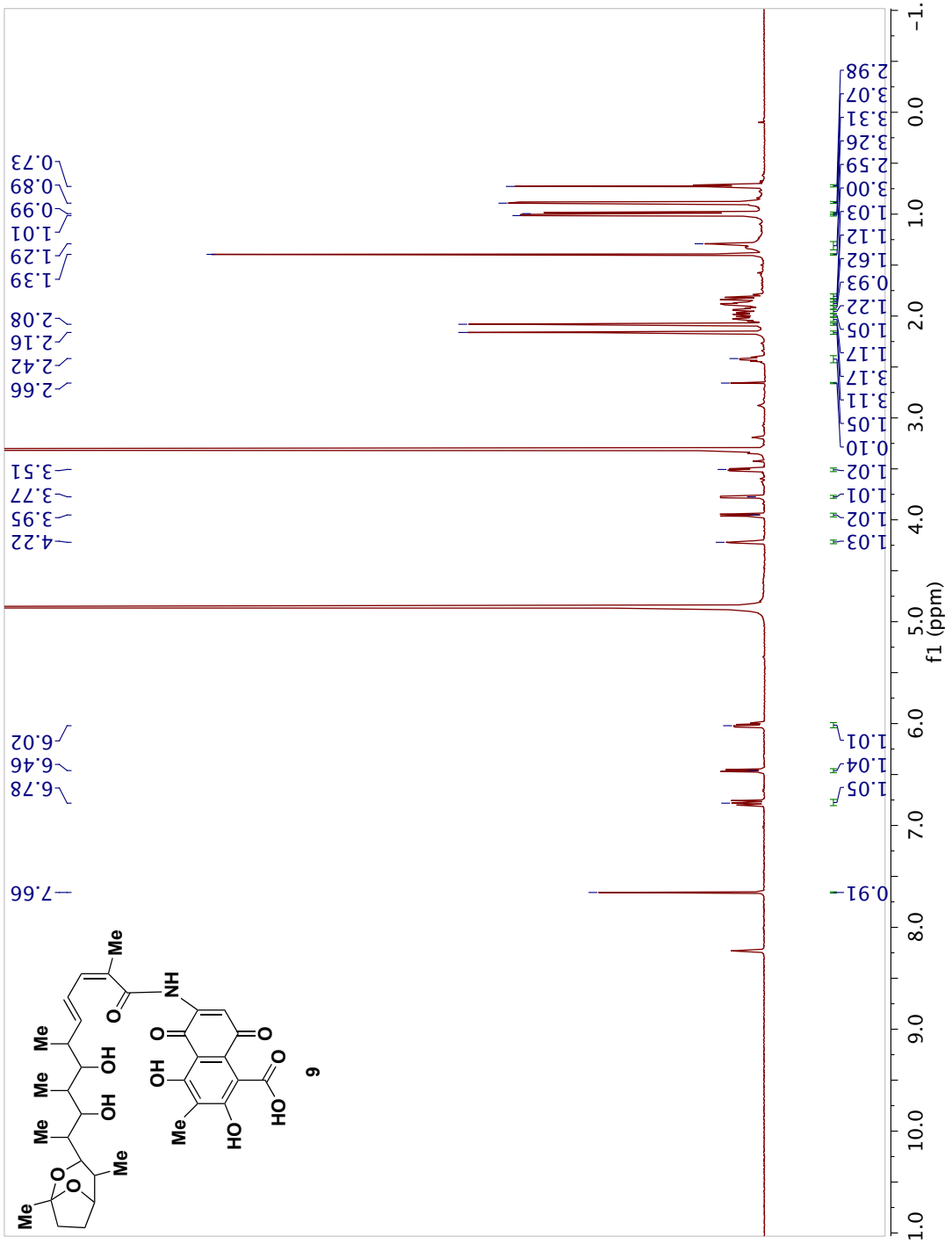

Figure 3A.2 ^{13}C- NMR of **9** in MeOH-d_4. 125 MHz

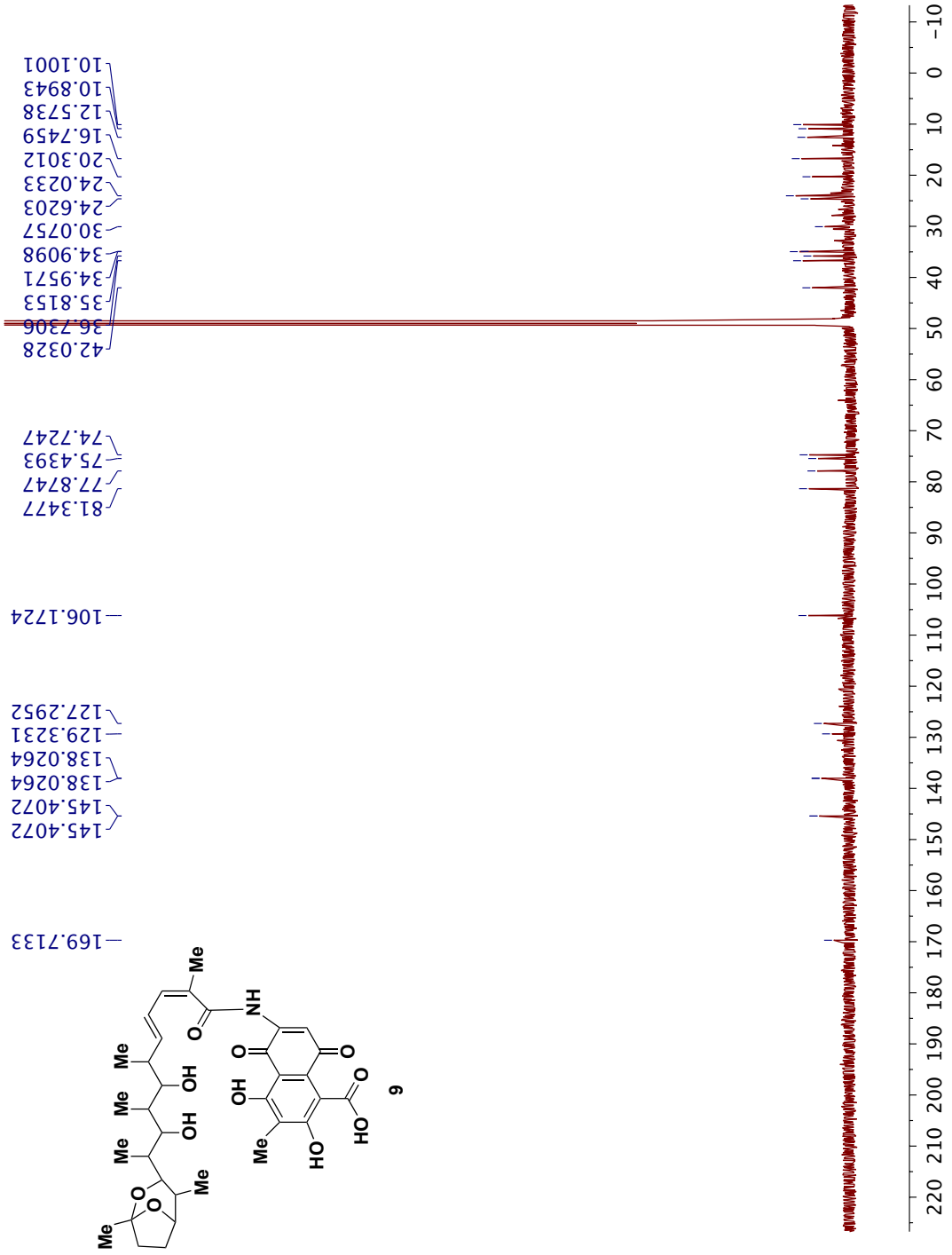

Figure 3A.3 gCOSY NMR of **9** in MeOH-d_4. 600 MHz

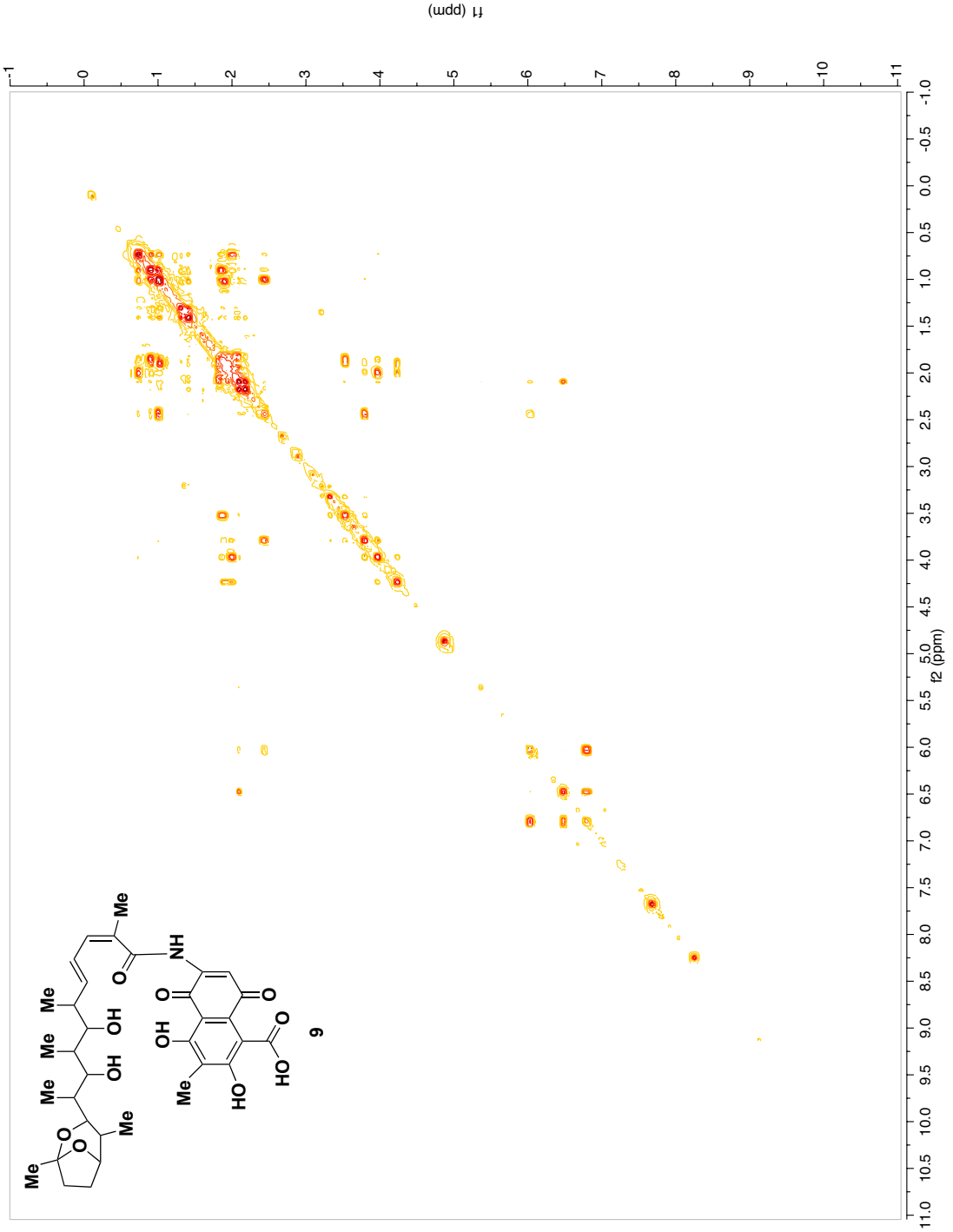

Figure 3A.4 gHSQC NMR of **9** in MeOH-d_4. 600 MHz

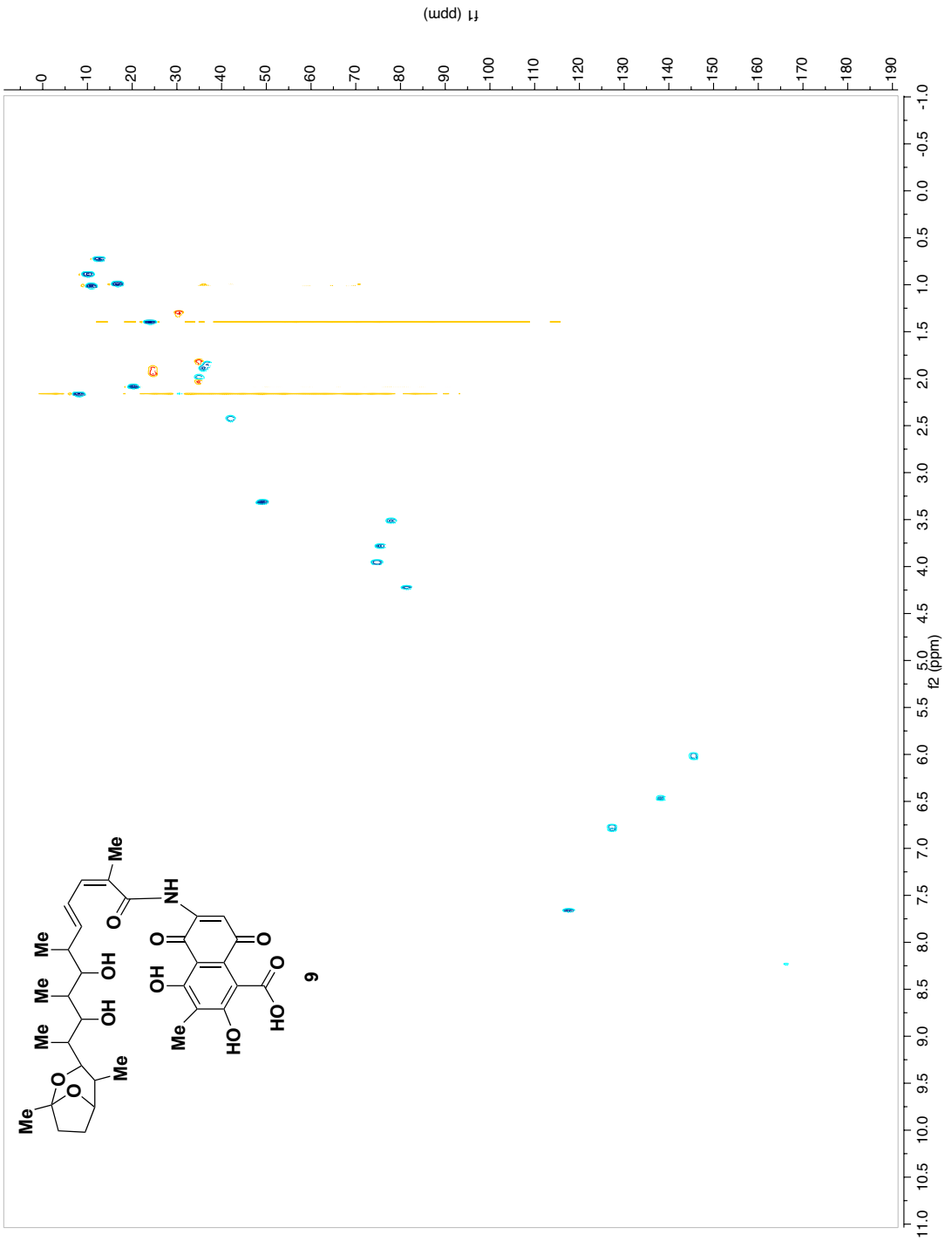

Figure 3A.5 gHMBC NMR of **9** in MeOH-d_4. 600 MHz

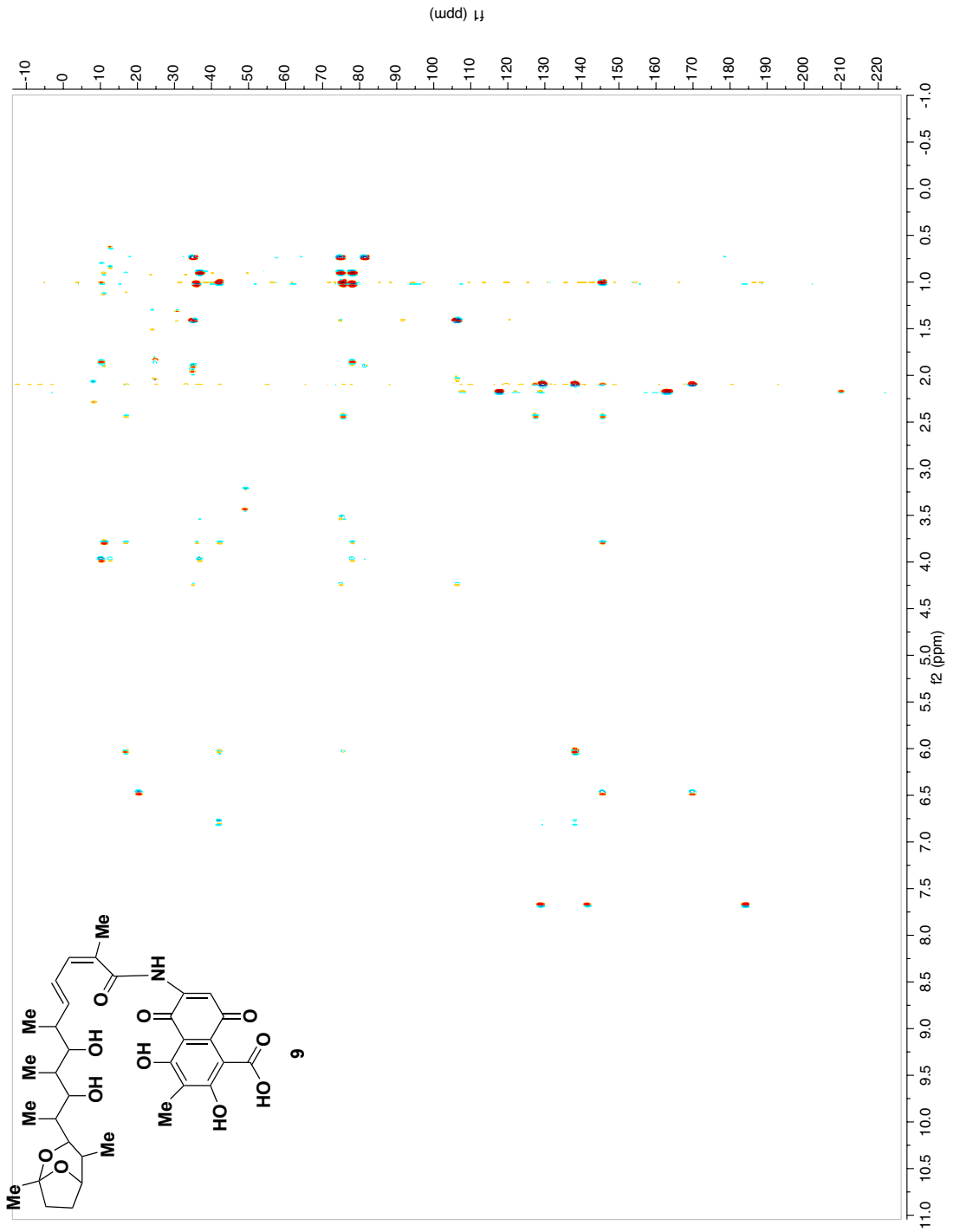

Figure 3A.6 Decoupling of H17 and H30 NMR of **9** in MeOH-d_4. 600 MHz

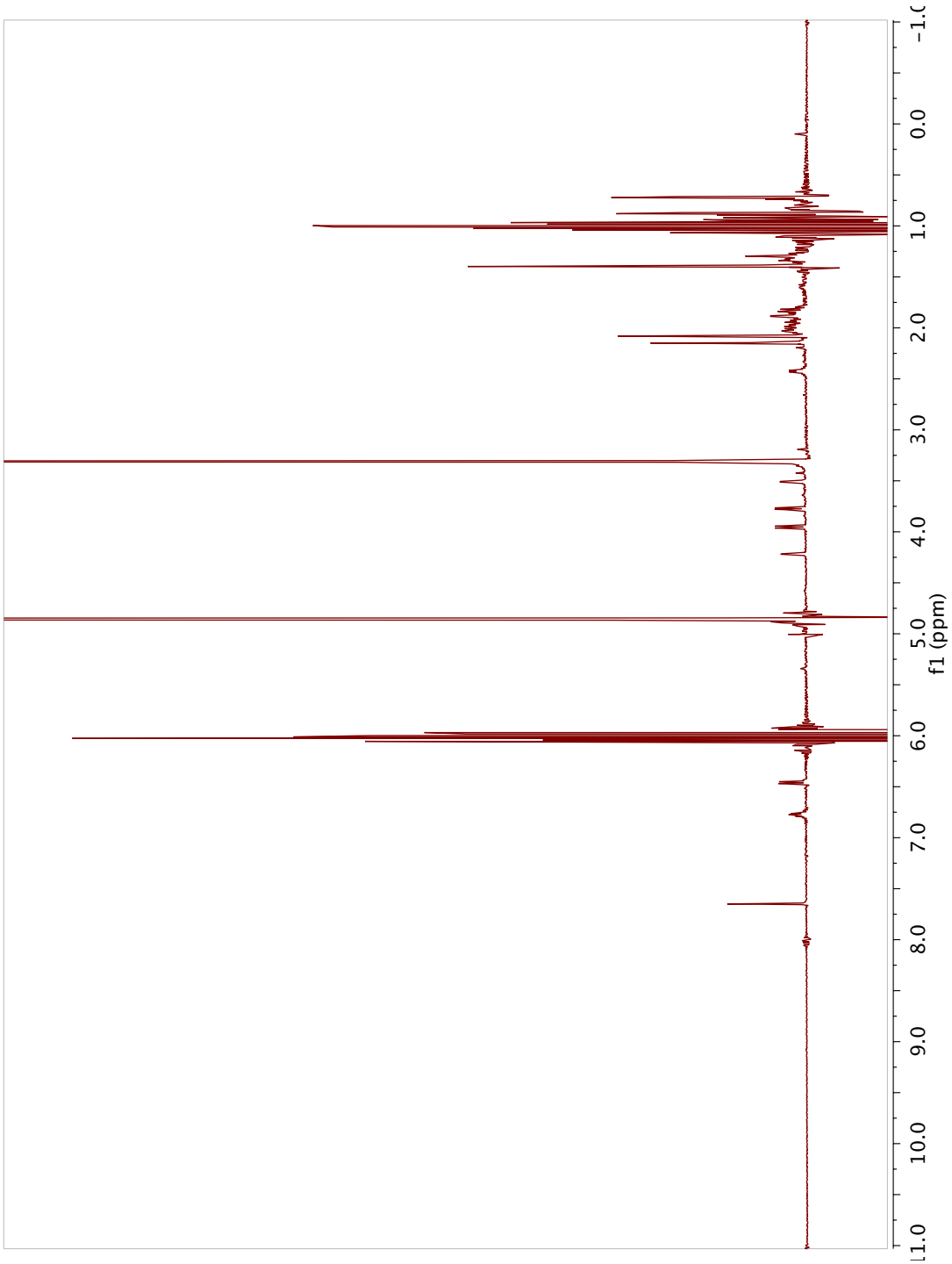

Figure 3A.7 Decoupling of H19 and H30 NMR of **9** in MeOH-d_4. 600 MHz

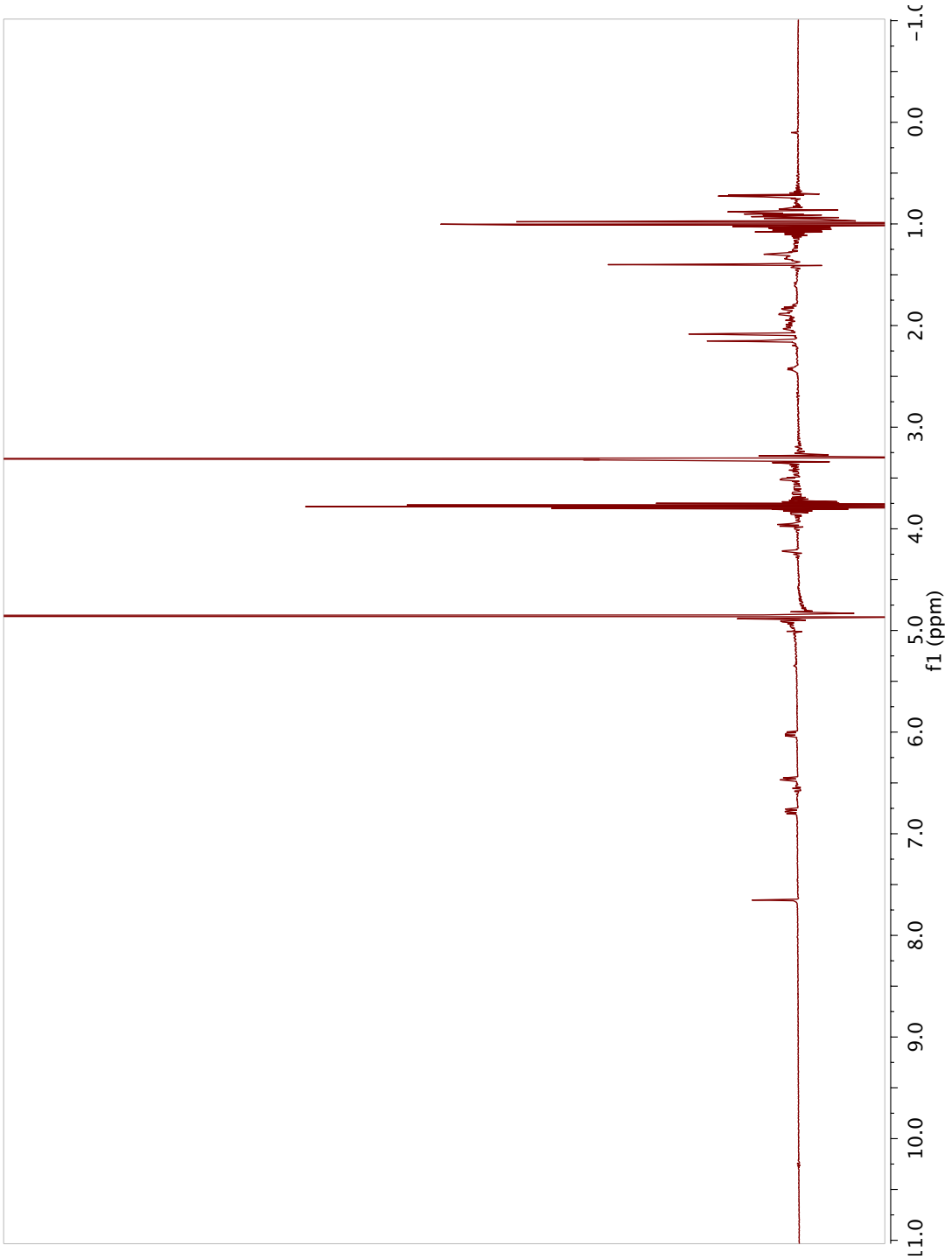

Figure 3A.8 Decoupling of H17 and H19 NMR of **9** in MeOH-d_4. 600 MHz

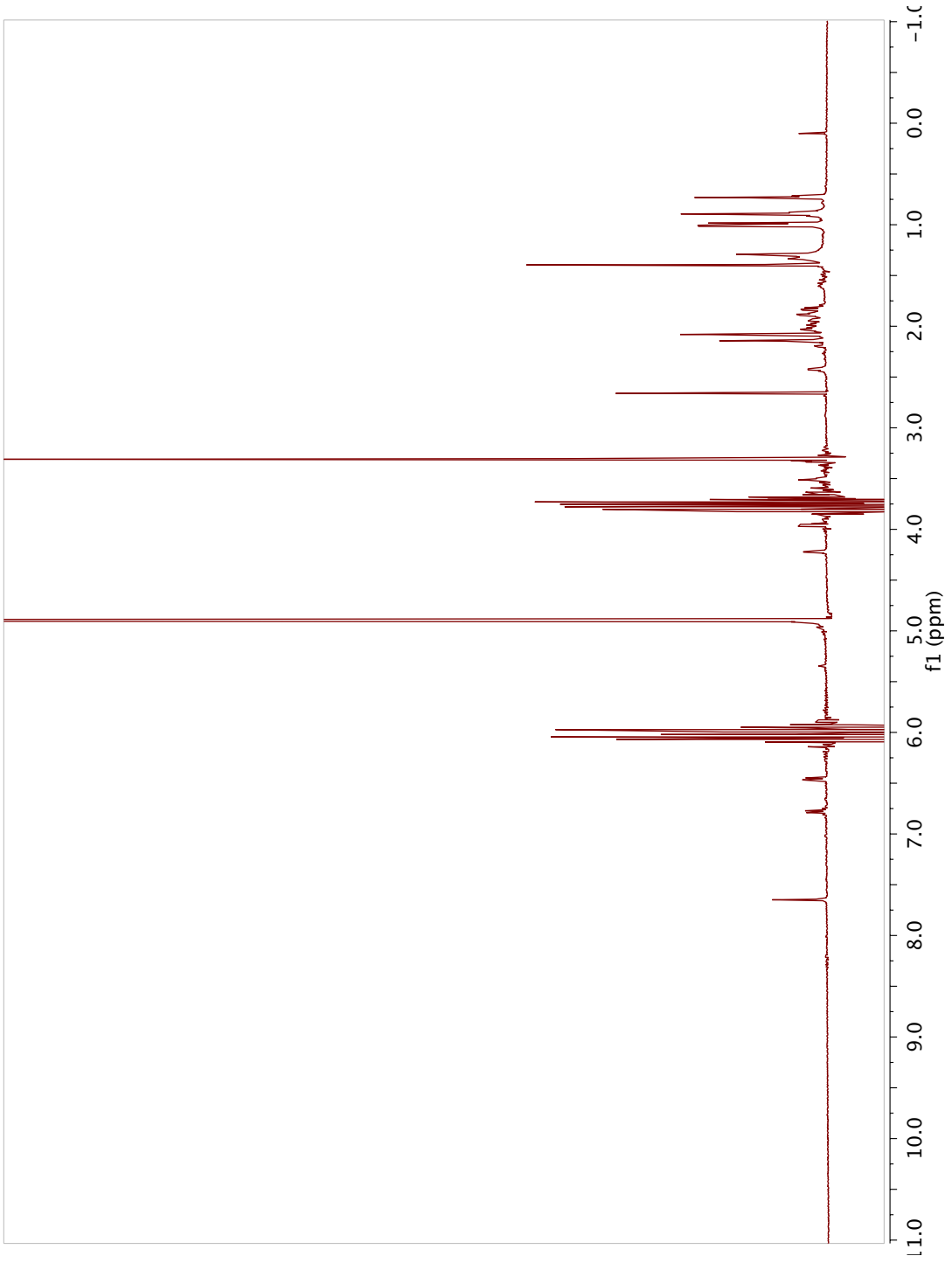

Figure 3A.9 ^{1}H NMR of **10** in MeOH-d_4. 600 MHz

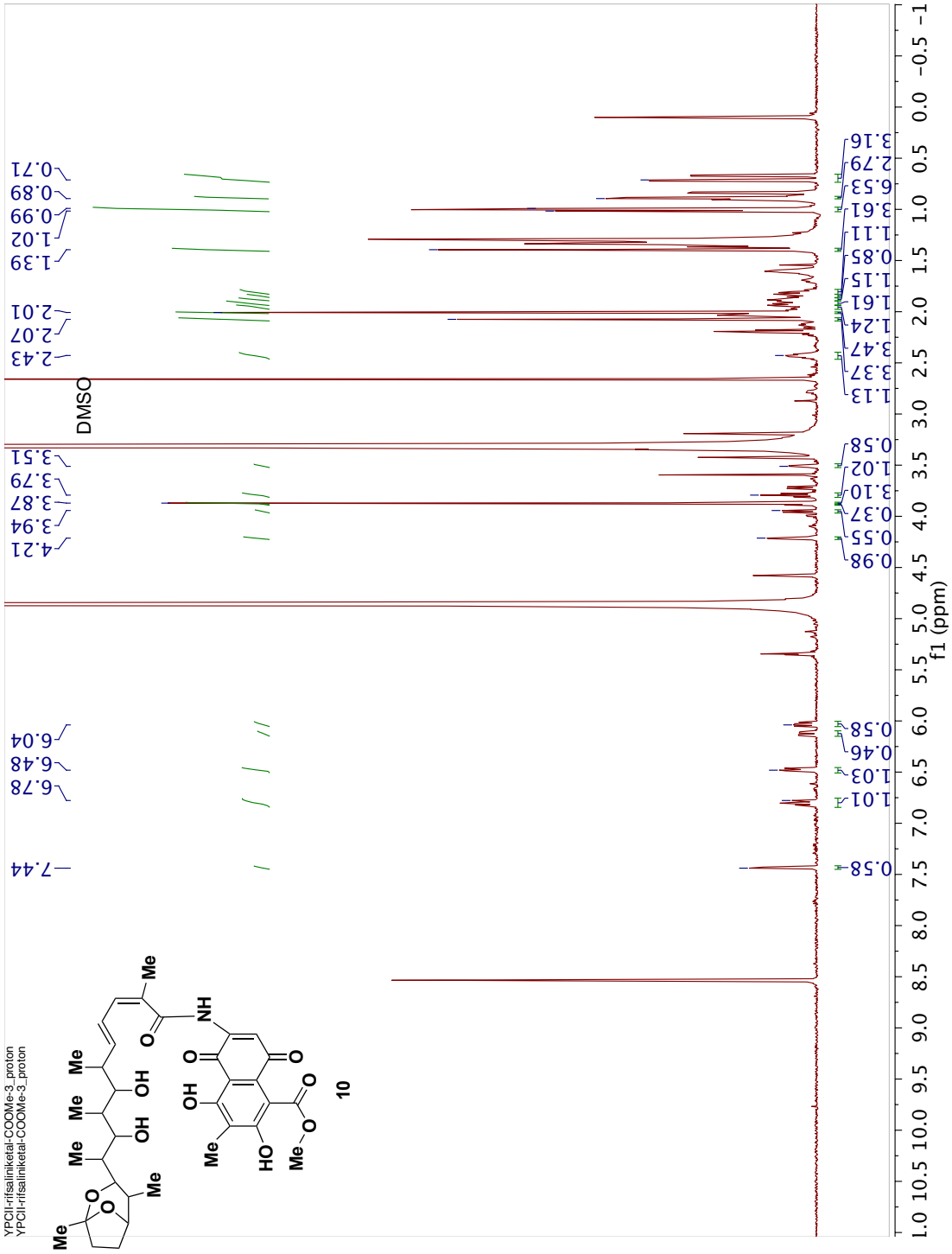

Figure 3A.10 HMBC NMR of **10** in MeOH-d_4. 600 MHz

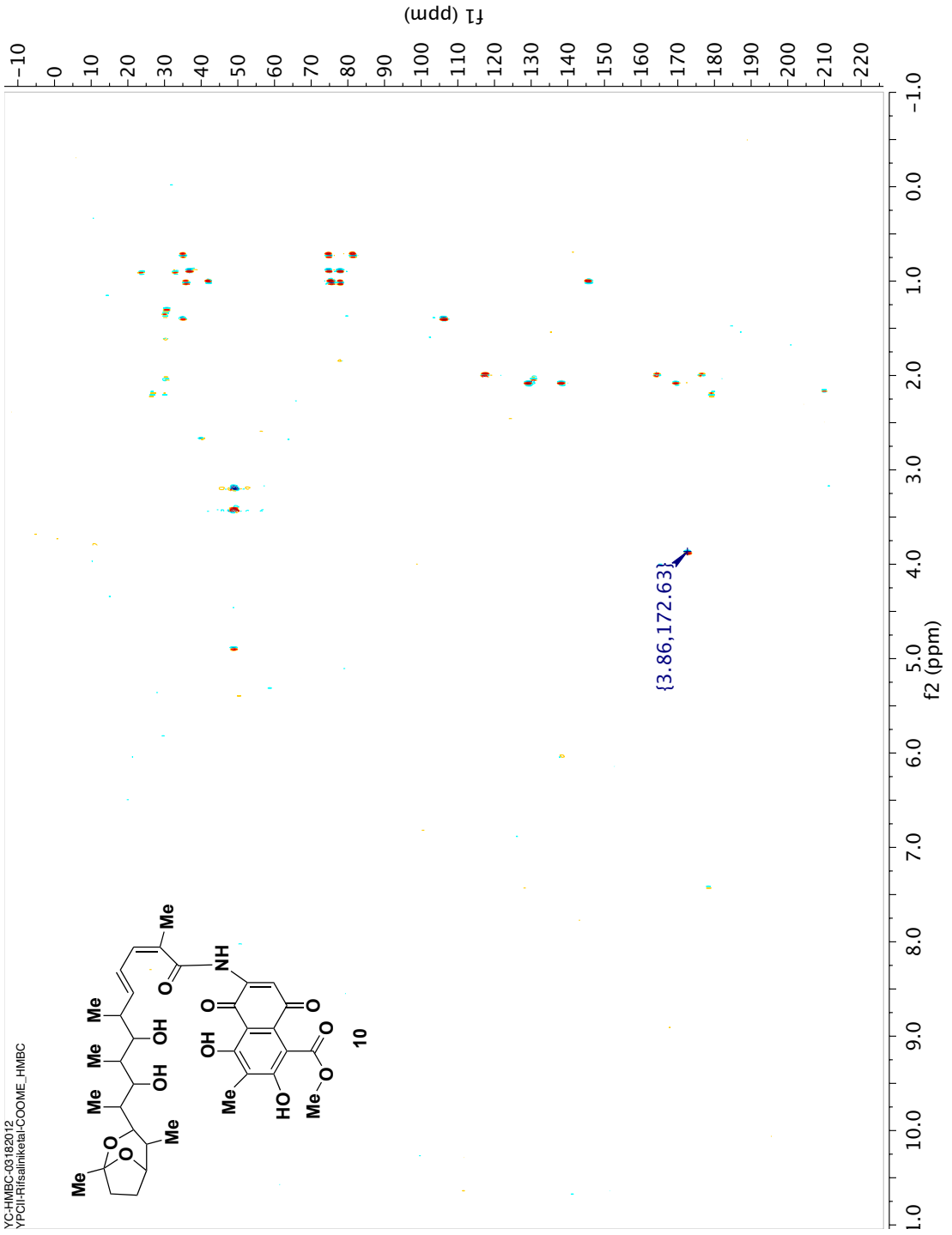

Table 3A.1 Disk diffusion assay of **9** and **10**. Diameter of inhibition in mm, including the disk zone of 6.0 mm, each compound was tested at a concentration of 2 mg/ml**.**

Strain	Rifsaliniketal	Rifsaliniketal-COOMe
P. aeruginosa	0.0	0
B. subtilis	0.0	6.0

Figure 3A.11 Stability of rifsaliniketal. **A**. LC- chromatograph of rifsaliniketal at 254nM. **B.** Ion extraction for $[M\text{-}H]^-$ 596 and $[M+H]^+$ 620 corresponding to salinisporamycin.

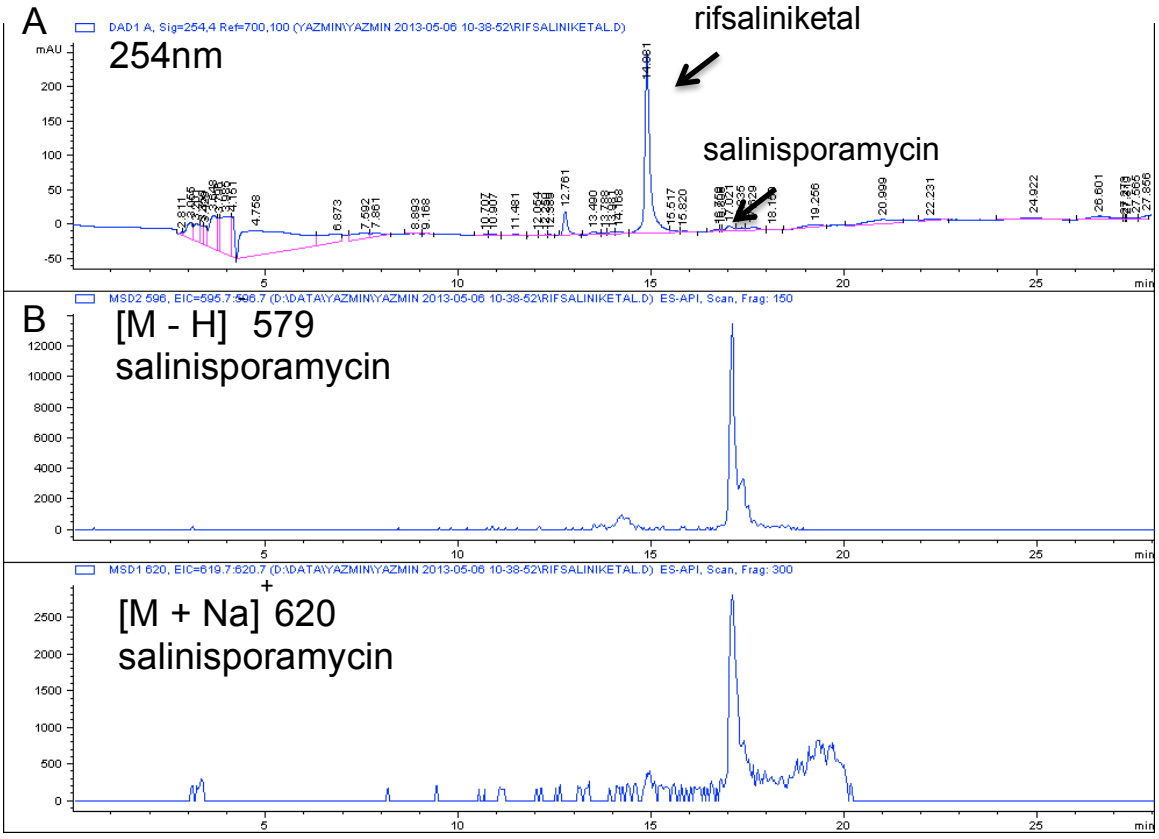

CHAPTER FOUR
Introduction

AN OUTLOOK ON THE INHIBITION OF CRM1 BY LEPTOMYCIN B

RESULTS/DATA IN THIS CHAPTER WERE OBTAINED WITH PERMISSION FROM PROCEEDINGS OF THE NATIONAL ACADEMY OF SCIENCES. *PNAS*. 2013, 110 (4), 1303-1308

4.1 Nuclear transport

The transport of macromolecules across the nuclear pore complex (NPC) is very important for the adequate functioning of eukaryotic cells. For example, transcription factors need to be translocated from the cytoplasm to the nucleus in order to regulate gene expression. [1] The shuttle of information through the NPC can be achieved by passive diffusion where small molecules, metabolites and ions are able to freely travel trough the nuclear envelope, and by an energy-dependent process where the NPC regulates the transport of macromolecules inside and outside the nucleus. This process is achieved by the interaction of macromolecules with specialized proteins called nuclear transport factors (NTF). The great majority of NTFs belong to the family of karyopherins. [2]

4.1.1 Nuclear export/import by karyopherins

Karyopherins (importins, exportins or transportins) are divided into two classes: 1) importins when they shuttle cargo from the cytoplasm into the nucleus and 2) exportins when they transport cargo from the nucleus to the cytoplasm. Ran-GTPase regulates the overall process of nuclear import and export by promoting the karyopherin's association or dissociation from its cargo.[3] In the cytoplasm, Ran is only found in its GDP-bound form, whereas in the nucleus it is found in its GTP-bound state. [4] The intrinsic ability of Ran to

hydrolyze GTP into GDP is achieved at a very slow rate; however cytoplasmic proteins Ran-GAP and RanBP1 can enhance this ability resulting in the conversion of Ran-GTP into Ran-GDP. [4] On the contrary, conversion of Ran-GDP into Ran-GTP is mediated by nuclear protein RCC1. [4] This difference in Ran state modulates the ability of karyopherins to bind or release cargo macromolecules (**Scheme 4.1**).[3]

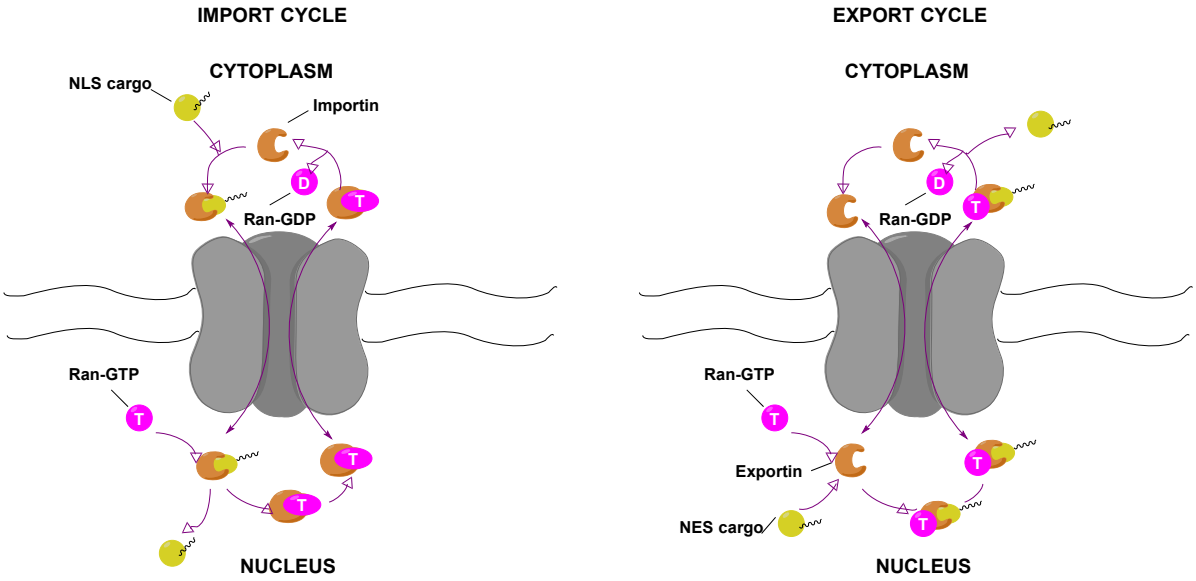

Scheme 4.1. Nucleocytoplasmic transport of cargo. [4]

The process of nuclear import is initiated in the cytoplasm where the concentration of Ran-GTP is low. A nuclear import receptor or importin is able to recognize its cargo via a nuclear localization signal (NLS), consisting of a short amino acid sequence containing mainly basic residues.[4] Upon binding of the importin to its cargo, this binary complex travels through the nuclear pore. Inside the nucleus, Ran-GTP binds to the importin-cargo complex causing a conformational change resulting in the release of its cargo. The importin-Ran-GTP complex is then recycled to the cytoplasm where Ran-GTP is hydrolyzed into Ran-GDP and the importin molecule is release to further interact with other cargo proteins (**Scheme 4.1**). [3-4]

Export of macromolecules is carried out in a similar fashion. Exportin identifies its cargo protein via a leucine-rich nuclear export signal (NES).[5] In the nucleus, binding of Ran-GTP to exportin allows for a better affinity towards the cargo protein, the newly formed ternary complex travels through the NPC where upon hydrolysis of Ran-GTP into Ran-GDP results in the dissociation of exportin from its cargo (**Scheme 4.1**). [3-5] This pathway allows the passage of macromolecules such as transcription factors, cell cycle regulators, RNPs and RNAs through the NPC for the regulation of important cellular processes.

4.1.2 Nuclear export receptor CRM1: A therapeutic target for the treatment of cancer

An important cellular export receptor involved in the shuttling of cargo from the nucleus into the cytoplasm is the nuclear export receptor CRM1 (chromosome region maintenance 1). Out of all the exportins known to date CRM1 has the broadest substrate range that includes mRNAs, ribonucleoproteins, and proteins. [5-6]

Mammalian cells utilize an intricate set of processes to protect themselves from uncontrolled cell growth, which may lead to cancer. One process they utilize is the regulation of transcription factors and tumor suppressors that require nuclear localization for their activation. In the case of aberrant cells this controlled event becomes deregulated, thus contributing to the development of cancer. Consequently, inhibition of the proteins responsible for the nuclear export of transcription factors and tumor suppressor to the cytoplasm could be exploited for the therapeutic intervention of cancer.[1] CRM1 has been shown to be responsible for the export of important cancer-related proteins such as p53, c-Abl and FOXO-3A. [1] For example, in normal dividing cells p53 is maintained at very low

levels but upon DNA-damage, hypoxia, ultraviolet light and hyperproliferation the levels of p53 increase. Accumulation of p53 leads to the activation of genes that promote apoptosis, cell cycle arrest and DNA repair.[7] Normal cells regulate p53 by enhancing its transport outside the nucleus for proteasomal degradation. [8] An important protein in this process is MDM2, a negative regulator of p53. Ubiquitination of p53 by MDM2 targets it for degradation. Moreover, p53 can be monoubiquitinated or polyubiquitinated by MDM2. When it is monoubiquitinated it exposes an NES sequence in its C-terminus that triggers a nuclear export response by CRM1 resulting in export of p53 and MDM2. Once they are in the cytoplasm MDM2 polyubiquitinates p53 leading to its degradation.[7] The overexpression of MDM2 results in the nuclear export of p53 resulting in its degradation and the development of cancer.[9] Consequently, an inhibitor of nuclear export will result in stabilization and activation of p53. [8]

4.2 Leptomycin B (LMB): An inhibitor of CMR1

4.2.1. An overview of LMB

Leptomycin B was isolated as an antifungal agent from a terrestrial bacteria *Streptomyces sp.* [10] The planar structure of this polyunsaturated polyketide was described in 1983 by Hamamoto and co-workers. [10b] The Kobayashi group predicted the absolute stereochemistry of LMB in 1998 based on similar spectral and structural characteristics to callystatin A, which the absolute configuration had been previously assigned. [11] The group was able to confirm their observations by its total synthesis (**Figure 4.1**). [11]

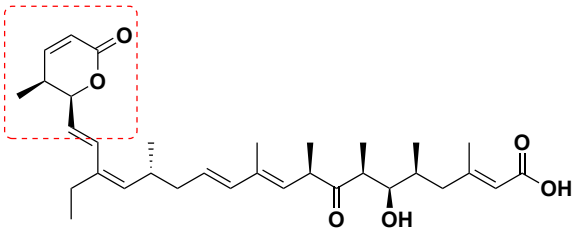

Figure 4.1. Leptomycin B. Red square represents LMB's warhead

Some of the important structural characteristics of LMB include its α, β- unsaturated δ-lactone, two conjugated dienes, a β-hydroxy-ketone moiety and a terminal carboxylate. LMB has been evaluated in clinical trials for the treatment of cancer but failed in phase I due to dose limiting toxicity that includes profound malaise, anorexia and gastrointestinal side effects. [12] This toxicity may in part be due to the remarkable affinity of LMB towards CRM1. Even though, LMB has been extensively studied it continues to be of interest to scientists because it can be utilized as a chemical probe to dissect the molecular interactions of CRM1. This interaction has led to the discovery of many CRM1- dependent nuclear export cargos. [5, 13]

4.2.2 Inhibition of CRM1 by LMB

To determine the molecular target of LMB a genomic library was created from an LMB-resistant mutant of *Schizosaccharomyces pombe.* The screen revealed a DNA fragment that conferred resistance to LMB and no cross-resistance to other chemical agents tested in the study. Sequencing of this small fragment of DNA revealed it was a mutant gene for the nuclear export receptor CRM1. [14] To obtain a more detailed mechanism of LMB's mode of action several CRM1 mutants of *S. pombe* were created. A highly resistant mutant to LMB only contained a single amino acid replacement, Cys-529 to a Ser. This suggested

that Cys-529 was involved in binding with LMB. To evaluate if the cysteine residue was necessary for LMB inhibition the Yoshida group looked at ^{35}S- labeled CRM1 in a binding assay. Wild type CRM1 and LMB-resistant CRM1 (S529, no cysteine residue for conjugate addition) were pre-incubated with an inactive analog of LMB (contains a saturated lactone ring) followed by a second incubation with biotinylated-LMB. Eluates from the binding assay were analyzed by SDS/PAGE. Wild type CRM1 interacted with biotinylated-LMB, contrary to inactive-LMB that did not bind to wild type CRM1. Furthermore, upon treatment of LMB-resistant CRM1 with biotinylated-LMB no binding was observed,[15] suggesting that the cysteine residue in CRM1 is involved in binding with LMB. Finally, the group confirmed their observations by examining LMB's binding to an 18 amino acid synthetic peptide of human-CRM1 (^{Hs}CRM1) containing Cys-528. Using mass spectrometry they observed a peak equivalent to the mass of LMB bound to the peptide (2644.06 Da), as well as a peak corresponding to the mass of free peptide (2104.02 Da). Additionally, the same experiment was performed but with a peptide containing a serine instead of cysteine, no peak was observed for the mass of LMB bound to peptide. Thus, LMB is able to alkylate the Cys residue found in the NES binding groove of CRM1 via a Michael addition to the α, β-unsaturated δ-lactone of LMB (**Scheme 4.2**). [15]

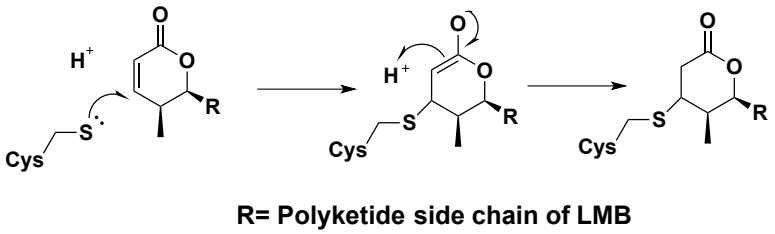

Scheme 4.2. Michael addition of the Cys residue of CRM1 to the α, β- unsaturated δ-lactone of LMB[16]

Furthermore, in the same study the authors were able to shed some light on the strong affinity of LMB towards CRM1. *In vivo* studies showed that LMB is able to selectively alkylate CRM1.[15]

4.2.3 Other inhibitors of CRM1

Several small molecules have been shown to prevent nuclear export by inhibition of CRM1. Some of these compounds include anguinomycin[17], ratjadone[18], goniothalamin [19] and CBS9106[20] just to mention a few (**Figure 4.2**). Similar to LMB these molecules inhibit CRM1 mediated-export by alkylating the reactive cysteine found in the NES binding groove.

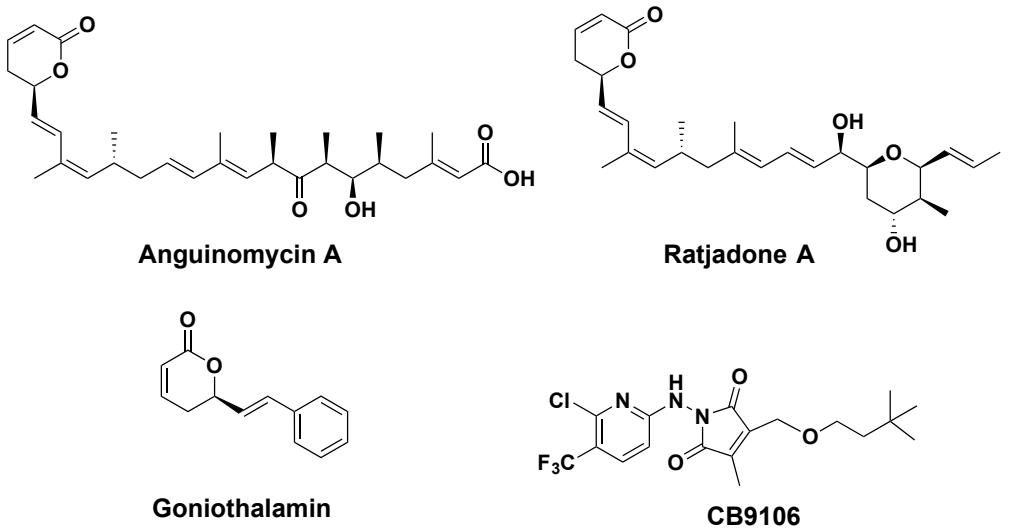

Figure 4.2. Other inhibitors of CRM1

4.2.4 Understanding the inhibition of CRM1 by LMB

It is important to understand the molecular basis of the interaction of CRM1 with LMB due to its ability to prevent the nuclear localization of important tumor suppressors and transcription factors that regulate cell growth. Because of it high affinity towards CRM1,

LMB represents a great chemical probe to study this interaction that can lead to the design of better small molecule inhibitors of CRM1 without any of the adverse effects associated with LMB.

In collaboration with the lab of Yuh Min Chook we set out to investigate the molecular interaction between CRM1 and LMB. The Chook lab had a surprising observation in a co-crystal structure of LMB and CRM1 that showed that the lactone ring of LMB was not only covalently bound to CRM1's cysteine residue, but the lactone ring had been hydrolyzed to the hydroxy acid. Subsequent analysis shows that this hydrolysis provides stabilization to a pocket of basic residues in the NES-binding groove of CMR1 resulting in additional binding energy. This further revealed that once the lactone ring has been hydrolyzed LMB irreversibly binds to CRM1.

Results and Discussion

4.3 A closer look at the interaction of LMB and CRM1

Prior to this work it was shown that LMB occupies part of the NES-binding groove of CRM1, [21] however it was not clear whether it interacted as an NES mimic or if a conformational change to CRM1 occurs by binding to the groove.

4.3.1 Crystal structure of CRM1 bound to LMB

A 1.8 to 2-Å-resolution crystal structure of LMB bound to the ternary complex of *Saccharomyces cerevisiae* CRM1 (^{Sc}CRM1), RanBP1, and human Ran•GppNHp was obtained (*crystal structure obtained by Qingxiang Sun, UTSW,*). The complex of CRM1 and

LMB did not crystallize on its own, contrary to LMB bound to the ternary complex of CRM1-RanBP1-Ran that formed crystals. Thr-539 (equivalent to Cys-528 of ^{Hs}CRM1)[16] of LMB-resistant ^{Sc}CRM1 was modified to cysteine for Michael conjugation to LMB, named ^{Sc}CRM1*. There are only few amino acid residues that are different between ^{Sc}CRM1 and ^{Hs}CRM1. The binding groove of ^{Sc}CRM1 was modified to match ^{Hs}CRM1 binding groove and these changes did not have a major impact in the structure of the yeast binding groove, validating ^{Sc}CRM1* as a mimic for ^{Hs}CRM1 by crystal structure. [16]

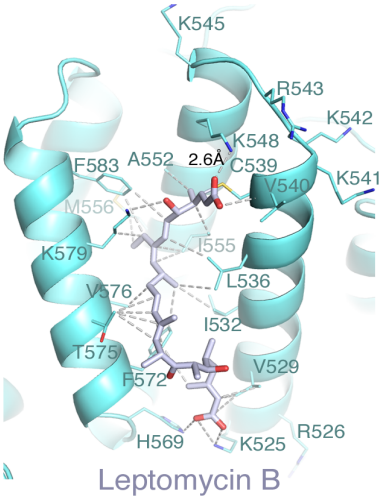

Figure 4.3. Crystal structure of CRM1 bound to LMB

Upon analysis of the crystal structure of CRM1 bound to LMB, the expected Michael addition adduct was observed (**Figure 4.3**). Interestingly, an open chain LMB was observed instead of the saturated lactone ring conjugated to cysteine. This open chain product was the hydrolysis of the lactone ring to the hydroxy acid (**Figure 4.4**).

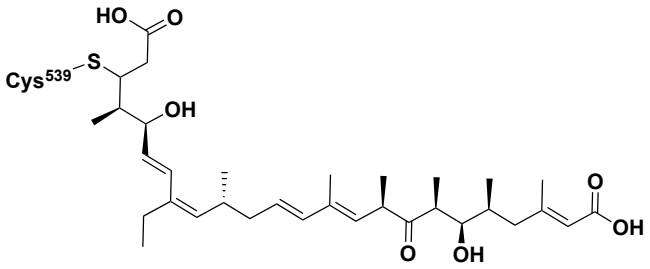

Figure 4.4. Hydrolysis of lactone ring in LMB.

The observation of the hydrolyzed lactone prompted the question of whether it was a product of experimental conditions. To address this concern, LMB alone was exposed to different pH conditions to determine if hydrolysis of the lactone ring was due to experimental pH. While no hydrolysis product was observed by ^{1}H-NMR of LMB at pH 3, 5, 7 and 8.5, at a pH of 10 traces of the hydrolysis product was detected (*^{1}H-NMR obtained by John MacMillan,* **Figure 4.5**). This result suggested that LMB is stable in the crystallization buffer at a pH of 6.6 and that possibly CRM1 is stabilizing the hydrolyzed lactone seen in the crystal structure.

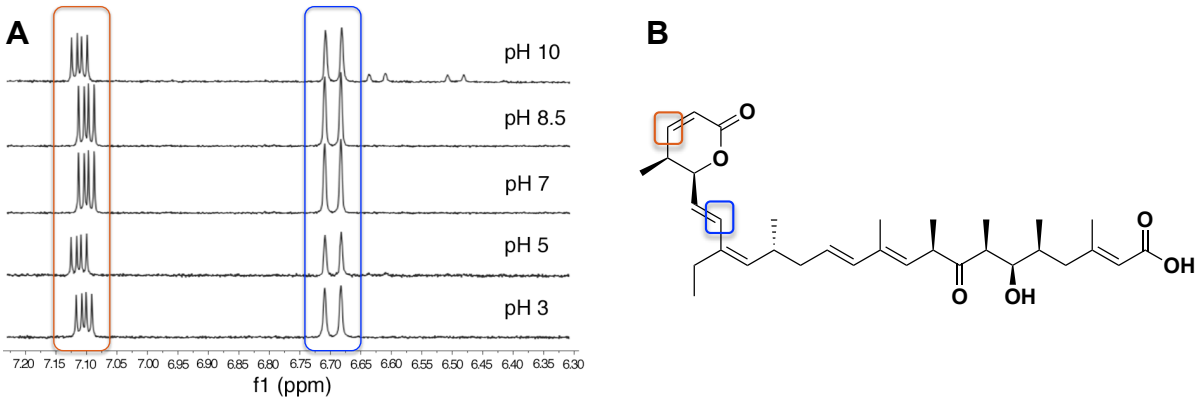

Figure 4.5. Effects of pH on LMB's lactone ring. **A**. ^{1}H-NMR of LMB at different pHs (new signals at 6.50ppm and 6.65ppm).**B**. Protons shown on spectra

Since hydrolyzed-LMB is not a product of experimental conditions during crystallization, several intriguing questions came to mind that can be best exemplified in **scheme 4.3.** For example, is cysteine conjugation to LMB reversible before it gets hydrolyzed? (**Scheme 4.3A**). Is CRM1 stabilizing the hydroxy acid product resulting from hydrolysis of the lactone ring? (**Scheme 4.3B**). Also, is cysteine conjugation reversible once the lactone ring has been hydrolyzed? Finally, if the lactone ring is chemically hydrolyzed, will it form a Michael-adduct with the cysteine of CRM1? (**Scheme 4.3C**). Is the hydrolyzed product stable in solution? (**Scheme 4.3D**). The answer to these questions can shed some light on the mechanistic detail of LMB's inhibition of CRM1, and provide information for the design of a less toxic compound that targets CRM1.

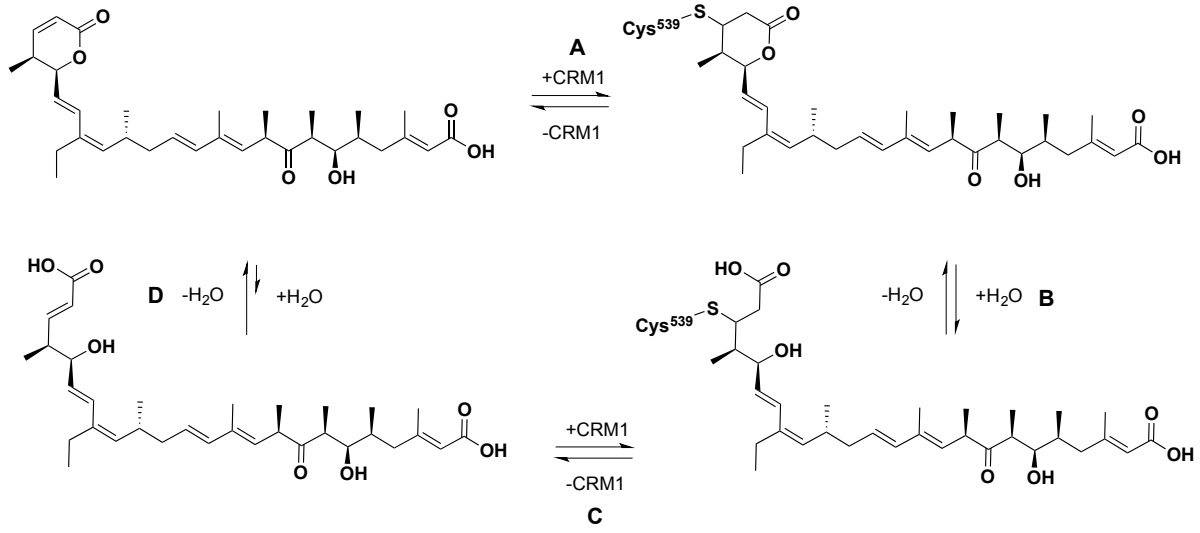

Scheme 4.3. Model showing the equilibria of conjugation and hydrolysis of LMB **A.** Reversibility of Michael conjugation before hydrolysis. **B.** Hydrolysis of lactone ring after Cys conjugation. **C.** Reversibility of Cys conjugation after hydrolysis. **D.** Hydrolysis of lactone ring before Michael conjugation.

4.3.2 Hydrolysis of LMB and its interaction with CRM1

To determine if chemically hydrolyzed-LMB (*hydrolysis of LMB by Youcai Hu, UTSW*) would interact with CRM1, a pull down assay was utilized with immobilized GST-$^{MVM\text{-}NS2}$NES beads (*pull down assay by Qingxiang Sun, UTSW*). This experiment would reveal if hydrolyzed-LMB can disrupt the interaction between CRM1and GST-NES beads (**Figure 4.6**). LMB or hydrolyzed-LMB were incubated with yeast or human CRM1 and then added to immobilized GST-$^{MVM\text{-}NS2}$NES beads and examined by SDS/PAGE. LMB is able to disrupt the interaction between ^{Sc}CRM1* and GST-NES as expected. Conversely, in the presence of hydrolyzed-LMB the nuclear export ^{Sc}CRM1* is able to interact with the NES beads. Similar results were observed with ^{Hs}CRM1. This observation suggests that conjugate addition of the Cys residue in the NES-binding groove of CRM1 happens first followed by hydrolysis of the lactone ring.

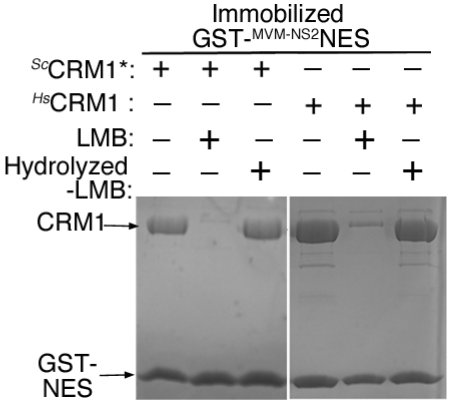

Figure 4.6. Hydrolyzed LMB fails to interact with ^{Hs}CRM1 and ^{Sc}CRM1* in a GST-$^{MVM\text{-}NS2}$NES pull down assay.

In accord with this observation, conjugate addition is more likely to happen in the lactone form than in its carboxylate form. This may be due to the decreased electrophilicity of the β-carbon in the hydrolyzed form of LMB (**Scheme 4.3**). [16]

4.3.3 Interaction of LMB with the NES binding groove of CRM1

LMB occupies an approximate of 70% of the NES-binding groove of ^{Sc}CRM1* and it has several electrostatic and hydrophobic interactions in the binding groove of CRM1. The resulting carboxyl from lactone hydrolysis has several interactions with neighboring amino acids such as the formation of a salt bridge with Lys-548, a polar interaction with the amide of Val-540 and a long-range electrostatic interaction with Arg-543. Additionally, the resulting hydroxyl group from lactone hydrolysis has an interaction with Lys-579 as shown in **figure 4.7**. The terminal carboxylic acid forms electrostatic interactions with Lys-525 and His-569 providing and extra anchor at the terminal end of LMB. The majority of carbons in LMB have an interaction with CRM1 with the exception of the β-hydroxy ketone moiety.

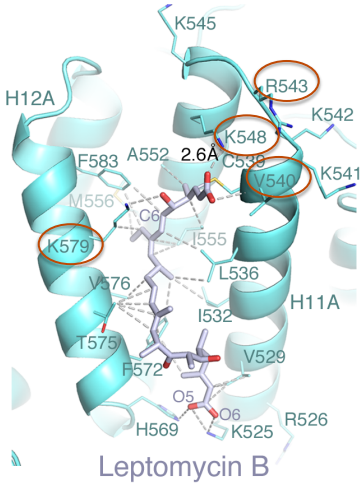

Figure 4.7. Stabilizing interactions (circled in red) of CRM1 that leads to the hydrolysis of the lactone ring in LMB

The presence of basic residues around the site of lactone hydrolysis raises the question if these residues are providing stabilization to the hydroxy acid product. To answer this question, the basic residues that come in contact with the hydrolyzed lactone were mutated (*mutation studies by Qingxiang Sun, UTSW*). Primarily, two residues K548 and K579 (^{Sc}CRM1* K548E, K579Q) were mutated and hydrolyzed-LMB conjugated to Cys was observed (**Figure 4.8A**). It appears that any basic residue around the lactone ring is enough for lactone hydrolysis. When K548 and K579 are mutated, an Arg-543 that is in close proximity is able to move into the groove and compensate for the missing basic residues leading to hydrolysis.

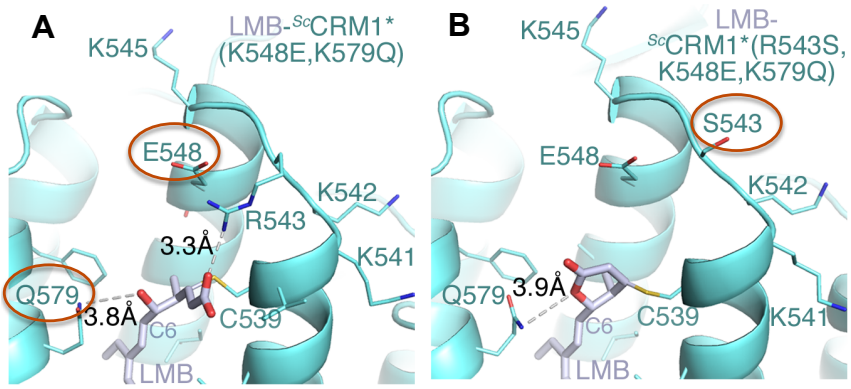

Figure 4.8. Structure of LMB- bound to ^{Sc}CRM1 mutants **A.** Double Mutant of ^{Sc}CRM1*, mutated residues are circled in red. **B.** Triple Mutant of ^{Sc}CRM1*, additional residue mutated is circled in red.

To observe if any positive charge is sufficient for lactone hydrolysis Arg-543 was mutated together with Lys-548 and Lys-579 in ^{Sc}CRM1* (R543S, K548E, K579Q, **Figure 4.8B**). Also, an additional mutant was formed where all the basic residues along the hydrolysis site were mutated [^{Sc}CRM1* (K541Q, K542Q, R543S, K545Q, K548Q, K579Q)]. In both cases LMB's lactone ring was intact and covalently bounded to CRM1 via Cys conjugation. So it appears that any basic residue around the lactone may be providing stabilization leading to the hydrolyzed product.

4.3.4 Verification of LMB hydrolysis by analytical methods

The insights into the hydrolysis of LMB by CRM1 to this point was solely based on the use of crystallographic analysis by the Chook lab, but we desired to have non-crystallographic data to support the hypothesis so an additional avenue was taken to understand this process. We have used crystal structure analysis and mutation studies to show that basic residues around the binding site provide stabilization of the hydrolyzed

lactone and that these sites are required for hydrolysis, as cysteine conjugation alone is not sufficient. To address the latter argument, the intrinsic hydrolysis of LMB vs a thiol conjugated LMB was examined. Thus, LMB bound to DTT (dithiothreitol, **Figure 4.9**) and LMB alone in buffer were analyzed by LCMS at the end of 26 hrs.

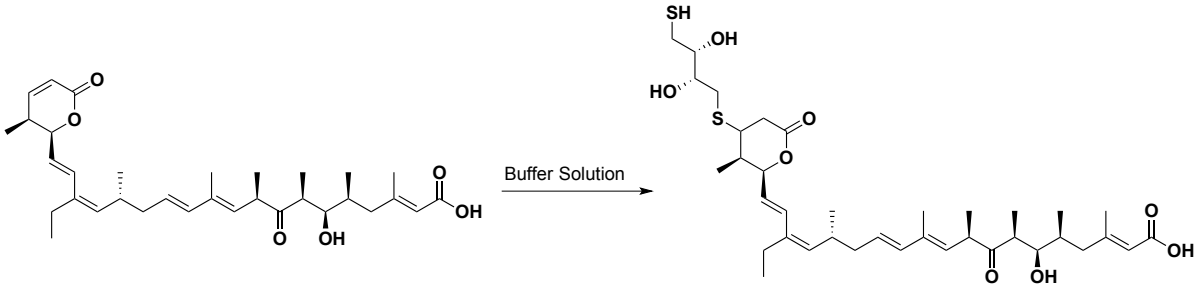

Figure 4.9. Conjugate addition of DDT to unsaturated α, β- unsaturated lactone ring

DTT was utilized as a mimic for Cys in order to provide similar electronics around the lactone ring as LMB covalently conjugated to CRM1. After 26hrs LMB-DTT is stable in solution and only a small amount of hydrolyzed-LMB is observed, suggesting that conjugation alone is not sufficient for hydrolysis of the lactone ring (**Figure 4.10, Table 4A.1**).

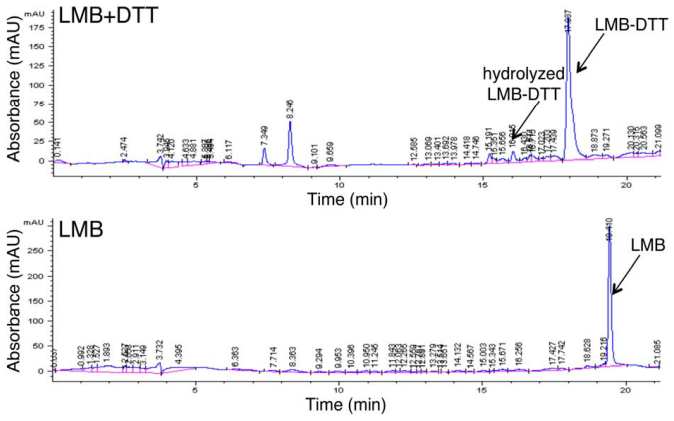

Figure 4.10. HPLC trace of LMB and LMB conjugated to DTT after 26hrs

To further understand if conjugation to the cysteine residue of CRM1 would have an impact on hydrolysis of LMB a series of experiments were performed using T539S mutant of LMB-insensitive CRM1 (^{y}CRM1). The overall experiment was carried out in the following manner: LMB and DTT were pre-incubated overnight in buffer followed by an incubation with ^{y}CRM1 in the presence or absence of hydroxylamine, each reaction was quenched after 26 hours (**Table 4A.2** contains quenching times of each reaction after 2, 6, and 8 hours, *Solutions used for analysis provided by Qingxiang Sun, UTSW*). Hydroxylamine was added since it is a commonly used reagent to increase the rate of hydrolysis of ester bonds. [22] The different complexes that can be formed from the reactions mentioned previously are shown in **figure 4.11**.

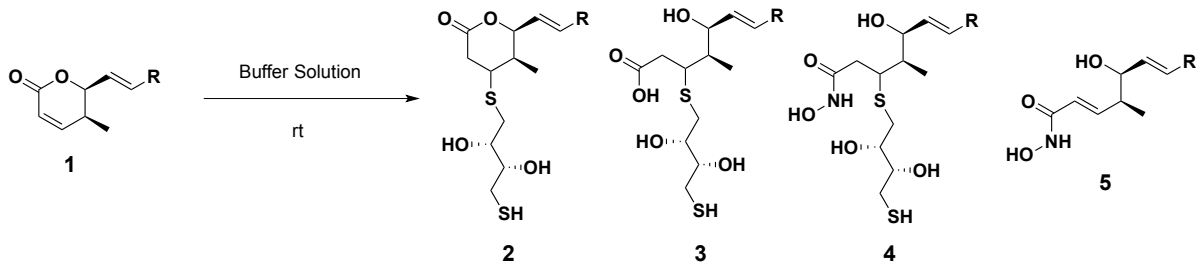

Figure 4.11. Complexes that can be formed from treating LMB-DTT with mutant CRM1 in the presence or absence of hydroxylamine

Complex **1** represents LMB alone no DTT addition, complex **2** is LMB with DTT addition but no hydrolysis of lactone ring, complex **3** illustrates LMB-DTT and hydrolysis of lactone ring, hydroxylamine addition to LMB-DTT is shown in complex **4,** and complex **5** represents no DTT addition to LMB but nucleophilic addition of hydroxylamine to the lactone ring. From **Table 4.1** we can observed only a trace amount of the hydrolysis product in LMB-DTT (+)-CRM1, contrary to LMB-DTT (-)-CRM1 where ~ 10% of the hydrolyzed

product is seen (**Table 4.1** lane **1** and lane **2**, respectively). A possible explanation is that hydrolysis is taking place at a slower rate in CRM1 due to limited access to the nucleophile in this case water. This may explain why we only see traces of hydrolyzed-LMB compared to the control experiment [(-)-CRM1], where LMB-DTT would have much more access to the nucleophile. A very encouraging result was the presence of the hydrolyzed product (~60%) in LMB-DTT (+)-CRM1 with hydroxylamine (**Table 4.1** lane **3**) compared to ~ 44% in the LMB-DTT (-)-CRM1 with hydroxylamine (**Table 4.1** lane **4**) suggesting that CRM1 is hydrolyzing the ring.

Table 4.1. Hydrolysis of LMB-DTT vs LMB-DTT treated with mutant CRM1 in the presence or absence of hydroxylamine

Entry	Enzyme	Thiol	Additive	1 (%)	2 (%)	3 (%)	4 (%)	5 (%)
1	^{y}CRM1	DTT	-	-	99.9	T	-	-
2	-	DTT	-	-	89.1	10.8	-	-
3	^{y}CRM1	DTT	NH_2OH	-	39.7	36.2	23.9	T
4	-	DTT	NH_2OH	-	52.5	20.0	24.2	3.1
5	-	-	-	100	-	-	-	-

% Obtained from integration of LC peak at 254nm. T =Trace amounts

Additionally, LMB alone in buffer has not been hydrolyzed in solution (**Table 4.1** lane **5** and **Figure 4.10**). Finally, the presence of complex **5** in **figure 4.11** suggests the reversibility of Michael conjugation a feature that can help explain the tenacious inhibition of LMB towards CRM1.

4.3.5 Stabilization of anionic intermediate by CRM1

LMB bound to ^{Sc}CRM1* with superposition of non-hydrolyzed-LMB with triple mutant ^{Sc}CRM1* (R543S, K548E, K579Q) provided information on a possible nucleophile, a water molecule that is 3.1 Å from the carbonyl carbon of the lactone ring in LMB *(Superposition by Qingxiang Sun, UTSW)*. It is located perpendicular to the plane of the carbonyl for nucleophilic attack (**Figure 4.12**).

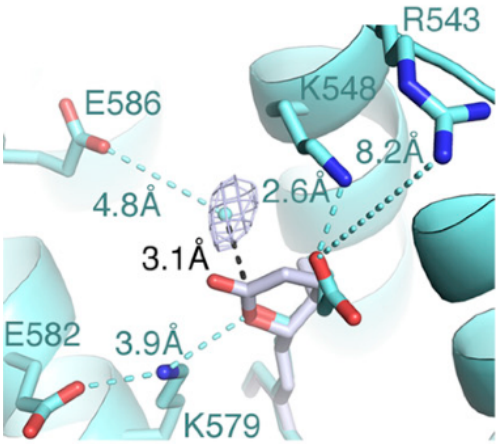

Figure 4.12. Superposition of LMB bound to CRM1 and of triple mutant bound to non-hydrolyzed LMB. The magenta structure is hydrolyzed-LMB and gray structure is non-hydrolyzed-LMB

Additionally, it can be observed that the basic residues around the hydrolysis site (Arg-543, Lys-548 and Lys-579) form an oxyanion hole that may allow the stabilization of the hydrolysis intermediate. Or perhaps the three positively charged residues could also contribute to hydrolysis by stabilizing the hydroxy acid product. Consistent with our previous argument hydrolyzed-LMB after 20 days in solution reverts back to the ring-closed LMB (**Figure 4.13**).

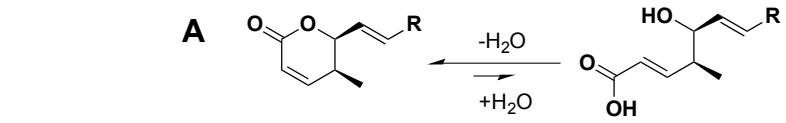

R= Polyketide side chain of LMB

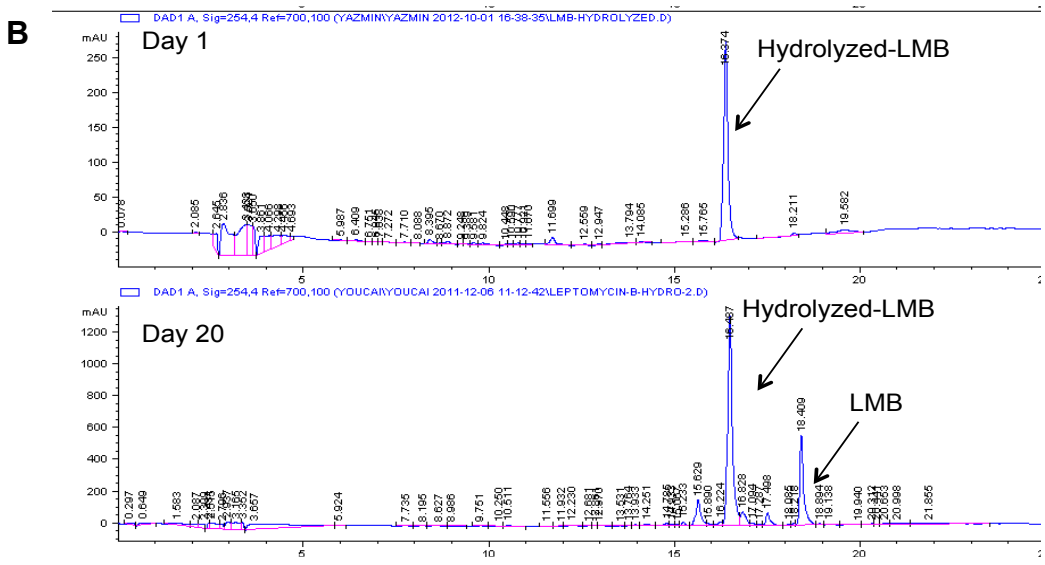

Figure 4.13. Reversibility of hydrolysis of LMB **A.** Equilibira of Hydrolysis of LMB **B.** HPLC trace of hydrolyzed-LMB at day 1 and the conversion back to LMB after 20 days of sitting in solution.

The low stability of hydrolyzed LMB in solution suggests that the three basic residues of CRM1 that are in close proximity to LMB's lactone ring may provide stabilization of hydrolyzed-LMB.

4.3.6 Reversibility of Michael conjugation

A new class of small molecules (KPT-185) was designed to specifically bind to the NES-binding groove of CRM1 (Karyopharm Therapeutics). A crystal structure of KPT-185 bound to ^{Sc}CRM1*-Ran-RanBP1 was recently reported. [23] KPT-185 structural characteristics

include a trifluoromethyl phenyl triazole moiety as well as an isopropyl acrylate for Michael conjugation with CRM1 (**Figure 4.14**).

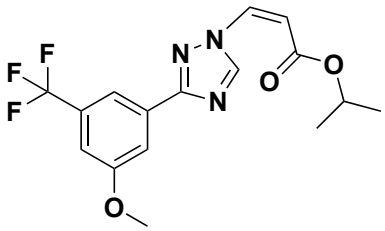

Figure 4.14. KPT-185

As expected, KPT-185 covalently modifies Cys-539 of the NES-binding groove of CRM1 via conjugate addition of its enone. From its crystal structure, it can be observed that KPT-185 occupies ~40% of the NES- binding groove of CRM1.[23a] Also, contrary to LMB that interacts with the NES groove through both electrostatic and hydrophobic interactions, KPT-185 interacts mostly through hydrophobic interactions. [16]

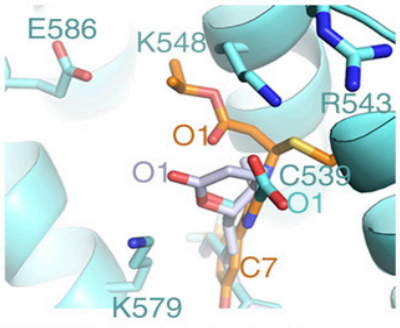

Figure 4.15. Superposition of KPT-185 and LMB bound to ^{Sc}CRM1* together with non-hydrolyzed LMB bound to triple mutant ^{Sc}CRM1* (R543S, K548Q, K579Q). Orange structure represent KPT-185, gray structure is non-hydrolyzed LMB and magenta structure is hydrolyzed-LMB *(superposition by Qingxiang Sun, UTSW)*.

More importantly, KPT-185 is not hydrolyzed by CRM1. It binds much deeper into the NES-groove restricting the access to the nucleophile for hydrolysis of its isopropyl

acrylate (**Figure 4.15**). Additionally, it seems that the hydrolyzed KPT-185 would have much less contact with CRM1 than its non-hydrolyzed counterpart, contrary to LMB that hydrolysis of the lactone ring forms more interactions with CRM1.[16]

The hydrolysis of LMB greatly compensates for a basic pocket in the groove of CRM1, contributing to the binding energy of the system. [16] Consequently, CRM1 inhibitors that have the ability to be hydrolyzed may bind more strongly than inhibitors that lack this ability. To see if the absence of hydrolysis would have an impact on covalent conjugation to cysteine, LMB bound to ^{Sc}CRM1* was compared to LMB bound to mutant ^{Sc}CRM1* (K541Q, K542Q, R543S, K545Q, K548Q, K579Q) that lacks the capability of hydrolyzing LMB (**Figure 4.16)**.

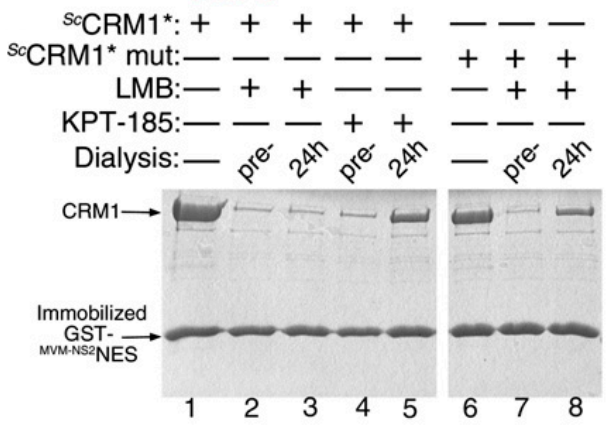

Figure 4.16. Stability of inhibitor conjugation. Inhibition assay of CRM1 after dialysis of ^{Sc}CRM1* treated with LMB and KPT-185 and ^{Sc}CRM1* (K541Q, K542Q, R543S, K545Q, K548Q, K579Q) treated with LMB.

Both proteins were incubated with LMB to afford full inhibition of CRM1 then were dialyzed for the removal of any unbound inhibitor. Both were compared by a pull-down inhibition assay using immobilized NES beads to ^{Sc}CRM1* treated with KPT-185, which lacks the ability to be hydrolyzed *(Inhibition assay by Qingxiang Sun, UTSW)*. In the case

where LMB was incubated with ^{Sc}CRM1*, it showed full inhibition and no reversal in cysteine conjugation, even after dialysis. Surprisingly, when LMB was incubated with ^{Sc}CRM1* (K541Q, K542Q, R543S, K545Q, K548Q, K579Q) it showed a decrease in inhibition of CRM1 after dialysis, suggesting that the covalent conjugation of LMB is reversible (**Figure 4.16).** Similarly, KPT-185 shows a decrease in inhibition after dialysis, suggesting that it reversibly binds to CRM1. These findings support the idea that hydrolysis of the lactone ring decreases the reversibility of cysteine conjugation leading to more persistent binding of the inhibitor, as is the case for LMB. Lactone hydrolysis is not necessary for inhibition of CRM1, however it seems that hydrolysis promoted by CRM1 may be the cause of prolonged inhibition by LMB. This may translate to the long-lived toxicity observed from this α, β- unsaturated lactone polyketide, even after removal of LMB. [12]

4.3.7 Is irreversibility of covalent conjugation the cause of LMB's toxicity?

KPT-185, a reversible inhibitor of CRM1 has been studied for its ability to inhibit nuclear export of important proteins that are dysregulated in human chronic lymphocytic leukemia (CLL). KPT-185 can restore the regulation of these proteins by preventing their cytoplasmic localization and cause apoptosis of CLL cells with minor toxicity to normal cells.[23a] These findings support the argument that the irreversibility of cysteine conjugation by LMB may be the cause of toxicity associated with the drug. To further explore this question, we set out to synthesize a model substrate that could not be hydrolyzed by CRM1. Then we could compare it to a hydrolysable analogue and in this manner compared their cytotoxic/toxicity profiles side by side. Ideally, one could synthesize an analogue of LMB

that would substitute its α, β- unsaturated lactone with a cyclohexenone lacking the capability of being hydrolyzed by CRM1. Unfortunately, due to the synthetic challenge that this endeavor poses, we decided to look at simpler scaffolds that could answer this question. One of these molecules is the styryl lactone (*R*)-goniothalamin (**6**), a natural product isolated form the bark of the genus *Goniothalamus* (**Figure 4.17**).[24] Compound **6** has been shown to inhibit nuclear export mediated by CRM1.[19] Aside from being an inhibitor of CRM1, **6** was selected because of its simplified structural complexity and because it is commercially available. Analogously, model substrate **7** has a similar core structure than **6** but lacks the lactone necessary for hydrolysis that has been replaced by a cyclohexenone moiety (**Figure 4.17**).

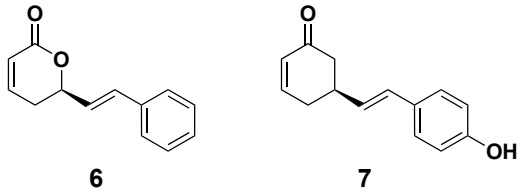

6 **7**

Figure 4.17. Goniothalamin (**6**) and model substrate (**7**)

4.3.8 Synthesis of model substrate

The synthesis of **7** turned out to be more challenging than expected due to the chirality of the cyclohexenone ring. Fortunately, the Sato group developed an efficient strategy for the synthesis of chiral cyclohexenone rings from commercially available starting materials that was utilized for the synthesis of the left fragment of **7** (**Figure 4.18**). [25]

The retrosynthetic analysis of **7** is shown in **scheme 4.4.** The model substrate comes from a 1,4 conjugated addition of styryl bromide **9** to cyclohexenone **8**.

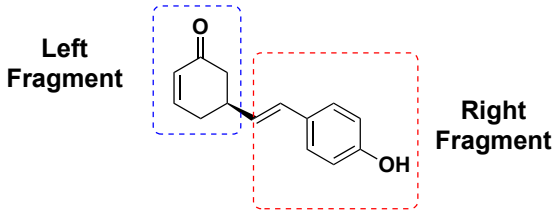

7

Figure 4.18. Model substrate **7**

The silyl ether dertivate **8** derives from intramolecular nucleophilic acyl substitution and intramolecular carbonyl addition [25] of commercially available ethyl-(*R*)-4-chloro-3-hydroxybutyrate (**10**). Styryl bromide **9** was obtained from a Hunsdiecker reaction of silyl ether protected *p*-coumaric acid (**11, Scheme 4.4**).[26]

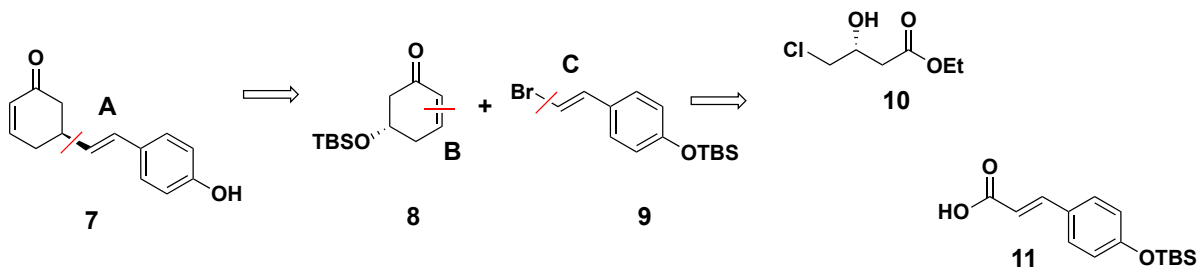

Scheme 4.4. Retrosynthetic analysis of **7**. **A.** 1,4- conjugate addition. **B**. Intramolecular nucleophilic acyl substitution and intramolecular carbonyl addition. **C**. Hunsdiecker reaction.

4.3.9 Synthesis of left fragment of model substrate

The commercially available chloro-butyrate **10** was converted into the iodo-butyrate derivate in 93% yield via a Finkelstein reaction using sodium iodide in acetone as shown in **Scheme 4.5**. [25]

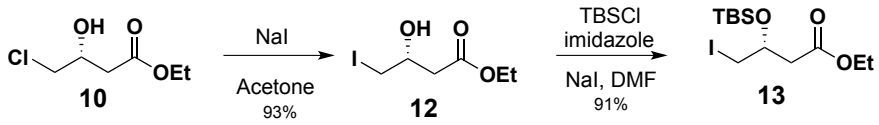

Scheme 4.5. Conversion of chloro-butyrate **10** to protected alcohol iodo-butyrate **13**.

TBS-protection of the secondary alcohol in **12** provided silyl ether **13** in 91% yield (**Scheme 4.5**). [25] Formation of **14** was achieved via divinyl magnesium cuprate addition to iodo-butyrate **13**, where the organocuprate was initially formed from vinylmagnesium bromide in the presence of DMPU, $(EtO)_3P$ and CuI. [25, 27] The use of DMPU for the preparation of the organocuprate resulted in lower yields (40%) and longer reaction times (12h). Instead, HMPA was utilized slightly increasing the yield to 51% and the time of the reaction was decrease to 3 hours (**Scheme 4.6**).

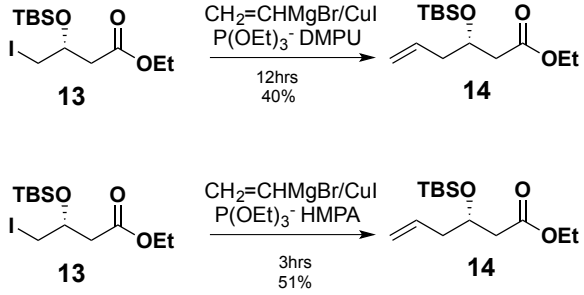

Scheme 4.6. Organocuprate addition of **13** to form vinyl derivate **14**

Vinyl **14** was treated with Ti(O*i*-Pr)$_4$ /2*i*-PrMgCl to afford cyclopropanol **15** via a tandem reaction of intramolecular nucleophilic acyl substitution and intramolecular carbonyl addition of **14**. The ring expansion product **8** was obtained from treatment of **15** with $FeCl_3$, followed by treatment with sodium acetate as shown in **Scheme 4.7**.

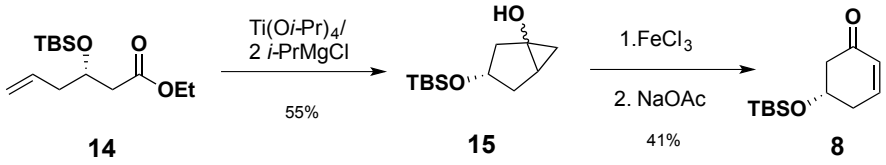

Scheme 4.7. Conversion of **14** to cyclohexenone **8**

4.3.10 Synthesis of right fragment of model substrate

An initial attempt at synthezing the right fragment of **7** (**Figure 4.18**) involved the use of selectfluor to generate Br^+ from KBr as shown in **scheme 4.8A**.[28] The resulting electrophile was reacted with *p*-coumaric acid to in theory generate the oxidative decarboxylation bromination reaction product as shown in **scheme 4.8B**. [29]

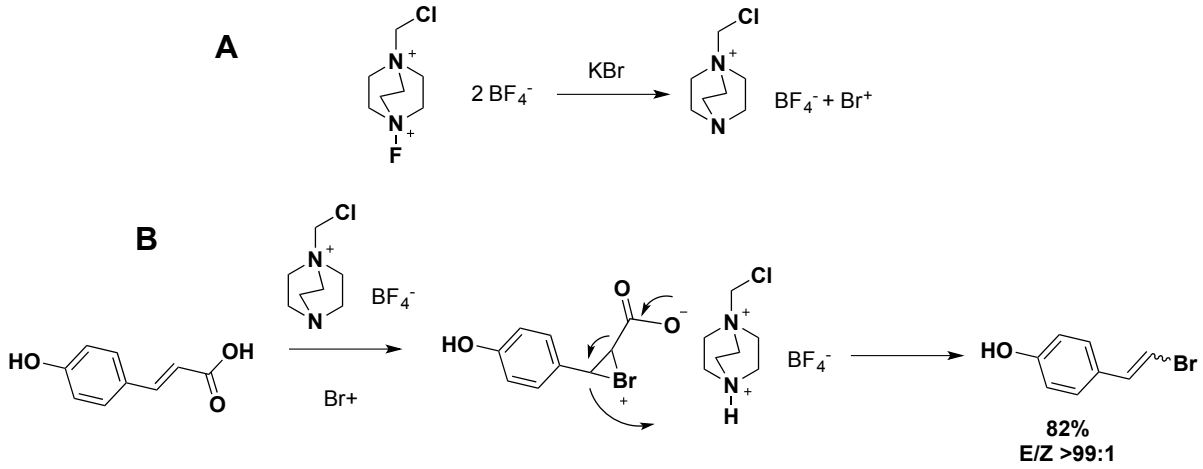

Scheme 4.8. A. Generation of electrophile using selectfluor. **B.** Formation of oxidative decarboxylation bromination reaction product. [29]

Unfortunately, contrary to the results from Ye and co-workers the reaction resulted in a combination of products difficult to separate by column chromatography. This may be the result of electrophilic aromatic substitution due to the electron-rich properties of substrate **17**. [30] To circumvent this problem, phenol **17** was protected using TBSCl and imidazole in DMF to afford **11** in 97% yield. The resulting silyl ether was then converted into **9** using NBS and lithium acetate. (**Scheme 4.9**). [26]

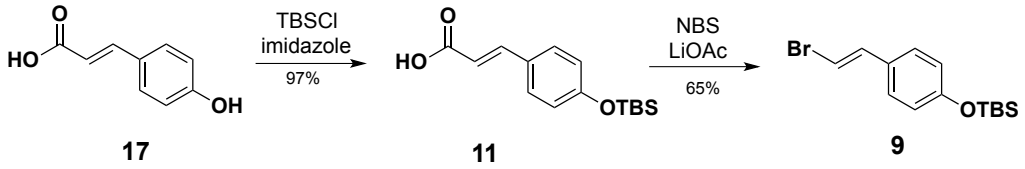

Scheme 4.9. Synthesis of the right fragment of **7**

4.3.11 Coupling of right and left fragment of model substrate

Coupling of the left fragment was envisioned to take place through conjugate addition via a higher-order cyanocuprate of the right fragment followed by desiloxylation to afford **7** as the phenol protected derivative.[25] In previous work, the Sato group reacted compound **8** with Gilman butylcuprate reagent and high-order butylcyanocuprate to afford the *trans*-**18** product with selectivities of 89:11 and 98.5:1.5, respectively (**Scheme 4.10**). [25, 31]

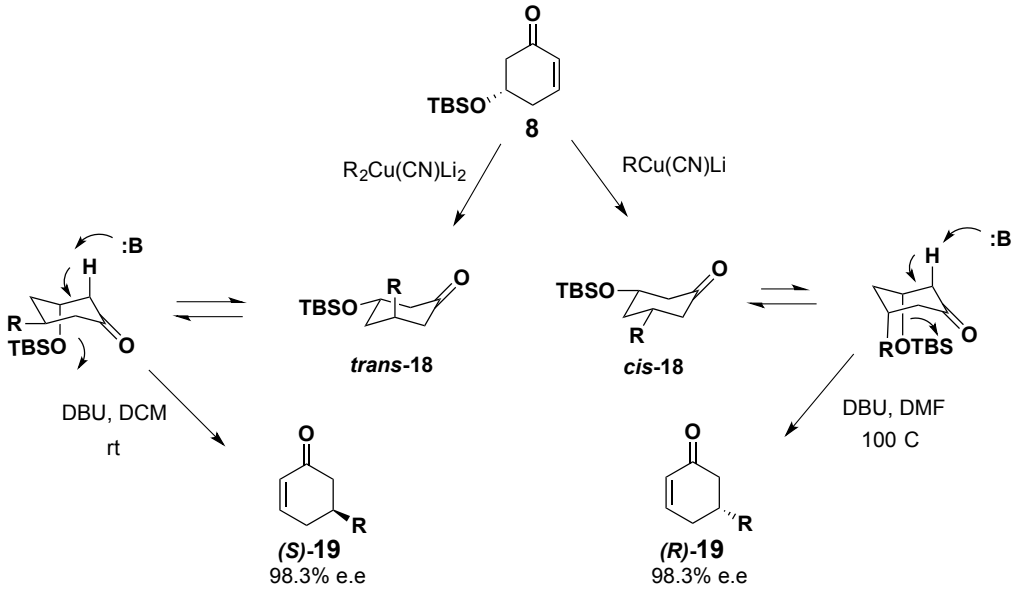

Scheme 4.10. Formation of chiral cyclohexenones via conjugate addition of low-order and high-order cyanocuprates onto **8** followed by desiloxylation[25]

Additionally, they observed that addition of low-order butylcyanocuprate resulted in the *cis*-**18** product. Treatment of both *trans*-**18** and *cis*-**18** with DBU provides the

desiloxylation products **19** in good yield. Furthermore, there was no racemization during the process of generating chiral cyclohexenones due to the very similar e.e. values for both **19** compounds to those from the starting material. The group then investigated the conjugate addition of **8** using a variety of high- and low-order cyanocuprates that include methyl, primary-alkyl, *sec*-alkyl, and *tert*-alkyl as well as phenyl and vinyl derivatives in good yields.[25] The use of low- or high-order cyanocuprates allows for access to both diasteromers of **18** and the desiloxylation step provides both enantiomers of **19** from a common chiral cyclohexenone ring **8**.

This powerful method allows for the access of both enantiomers of **7**, which could provide more information on the binding of these molecules to CRM1. As seen by the synthesis of (*S*)-goniothalamin where differences in cytotoxicity were observed when comparing both enantiomers.[32]

The coupling of **8** with **9** has proven to be more challenging than expected due to the inability to generate the coupling product **20** (**Scheme 4.11**). One difference in our strategy from that of Sato's is that he utilizes cyanocuprates that are mainly generated from commercially available lithium reagents whereas we have to generate the organolithium in the laboratory.

Another difficulty has been the low stability of compound **8**,[25] which slows down the process of optimizing the reaction conditions because only small quantities of compound **8** are generated to limit the decomposition of large quantities of material.

To generate the organolithium, the butyllithium reagent was slowly added at -78°C to a THF solution of **9** and was let to stir for 50 mins. This solution was then transferred to a

Schlenk tube with CuCN in THF and stirred for 1 hour followed by addition of **8** dissolved in THF at -78°C. [25] After quenching the reaction there was no trace of **20** only what appeared to be the styryl derivative of **9**, suggesting that the organolithium of **9** was generated but did not reacted with enone **8** (**Scheme 4.11**).

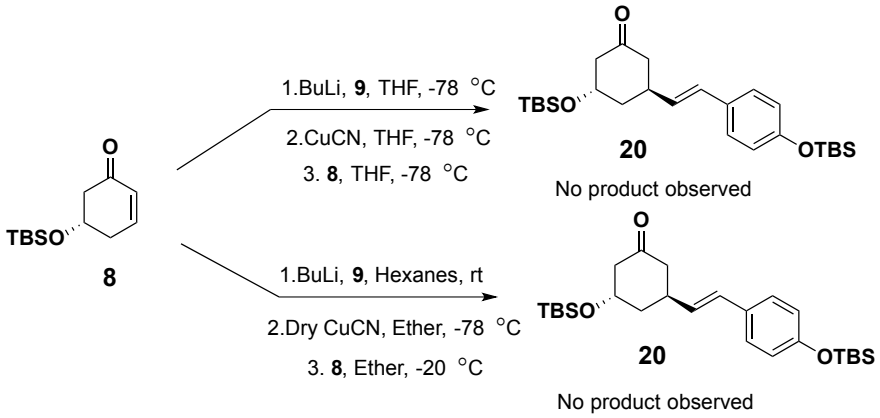

Scheme 4.11. Coupling reaction of **8** with **9**

After several attempts at this reaction and no success, we started wondering if perhaps our copper source was wet. Consequently, CuCN was dried under vacuum at 60°C for 2 hours before use.[33]

Additionally, the solvent was changed from THF to hexanes for the generation of the organolithium as shown by Utimoto and co-workers, which proved to be the best solvent for their metal-halogen exchange reaction.[34] Unfortunately, the desired product was not observed under these conditions (**Scheme 4.11**).

To avoid loosing more of the coupling partner **9** and to test the quality of the reagents**,** butyllithium was utilized under the same reactions conditions developed by Sato and co-workers with the exception that the CuCN used for this reaction was dried[33], unfortunately the desired product **21** was not observed (**Scheme 4.12**). A possible explanation of why the

conjugate addition reaction is not taking place is that the buthyllithium reagent utilized for the reaction had decomposed while stored in solution. Consequently, for the next reaction in **scheme 4.12** a new bottle of butyllithium was utilized as well as a new source of copper (CuI) to generate a Gilman butylcuprate reagent instead of the high-order butylcyanocuprate used in the previous reaction. [35]

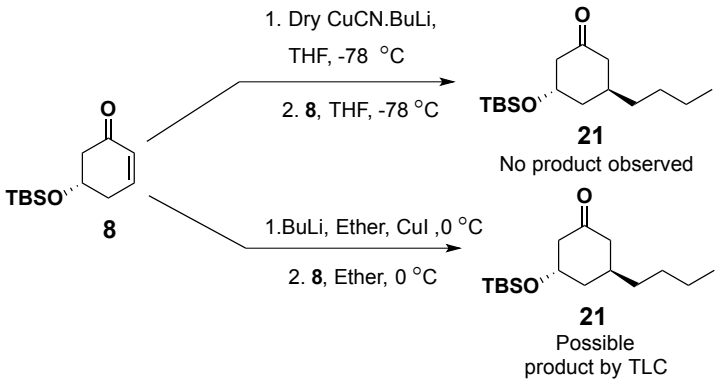

Scheme 4.12. 1,4-Conjugate addition of enone **8** with buthyllithium

Interestingly, upon checking the reaction by TLC a new spot in the plate appeared indicating that the reaction may have worked, unfortunately the reaction was carried out at a very small scale that there was not enough material for examination by NMR. Nonetheless, this result gave us confidence to try the same reaction conditions with substrate **9** (**Scheme 4.13**).[34-35] Regrettably the desired product was not observed and appears that the starting material **8** decomposed.

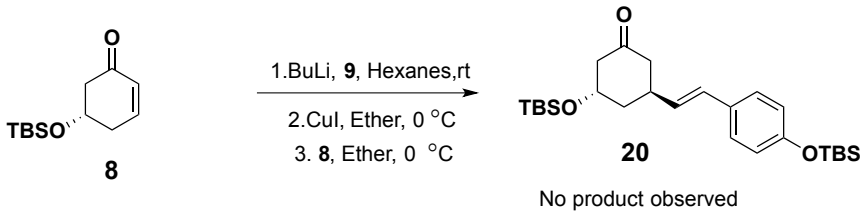

Scheme 4.13. 1,4-Conjugate addition of **8** with styrylcuprate

After trying different temperatures, solvents, copper sources, coupling patterns to conjugate with **8**, one avenue left to be explored was the left fragment of **7**, enone **8**. Perhaps, the low stability of **8** may play a role during the reaction, leading to its decomposition and no reaction. To test for this hypothesis we looked at the simplest cyclohexenone (**22)** as seen in **Scheme 4.14**. The progress of the reaction was monitored by TLC and after 3 hours the reaction was finalized. Based on our NMR studies the desired product was present.

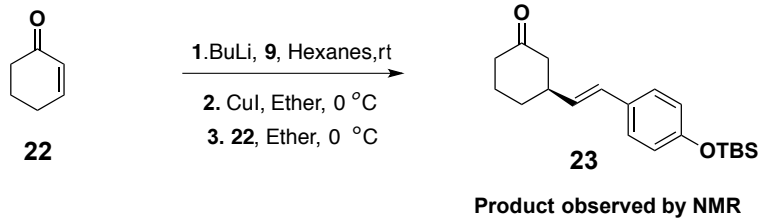

Scheme 4.14. 1,4-Conjugate addition of **22** with styrylcuprate

Although this is an encouraging result the 1,4-conjugate addition of **8** with **9** waits to be completed. Considering the low stability of **8** and that it is stored over calcium hydride, [25] a strong desiccating agent, it appears that **8** is a contributing factor of why its coupling with **9** has not worked so far. It may be that it is decomposing during experimental conditions due to the small scale of the reaction that any residual water present may be affecting its stability.

In the future, the reaction of **8** with **9** via conjugate addition will be revisited using the same conditions as in **scheme 4.14** but at a larger scale to prevent any decomposition of enone **8**. If this approach succeeds, the next attempt will be to do the conjugate addition

reaction using the high-order cyanocuprate of **9,** due to the better diastereoselectivity [25, 31] observed by the Sato group from using this organocuprate complex instead of the Gilman reagent. This will follow the synthesis of the enantiomer of **7** by simply switching to the low-order cyanocuprate of **9** in the conjugate addition step. Additionally, in an effort to optimize the conjugate addition reaction, a non-transferable group such as 2-thienyl can be utilized for the formation of the organocuprate of **9** to preserve this compound for future conjugate addition reactions.

4.3.12 Biotinalytion of LMB

The affinity/inhibition of LMB to CRM1 is indirectly determined by looking at CRM1's ability to interact with the immobilized NES beads in a pull-down inhibition assay.

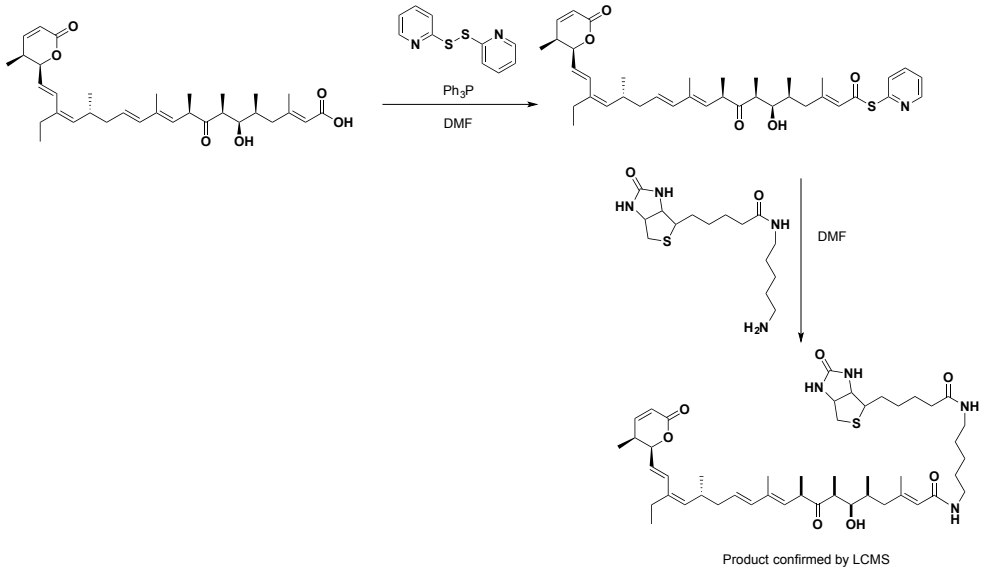

Scheme 4.15. Biotinylation of LMB

A caveat to this is that CRM1 mutants have little affinity to no affinity towards the NES immobilized beads. Consequently, biotinylated-LMB can be utilized to compare LMB inhibition towards CRM1 and its mutants directly.

For the synthesis of biotinylated-LMB, the terminal carboxylic acid was activated with dipyridyl disulfide and triphenyl phosphine.[36] Once the pyridinethiol ester was formed biotin cadaverine was added resulting in biotinylated LMB,[37] which was confirmed by LCMS (**Scheme 4.15**). The inhibition/affinity of LMB and its mutants towards CRM1 is currently under investigation.

4.3.13 An overview of LMB's interaction with CRM1

A more detailed understanding of LMB's interaction with CRM1 has been obtained. Some of the questions asked earlier in the chapter can now be addressed (**Scheme 4.16**). Once LMB forms a Michael adduct with cysteine it is immediately hydrolyzed due to stabilization of the anionic intermediate by basic residues around the hydrolysis site (**Scheme 4.16B**). Additionally, the low stability of hydrolyzed-LMB in solution displays CRM1's stabilization of the hydrolyzed product (**Scheme 4.16D**). Furthermore, LMB hydrolysis provides stabilization to the complex by compensating for a basic pocket residue in CRM1, leading to irreversible cysteine conjugation of LMB (**Scheme 4.16C**). In the event where CRM1 doesn't hydrolyze LMB, as in the case of the triple mutant of ^{Sc}CRM1*(**Figure 4.12**), conjugate addition is reversible as shown in **scheme 4.16A**.

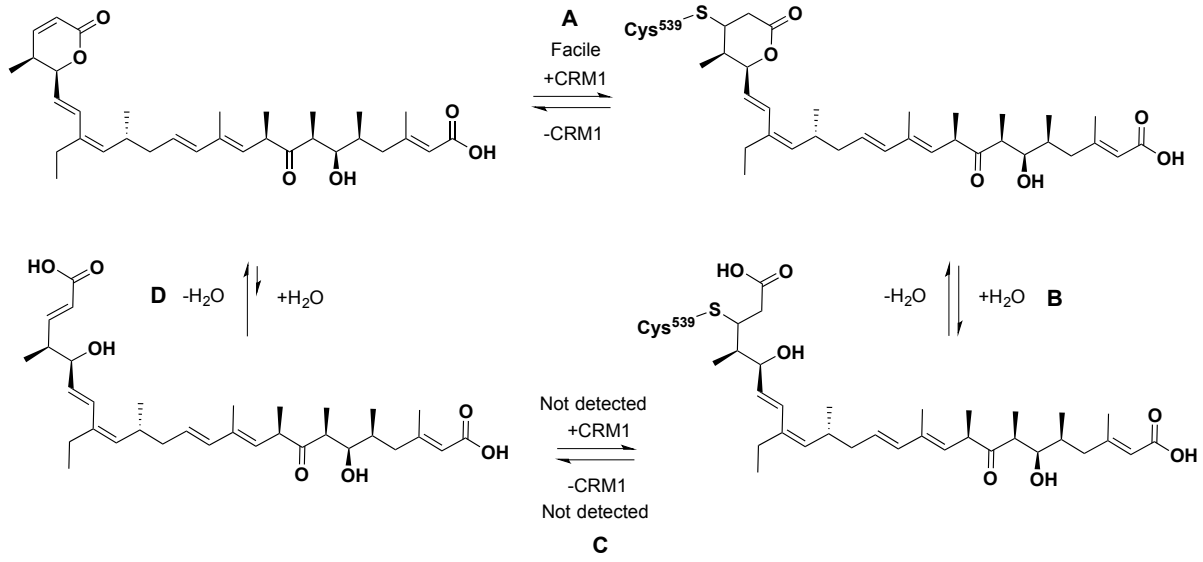

Scheme 4.16. Model showing the equilibria of conjugation and hydrolysis of LMB **A.** Reversibility of Michael conjugation before hydrolysis. **B.** Hydrolysis of lactone ring after Cys conjugation. **C.** Reversibility of Cys conjugation after hydrolysis. **D.** Hydrolysis of lactone ring before Michael conjugation.

Conclusion

4.4 Understanding the interaction of LMB and CRM1

CRM1 has been validated as a target for the treatment of cancer due to its ability to localize important tumor suppressors and negative cell cycle regulators to the cytoplasm, rendering them inactive. An important inhibitor of this nuclear export LMB, interacts with the NES binding groove of CRM1 by alkylating its cysteine residue via a Michael conjugation of LMB's α,β- unsaturated lactone ring. Due to a basic pocket of CRM1 near the lactone ring of LMB, the karyopherin is able to hydrolyze the lactone to compensate for this basic pocket providing stabilization to the system. This hydrolyzation event prevents the

reversibility of Michael conjugation of LMB perhaps leading to an increase in inhibitor potency. The synthesis of a model substrate is underway that would shed more light into the relation between potency and reversibility of cysteine conjugation. This is the first time that a karyopherin is able to drive a chemical reaction.

Experimental Section

4.5 Materials and methods

4.5.1 *General procedure*

All reactions were performed under a nitrogen atmosphere, using flame-dried glassware and monitored by TLC (Silicycle 60 F-254); visualization was done with UV /$KMnO_4$. ^{1}H and ^{13}C NMR were performed at 500 MHz and 100 MHz, respectively; chemical shifts are reported as ppm and referenced to $CDCl_3$ (7.26 and 77.0 ppm, respectively). All reagents were purchased from commercially available sources and used without further purification. Flash column chromatography was performed using silica gel purchased from Silicycle (particle size 0.032-0.063 mm)

*4.5.2 Synthesis of **12***

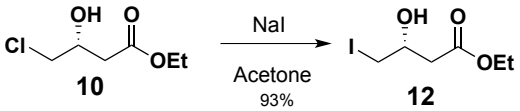

To a flame dried flask **10** (10 g, 60 mmol) was added in dry acetone (120 mL)followd by adding dry NaI (36 g, 240 mmol). The mixture was let to stir under reflux for 3 days. Acetone was mainly evaporated in vacuo, and the resulting residue was diluted with water

(50 mL). The mixture was extracted with ether (3 x 50 mL) and washed with saturated $Na_2S_2O_3$. The organic layer was dried over $MgSO_4$ and evaporation of the solvent gave an oil which was passed through a silica pad (Hexanes:Ether = 1:1) to yield **12** (14.4 g, 93%). ^{1}H NMR (500 MHz, $CDCl_3$) δ 4.16 (q, *J* = 7.2 Hz, 2H), 3.98 (m, 1H), 3.31 (dd, *J* = 10.4 Hz, 5.2 Hz, 1H), 3.28 (dd, *J* = 10.4 Hz, 5.6 Hz, 1H), 2.63 (dd, *J* = 16.5 Hz, 4.3 Hz, 1H), 2.58 (dd, *J* = 16.5 Hz, 7.8 Hz, 1H), 1.25 (t, *J* = 7.1 Hz, 3H). [25]

*4.5.3 Synthesis of **13***

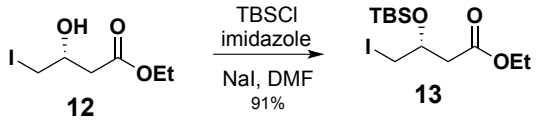

To a flame dried flask with a solution of **12** (2 gr, 7.7 mmol) and anhydrous DMF (16 mL) was added NaI (2.3 g, 15.4 mmol) and imidazole (1.04g, 15.4). TBSCl (1.74 g, 11.5 mmol) was added portion wise at 0°C followed by stirring for 16hrs from 0°C to rt. The mixture was diluted with water (20 mL) and extracted with ether (3 x 20 mL). The organic layer was dried over $MgSO_4$ and the solvent was dried in vacuo to yield **13** (1.25 g, 91%) as an oil. ^{1}H NMR (500 MHz, $CDCl_3$) δ 4.13 (m, 2H), 4.02 (m, 1H), 3.27 (dd, *J* = 10.1 Hz. 4.2 Hz, 1H), 3.24 (dd, *J* = 10.1 Hz, 6.2 Hz, 1H), 2.66 (dd, *J* = 15.2 Hz, 4.8 Hz, 1H), 2.52 (dd, *J* = 15.2 Hz, 7.4 Hz, 1H), 1.26 (t, *J* = 7.2 Hz, 3H), 0.88 (s, 9H), 0.11 (s, 3H), 0.06 (s, 3H). ^{13}C NMR (100 MHz, $CDCl_3$) δ 170.5, 68.3, 60.3, 42.4, 25.6, 17.8, 14.1, 12.9, -4.5, -4.9. [25]

*4.5.4 Synthesis of **14***

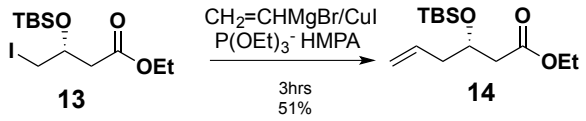

To a solution of CuI (1.3 g, 7.01 mmol) in freshly distilled THF (14 mL) was added at -35°C vinylmagnesium bromide (1.0M in THF, 14.0 ml, 14 mmol), the resulting orange slurry was stirred for 25 mins followed by addition of HMPA (2.4 ml, 14.0 mmol) and $P(OEt)_3$ (2.4 mL, 14.0mmol) at -35°C. The resulting mixture was stirred for 15 mins and a solution of **13** in THF (2.6g, 7.0 mmol) was added slowly. The mixture was stirred for 1hr at -35°C and was let to reach rt. The solution turned black and was stop after 3hr. The reaction was quenched at 0°C with saturated NH_4Cl and stirred at rt for 30mins. The product was extracted with ether (3X) and dried over $MgSO_4$. Evaporation of the solvent gave an oil which was purified by flash column chromatography (SiO_2; Hexanes:DCM) to yield **14** (970.4 mg, 51%). ^{1}H NMR (500 MHz, $CDCl_3$) δ 5.76 (ddt, *J*=16.9 Hz, 9.7 Hz, 7.2 Hz, 1H), 5.05 (m, 2H), 4.18 (quint, *J*=6.5 Hz, 1H), 4.09 (m, 2H), 2.40 (d, *J* = 6.9 Hz, 1H), 2.40 (d, *J* = 5.7 Hz, 1H), 2.25 (m, 2H), 1.23 (t, *J* = 7.2 Hz, 3H), 0.84 (s, 9H), 0.05 (s, 3H), 0.02 (s, 3H). [25]

*4.5.5 Synthesis of **15***

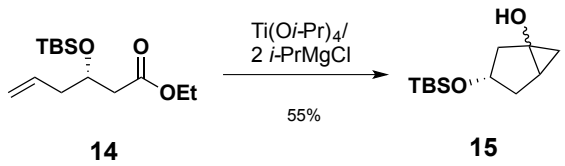

To a solution of vinyl **14** (351.4 mg, 1.28 mmol) in freshly distilled ether (6.5 ml) was added $Ti(O\text{-}iPr)_4$ (0.760 ml, 2.57mmol) at rt, to the resulting colorless mixture was added *i*-PrMgCl (2.56 ml, 5.12 mmol) slowly at -45°C. The solution turned a burgundy color and was let to stir for 1hr at -45°C; then, the reaction was let to reach rt over a period of 90 mins and stirring was continued for 2 hours at rt. Upon completion the reaction was hydrolyzed at 0°C with saturated NH_4Cl and stirred for 30 mins at rt. Extraction with ether (3X) and drying with $MgSO_4$ gave after evaporation of the solvent an oil which was purified by flash column chromatography (SiO_2; 10% Ethyl acetate: 90 % Hexanes) to yield **15** (162 mg, 55%). ^1H NMR (500 MHz, $CDCl_3$) δ 4.26 (m, 1H), 3.79 (m, 1H), 2.35 (dd, *J*=11.8Hz, 7.0 Hz, 1H), 2.21 (m, 2H), 2.07 (d, *J* = 13.0 Hz, 1H), 2.02-1.78 (m, 3H), 1.51 (d, *J*= 13.6 Hz, 1H), 1.35 (m, 2H), 1.08 (t, *J* = 4.5 Hz, 1H), 0.91- 0.77(m, 2H), 0.86 (s, 9H), 0.84 (s, 9H), 0.04 (dd, *J* = 5.5Hz, 4.5 Hz, 1H), 0.01 (s, 3H), 0.01 (s, 3H), -0.01 (s, 3H), -0.02 (s, 3H). [25]

*4.5.6 Synthesis of **8***

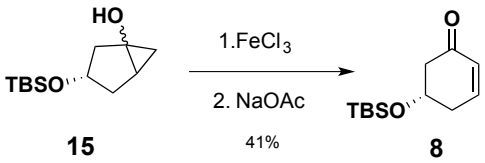

To a flame-dried flask was added $FeCl_3$ (253.0 mg, 1.56 mmol) and was cooled to -5°C using an ice bath, DMF (820 µL) was slowly added while vigorously stirring. Once $FeCl_3$ was added, the ice bath was removed and pyridine (57 µL, 0.711 mmol) was added followed by a solution of **15** (162.2 mg, 0.711 mmol) in DMF (79 µL). The reaction was let

to stir for 40min at rt. and diluted with water. The organic layer was extracted with ether and dried over $MgSO_4$, which gave after evaporation of the solvent an oil that was diluted with MeOH (790 µL). The solution was then charged with NaOAc (291.2 mg, 3.55 mmol) and was let to stir of 90 mins. Reaction mixture was diluted with water, extracted with DCM (3X) and dried over $MgSO_4$. The afforded oil was rapidly purified by flash column chromatography (SiO_2; 5% Ethyl acetate: 95 % Hexanes) and stored over CaH_2 at rt.

^{1}H NMR (500 MHz, $CDCl_3$) δ 6.87 (ddd, *J*=10.2 Hz, 5.3 Hz, 3.2 Hz, 1H), 6.06 (dt, *J* = 10.2 Hz, 1.7 Hz, 1.7 Hz, 1H), 4.22 (dddd, *J*= 9.7 Hz, 7.6 Hz, 4.3 Hz, 4.3 Hz, 1H), 2,66 (dd, *J* = 15.8 Hz , 4.3 Hz, 1H), 2.61 (m, 1H), 2.49 (dd, *J* = 15.8 Hz, 9.7 Hz, 1H), 2.39 (dddd, *J*=18.4 Hz, 7.6 Hz, 3.0 Hz, 3.0 Hz, 1H),0.87 (s, 9H), 0.06 (s, 6H). [25]

*4.5.7 Synthesis of **11***

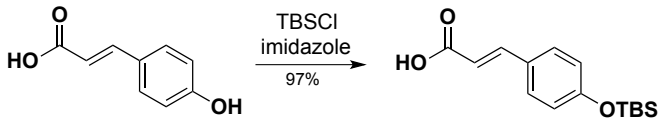

17 **11**

In a flame-dried flask were added *p*-coumaric acid (3 g, 18.2 mmol), TBSCl (3.3 g, 21.8 mmol) and imidazole (7.4 g, 109.2 mmol) followed by DMF (7.6 mL). The reaction mixture was allowed to stir at rt for 16hrs followed by dilution with DCM. The organic mixture was washed with brine (2X) and water (2X). The combined organic layers were dried over $MgSO_4$ and purified via flash column chromatography (SiO_2; 5% Methanol: 95 % DCM) to give a white wax (4.9 g, 97%).

^{1}H NMR (500 MHz, $CDCl_3$) δ 7.75 (d, *J*= 16.0 Hz, 1H), 7.46 (d, *J* = 8.8 Hz, 2H), 6.86 (d, *J*=

8.8 Hz, 2H), 6.33(d, *J* = 16.0 Hz, 1H), 0.98 (s, 9H), 0.22 (s, 6H). [26]

*4.5.8 Synthesis of **9***

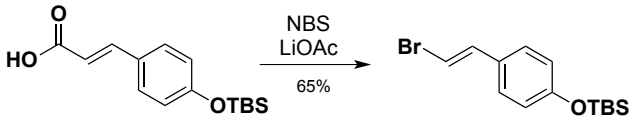

11 **9**

A solution of **11** (1g, 3.59 mmol) in CH3CN: H2O (7:1, 8.9 mL) was stirred at 60°C until most of **11** dissolved, then NBS (0.797 g, 4.48 mmol) was added and solution turned green. LiOAc (0.058g, 0.89 mmol) was subsequently added and the solution turned yellow, reaction was let to stir at 60°C for 1 hr. Solvent was removed and the mixture was purified by flash column chromatography (SiO_2; 10% DCM: 90 % Hexanes) that yielded an oil (806.5 mg, 65%). ^{1}H NMR (500 MHz, $CDCl_3$) δ 7.19 (d, *J*= 8.6 Hz, 2H), 7.06 (d, *J* = 13.9 Hz, 1H), 6.82 (d, *J*= 8.6 Hz, 2H), 6.63(d, *J* = 13.9 Hz, 1H), 1.01 (s, 9H), 0.22 (s, 6H). ^{13}C NMR (100 MHz, $CDCl_3$) δ 155.9, 136.6, 129.4, 127.3, 120.2, 104.2, 25.7, 18.2, -4.29. [26]

4.5.9 Synthesis of biotinylated-LMB

The solution of LMB in ethanol was dried (carefully removing solvent due to LMB's instability when dried) under nitrogen blowers followed by addition of toluene to avoid drying LMB completely. Solution was immediately transferred to a flame-dried vial, flushed with N_2 and addition of DMF. To this solution was added Ph_3P and dithiodipyride (DTP), the mixture was let to stir at rt for 24hrs. Subsequent addition of biotin cadaverine, the reaction was stopped after 24 hrs. The mixture was diluted with ethyl acetate and washed with water.

The aqueous layer was washed with ethyl acetate (2X). The organic layer was almost dried and was redissolved in methanol for reverse phase HPLC on a C18 column (10% acetonitrile in water to 100% acetonitrile over 23 mins followed by 100% acetonitrile for 8 mins). Product was verified by ESI-MS *m/z* 851 $[M+H]^+$, 849 $[M-H]^-$. [37]

4.5.10 LCMS Analysis

LC- MS analysis of LMB derivatives in buffer (**Table 4.1 in, 4A.1 and 4A.2**) were analyzed by LC-UV-MS using a Phenomenex C18 Luna HPLC column (4.6 × 100 mm) with a solvent gradient from 90:10 H_2O: CH_3CN to 0:100 H_2O: CH_3CN over 17 min and then, 0:100 H_2O:CH_3CN for 10 min. Detection of LMB derivatives was accomplished at 254 nm and with MS $[M + H]^+$ ion extraction. Integrals for each peak were achieved from LC chromatogram at 254nm.

References

1. Mutka, S. C.; Yang, W. Q.; Dong, S. D.; Ward, S. L.; Craig, D. A.; Timmermans, P. B.; Murli, S., Identification of nuclear export inhibitors with potent anticancer activity in vivo. *Cancer research* **2009,** *69* (2), 510-7.
2. Strambio-De-Castillia, C.; Niepel, M.; Rout, M. P., The nuclear pore complex: bridging nuclear transport and gene regulation. *Nature reviews. Molecular cell biology* **2010,** *11* (7), 490-501.
3. Wente, S. R.; Rout, M. P., The nuclear pore complex and nuclear transport. *Cold Spring Harbor perspectives in biology* **2010,** *2* (10), a000562.
4. Freitas, N.; Cunha, C., Mechanisms and signals for the nuclear import of proteins. *Current genomics* **2009,** *10* (8), 550-7.
5. Kutay, U.; Guttinger, S., Leucine-rich nuclear-export signals: born to be weak. *Trends in cell biology* **2005,** *15* (3), 121-4.
6. Hutten, S.; Kehlenbach, R. H., CRM1-mediated nuclear export: to the pore and beyond. *Trends in cell biology* **2007,** *17* (4), 193-201.
7. Davis, J. R.; Mossalam, M.; Lim, C. S., Controlled access of p53 to the nucleus regulates its proteasomal degradation by MDM2. *Molecular pharmaceutics* **2013,** *10* (4), 1340-9.
8. Vousden, K. H.; Vande Woude, G. F., The ins and outs of p53. *Nature cell biology* **2000,** *2* (10), E178-80.
9. (a) Chen, L.; Yin, H.; Farooqi, B.; Sebti, S.; Hamilton, A. D.; Chen, J., p53 alpha-Helix mimetics antagonize p53/MDM2 interaction and activate p53. *Molecular cancer therapeutics* **2005,** *4* (6), 1019-25; (b) Chene, P., Inhibiting the p53-MDM2 interaction: an important target for cancer therapy. *Nature reviews. Cancer* **2003,** *3* (2), 102-9.
10. (a) Hamamoto, T.; Gunji, S.; Tsuji, H.; Beppu, T., Leptomycins A and B, new antifungal antibiotics. I. Taxonomy of the producing strain and their fermentation, purification and characterization. *The Journal of antibiotics* **1983,** *36* (6), 639-45; (b) Hamamoto, T.; Seto, H.; Beppu, T., Leptomycins A and B, new antifungal antibiotics. II. Structure elucidation. *The Journal of antibiotics* **1983,** *36* (6), 646-50.
11. Kobayashi, M.; Wang, W. Q.; Tsutsui, Y.; Sugimoto, M.; Murakami, N., Absolute stereostructure and total synthesis of leptomycin B. *Tetrahedron Lett* **1998,** *39* (45), 8291-8294.
12. Newlands, E. S.; Rustin, G. J.; Brampton, M. H., Phase I trial of elactocin. *British journal of cancer* **1996,** *74* (4), 648-9.
13. (a) Matsuyama, A.; Arai, R.; Yashiroda, Y.; Shirai, A.; Kamata, A.; Sekido, S.; Kobayashi, Y.; Hashimoto, A.; Hamamoto, M.; Hiraoka, Y.; Horinouchi, S.; Yoshida, M., ORFeome cloning and global analysis of protein localization in the fission yeast Schizosaccharomyces pombe. *Nature biotechnology* **2006,** *24* (7), 841-7; (b) Xu, D.; Farmer, A.; Chook, Y. M., Recognition of nuclear targeting signals by Karyopherin-beta proteins. *Current opinion in structural biology* **2010,** *20* (6), 782-90.
14. Nishi, K.; Yoshida, M.; Fujiwara, D.; Nishikawa, M.; Horinouchi, S.; Beppu, T., Leptomycin-B Targets a Regulatory Cascade of Crm1, a Fission Yeast Nuclear-Protein,

Involved in Control of Higher-Order Chromosome Structure and Gene-Expression. *J Biol Chem* **1994,** *269* (9), 6320-6324.
15. Kudo, N.; Matsumori, N.; Taoka, H.; Fujiwara, D.; Schreiner, E. P.; Wolff, B.; Yoshida, M.; Horinouchi, S., Leptomycin B inactivates CRM1/exportin 1 by covalent modification at a cysteine residue in the central conserved region. *Proceedings of the National Academy of Sciences of the United States of America* **1999,** *96* (16), 9112-7.
16. Sun, Q.; Carrasco, Y. P.; Hu, Y.; Guo, X.; Mirzaei, H.; Macmillan, J.; Chook, Y. M., Nuclear export inhibition through covalent conjugation and hydrolysis of Leptomycin B by CRM1. *Proceedings of the National Academy of Sciences of the United States of America* **2013,** *110* (4), 1303-8.
17. Bonazzi, S.; Eidam, O.; Guttinger, S.; Wach, J. Y.; Zemp, I.; Kutay, U.; Gademann, K., Anguinomycins and derivatives: total syntheses, modeling, and biological evaluation of the inhibition of nucleocytoplasmic transport. *Journal of the American Chemical Society* **2010,** *132* (4), 1432-42.
18. Meissner, T.; Krause, E.; Vinkemeier, U., Ratjadone and leptomycin B block CRM1-dependent nuclear export by identical mechanisms. *FEBS letters* **2004,** *576* (1-2), 27-30.
19. Wach, J. Y.; Guttinger, S.; Kutay, U.; Gademann, K., The cytotoxic styryl lactone goniothalamin is an inhibitor of nucleocytoplasmic transport. *Bioorganic & medicinal chemistry letters* **2010,** *20* (9), 2843-6.
20. Sakakibara, K.; Saito, N.; Sato, T.; Suzuki, A.; Hasegawa, Y.; Friedman, J. M.; Kufe, D. W.; Vonhoff, D. D.; Iwami, T.; Kawabe, T., CBS9106 is a novel reversible oral CRM1 inhibitor with CRM1 degrading activity. *Blood* **2011,** *118* (14), 3922-31.
21. (a) Dong, X.; Biswas, A.; Suel, K. E.; Jackson, L. K.; Martinez, R.; Gu, H.; Chook, Y. M., Structural basis for leucine-rich nuclear export signal recognition by CRM1. *Nature* **2009,** *458* (7242), 1136-41; (b) Monecke, T.; Guttler, T.; Neumann, P.; Dickmanns, A.; Gorlich, D.; Ficner, R., Crystal structure of the nuclear export receptor CRM1 in complex with Snurportin1 and RanGTP. *Science* **2009,** *324* (5930), 1087-91.
22. (a) Jencks, W. P., The Reaction of Hydroxylamine with Activated Acyl Groups .2. Mechanism of the Reaction. *Journal of the American Chemical Society* **1958,** *80* (17), 4585-4588; (b) Caplow, M.; Jencks, W. P., The Chymotrypsin-Catalyzed Hydrolysis and Synthesis of N-Acetyl-L-Tyrosine Hydroxamic Acid. *J Biol Chem* **1964,** *239*, 1640-52.
23. (a) Lapalombella, R.; Sun, Q.; Williams, K.; Tangeman, L.; Jha, S.; Zhong, Y.; Goettl, V.; Mahoney, E.; Berglund, C.; Gupta, S.; Farmer, A.; Mani, R.; Johnson, A. J.; Lucas, D.; Mo, X.; Daelemans, D.; Sandanayaka, V.; Shechter, S.; McCauley, D.; Shacham, S.; Kauffman, M.; Chook, Y. M.; Byrd, J. C., Selective inhibitors of nuclear export show that CRM1/XPO1 is a target in chronic lymphocytic leukemia. *Blood* **2012,** *120* (23), 4621-34; (b) Etchin, J.; Sun, Q.; Kentsis, A.; Farmer, A.; Zhang, Z. C.; Sanda, T.; Mansour, M. R.; Barcelo, C.; McCauley, D.; Kauffman, M.; Shacham, S.; Christie, A. L.; Kung, A. L.; Rodig, S. J.; Chook, Y. M.; Look, A. T., Antileukemic activity of nuclear export inhibitors that spare normal hematopoietic cells. *Leukemia* **2013,** *27* (1), 66-74.
24. Jewers, K.; Blunden, G.; Wetchapi.S; Dougan, J.; Manchand.Ah; Davis, J. B.; Kyi, A., Goniothalamin and Its Distribution in 4 Goniothalamus Species. *Phytochemistry* **1972,** *11* (6), 2025-&.

25. Hareau, G. P. J.; Koiwa, M.; Hikichi, S.; Sato, F., Synthesis of optically active 5-(tert-butyldimethylsiloxy)-2-cyclohexenone and its 6-substituted derivatives as useful chiral building blocks for the synthesis of cyclohexane rings. Syntheses of carvone, penienone, and penihydrone. *Journal of the American Chemical Society* **1999,** *121* (15), 3640-3650.
26. Georgiades, S. N.; Clardy, J., Synthetic libraries of tyrosine-derived bacterial metabolites. *Bioorganic & medicinal chemistry letters* **2008,** *18* (10), 3117-21.
27. Yamada, T.; Iritani, M.; Minoura, K.; Numata, A.; Kobayashi, Y.; Wang, Y. G., Absolute stereostructures of cell adhesion inhibitors, macrosphelides H and L, from Periconia byssoides OUPS-N133. *The Journal of antibiotics* **2002,** *55* (2), 147-54.
28. Syvret, R. G.; Butt, K. M.; Nguyen, T. P.; Bulleck, V. L.; Rieth, R. D., Novel process for generating useful electrophiles from common anions using Selectfluor (R) fluorination agent. *Journal of Organic Chemistry* **2002,** *67* (13), 4487-4493.
29. Ye, C. F.; Shreeve, J. M., Structure-dependent oxidative bromination of unsaturated C-C bonds mediated by selectfluor. *Journal of Organic Chemistry* **2004,** *69* (24), 8561-8563.
30. Kurti, L. a. C., B., *Strategic Applications of Named Reactions in Organic Synthesis*. Paperback ed.; Elsevier Academic Press: 2005.
31. Hikichi, S.; Hareau, G. P. J.; Sato, F., Efficient and practical synthesis of optically active 5-t-butyldimethylsiloxy-2-cyclohexenone as a convenient chiral 2,5-cyclohexadienone synthon. *Tetrahedron Lett* **1997,** *38* (48), 8299-8302.
32. Fatima, A.; Kohn, L. K.; Carvalho, J. E.; Pilli, R. A., Cytotoxic activity of (S)-goniothalamin and analogues against human cancer cells. *Bioorganic & medicinal chemistry* **2006,** *14* (3), 622-31.
33. Huang, H.; Alvarez, K.; Lui, Q.; Barnhart, T. M.; Snyder, J. P.; PennerHahn, J. E., Infrared spectroscopic characterization of cyanocuprates. *Journal of the American Chemical Society* **1996,** *118* (37), 8808-8816.
34. Shinokubo, H.; Miki, H.; Yokoo, T.; Oshima, K.; Utimoto, K., A Facile Preparation of Alkenylmetallic and Allenylmetallic Compounds by Means of Iodine-Metal Exchange and Their Use in Organic-Synthesis. *Tetrahedron* **1995,** *51* (43), 11681-11692.
35. Valot, G.; Garcia, J.; Duplan, V.; Serba, C.; Barluenga, S.; Winssinger, N., Diversity-oriented synthesis of diverse polycyclic scaffolds inspired by the logic of sesquiterpene lactones biosynthesis. *Angewandte Chemie* **2012,** *51* (22), 5391-4.
36. (a) Mukaiyama, T.; Matsueda, R.; Suzuki, M., Peptide synthesis via the oxidation-reduction condensation by the use of 2,2'-dipyridyldisulfide as a oxidant. *Tetrahedron Lett* **1970,** (22), 1901-4; (b) Corey, E. J.; Nicolaou, K. C., Efficient and Mild Lactonization Method for Synthesis of Macrolides. *Journal of the American Chemical Society* **1974,** *96* (17), 5614-5616.
37. Kudo, N.; Wolff, B.; Sekimoto, T.; Schreiner, E. P.; Yoneda, Y.; Yanagida, M.; Horinouchi, S.; Yoshida, M., Leptomycin B inhibition of signal-mediated nuclear export by direct binding to CRM1. *Experimental cell research* **1998,** *242* (2), 540-7.

APPENDIX 4A

Table 4A.1 Hydrolysis of LMB and DTT-LMB

Time	Thiol	LMB*	LMB-DTT*	Hydrolyzed-LMB
26h	-	1	0	0
26h	DTT	0	0.89	0.11

* Ratio obtained from integration of LC chromatogram peak at 254nm.

Table 4A.2 Hydrolysis of LMB-DTT vs LMB-DTT treated with CRM1 in the presence or absence of hydroxylamine

Entry	Time	Enzyme	Thiol	Additive	1	2	3	4	8
1	2h	^{y}CRM1	DTT	-	-	99.9	T	-	-
2	8h	^{y}CRM1	DTT	-	-	99.9	T	-	-
3	26h	^{y}CRM1	DTT	-	-	99.9	T	-	-
4	26h	-	DTT	-	-	89.1	10.8	-	-
5	2h	^{y}CRM1	DTT	NH_2OH	-	85.5	7.0	7.3	T
6	8h	^{y}CRM1	DTT	NH_2OH	-	68.9	15.3	15.7	T
7	26h	^{y}CRM1	DTT	NH_2OH	-	39.7	36.2	23.9	T
8	26h	-	DTT	NH_2OH	-	52.5	20.0	24.2	3.1
9	26h	-	-	-	100	-	-	-	-

% Obtained from integration of LC chromatogram peak at 254nm. T= Trace amounts

Figure 4A.1 ^{1}H- NMR of **12** in $CDCl_3$. 500 MHz

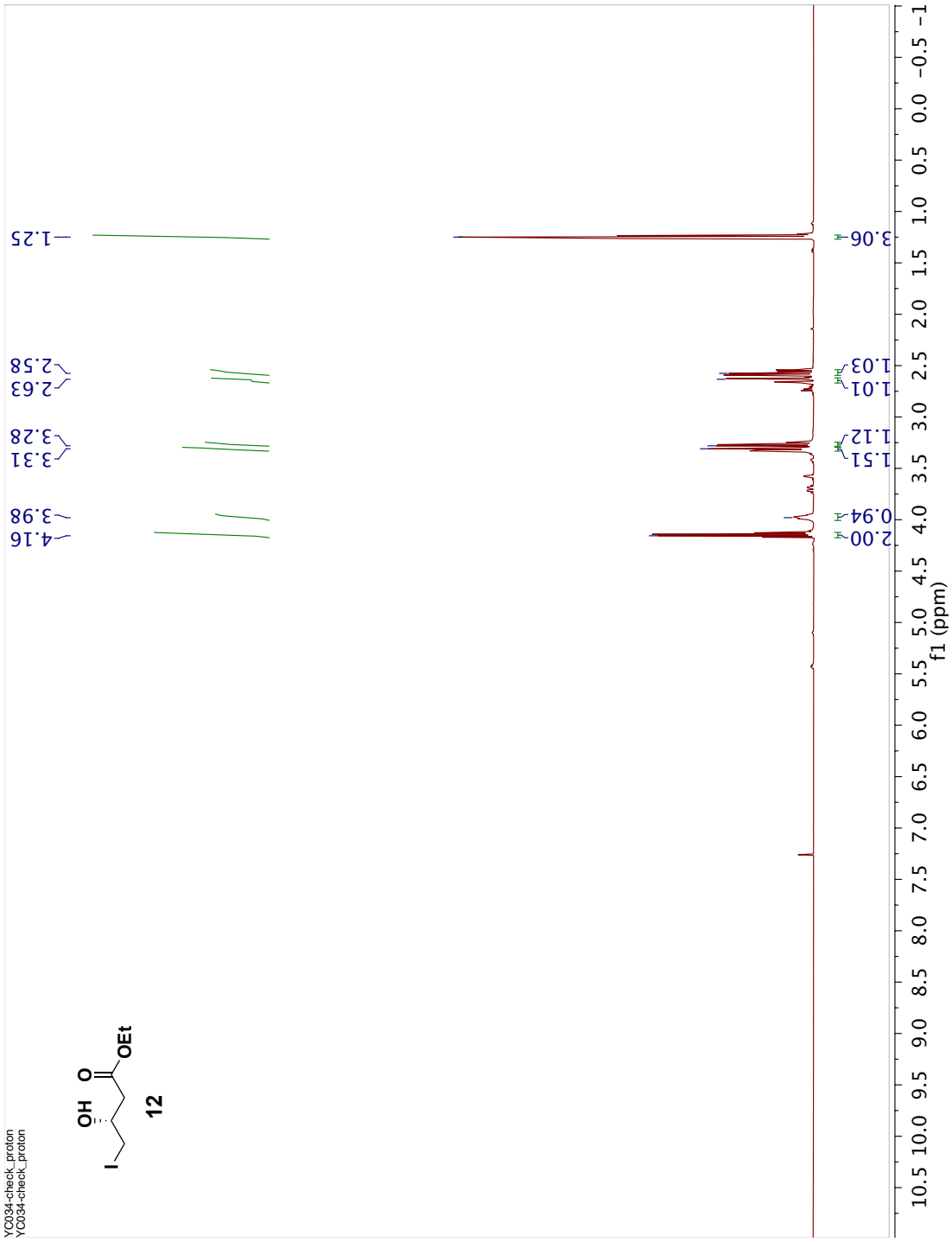

Figure 4A.2 ^{1}H- NMR of **13** in $CDCl_3$. 500 MHz

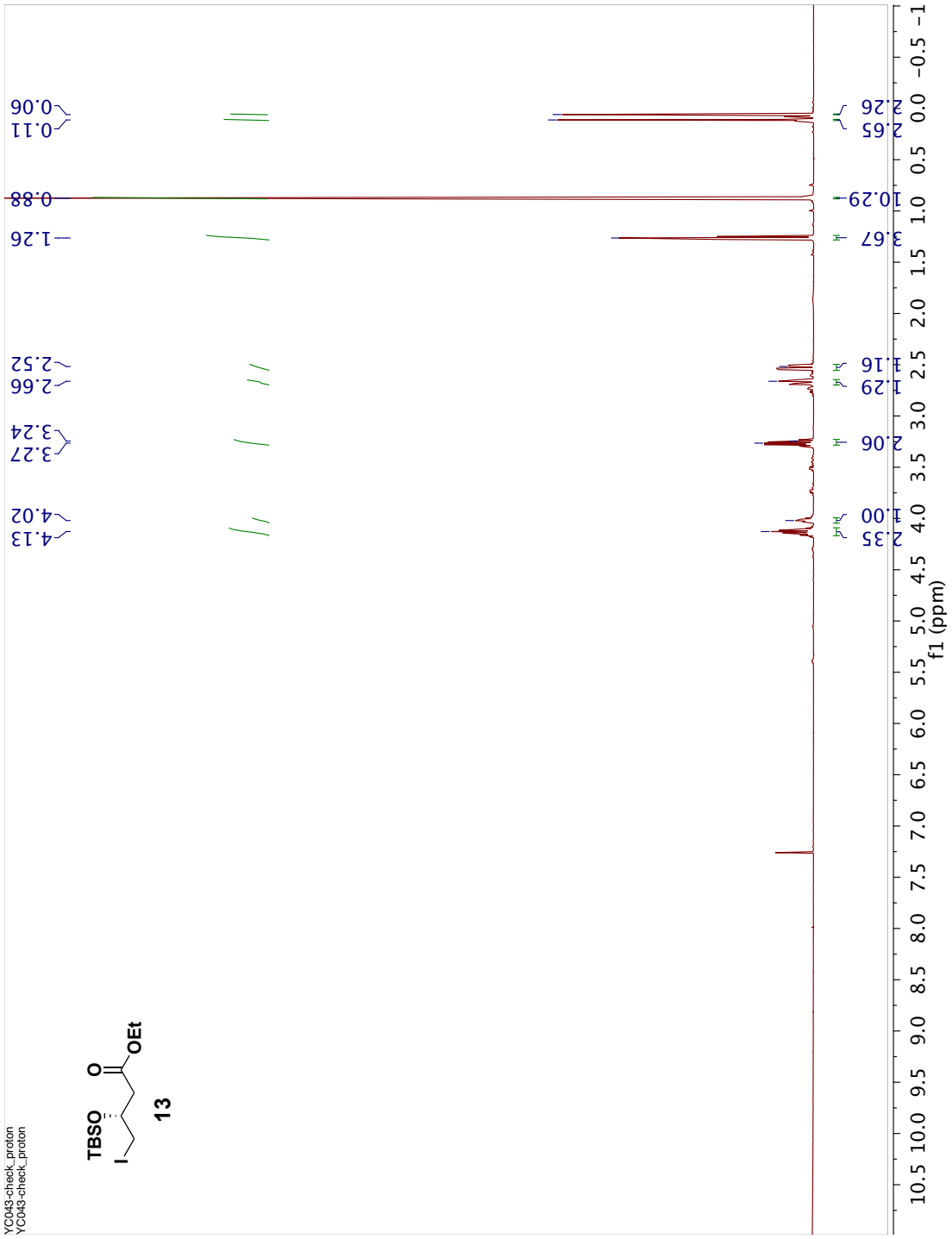

Figure 4A.3 ^{1}H- NMR of **14** in $CDCl_3$. 500 MHz

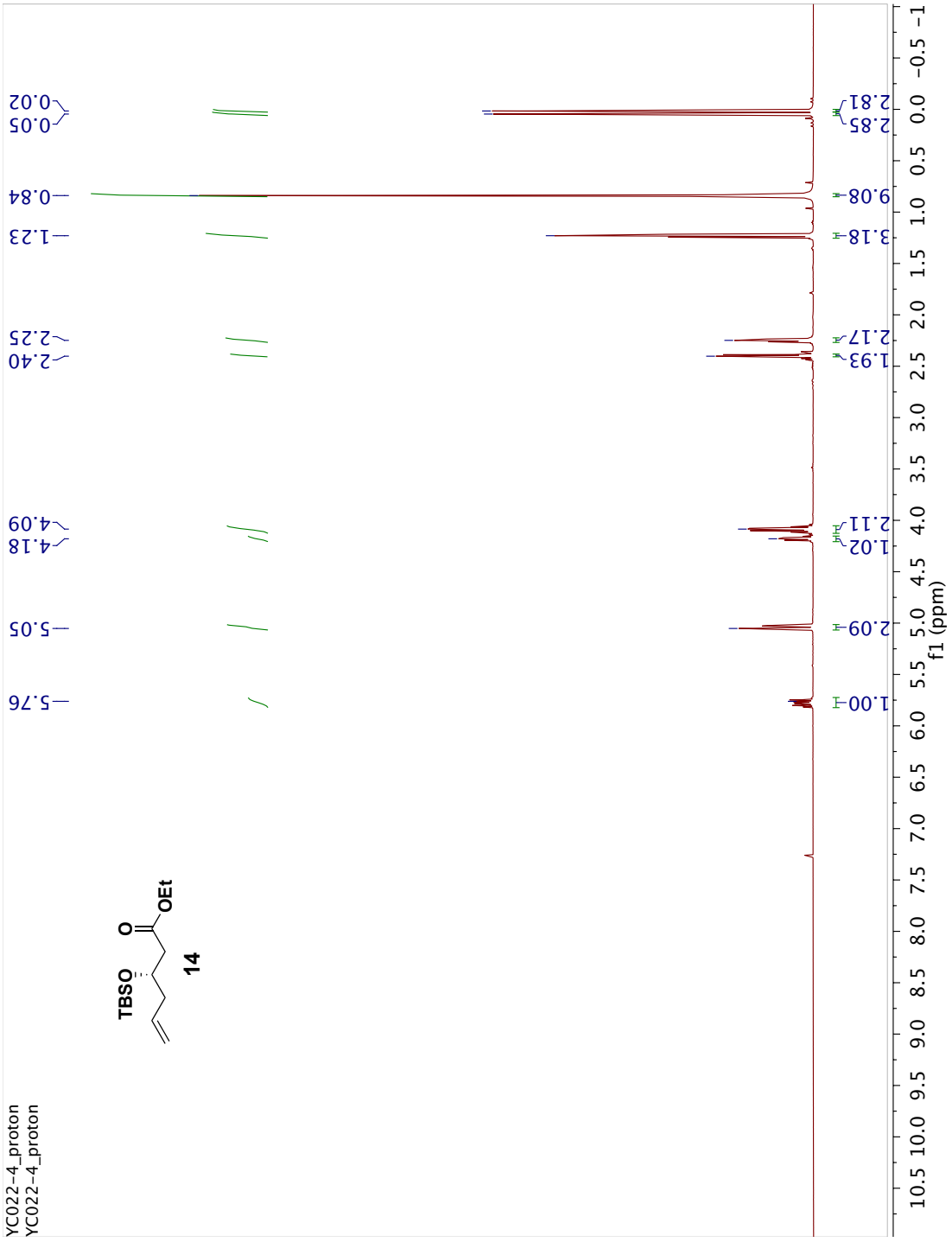

Figure 4A.4 ^{1}H- NMR of **15** in $CDCl_3$. 500 MHz

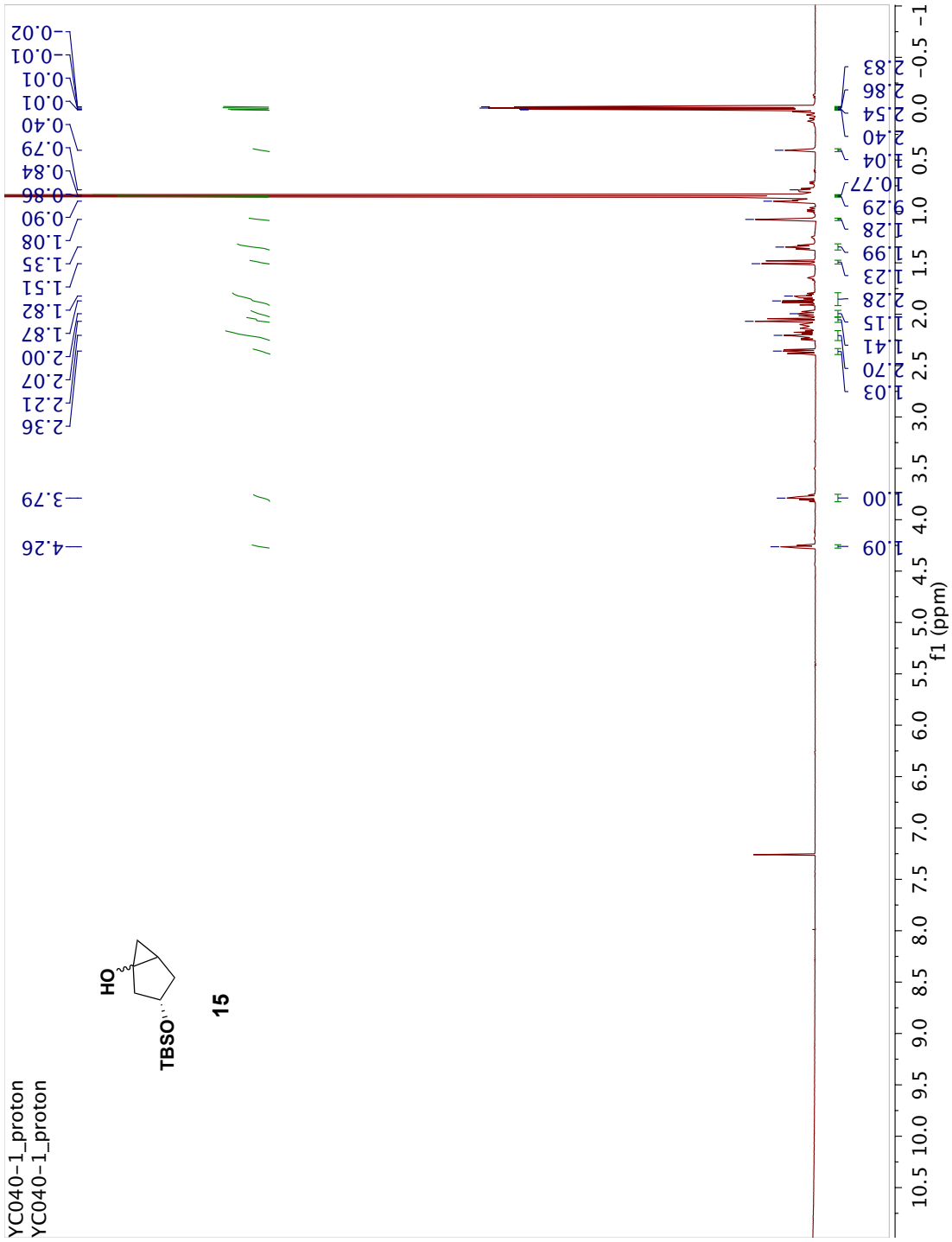

Figure 4A.5 ^{1}H- NMR of **8** in $CDCl_3$. 500 MHz

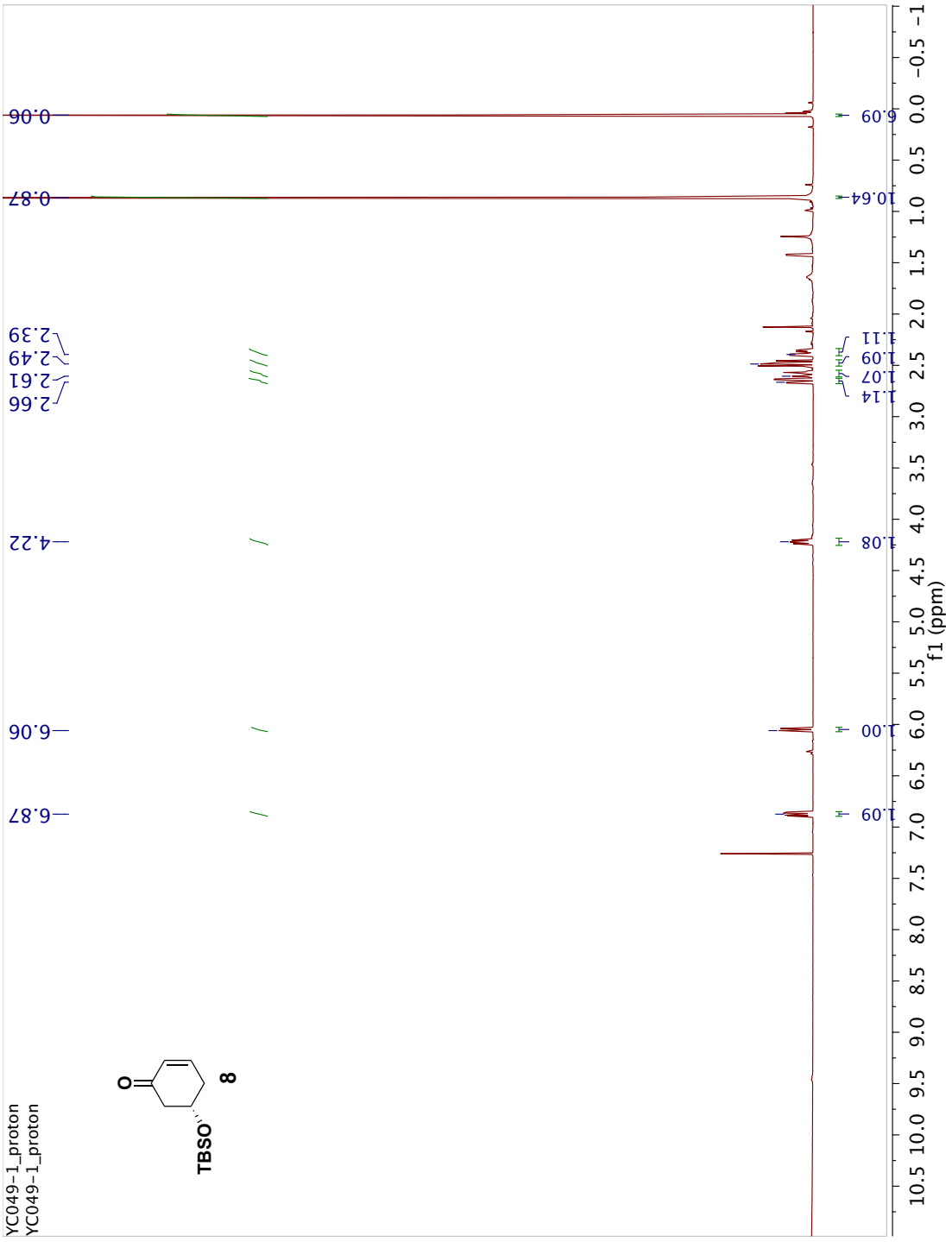

Figure 4A.6 ^{1}H- NMR of **11** in $CDCl_3$. 500 MHz

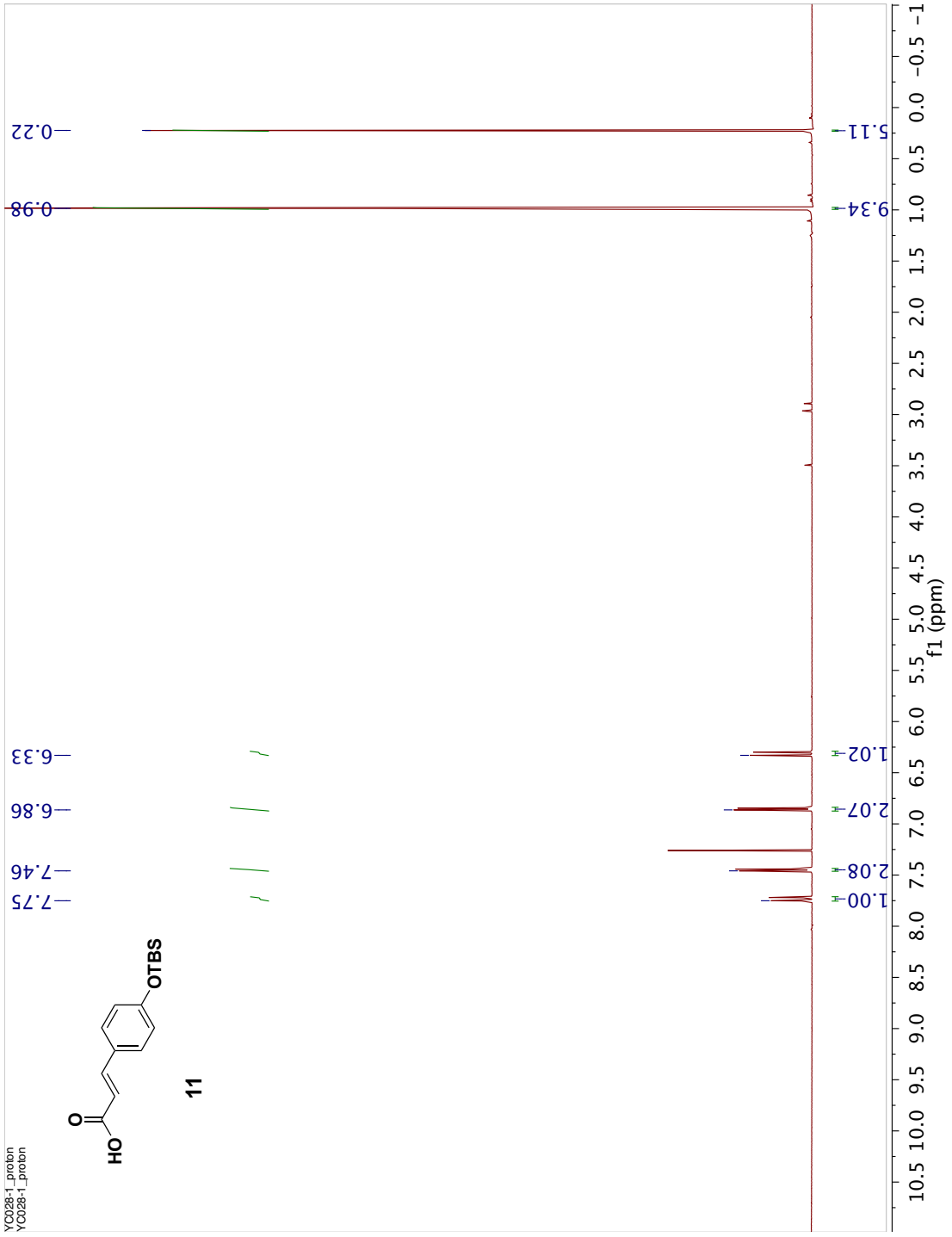

Figure 4A.7 ^{1}H- NMR of **9** in $CDCl_3$. 500 MHz

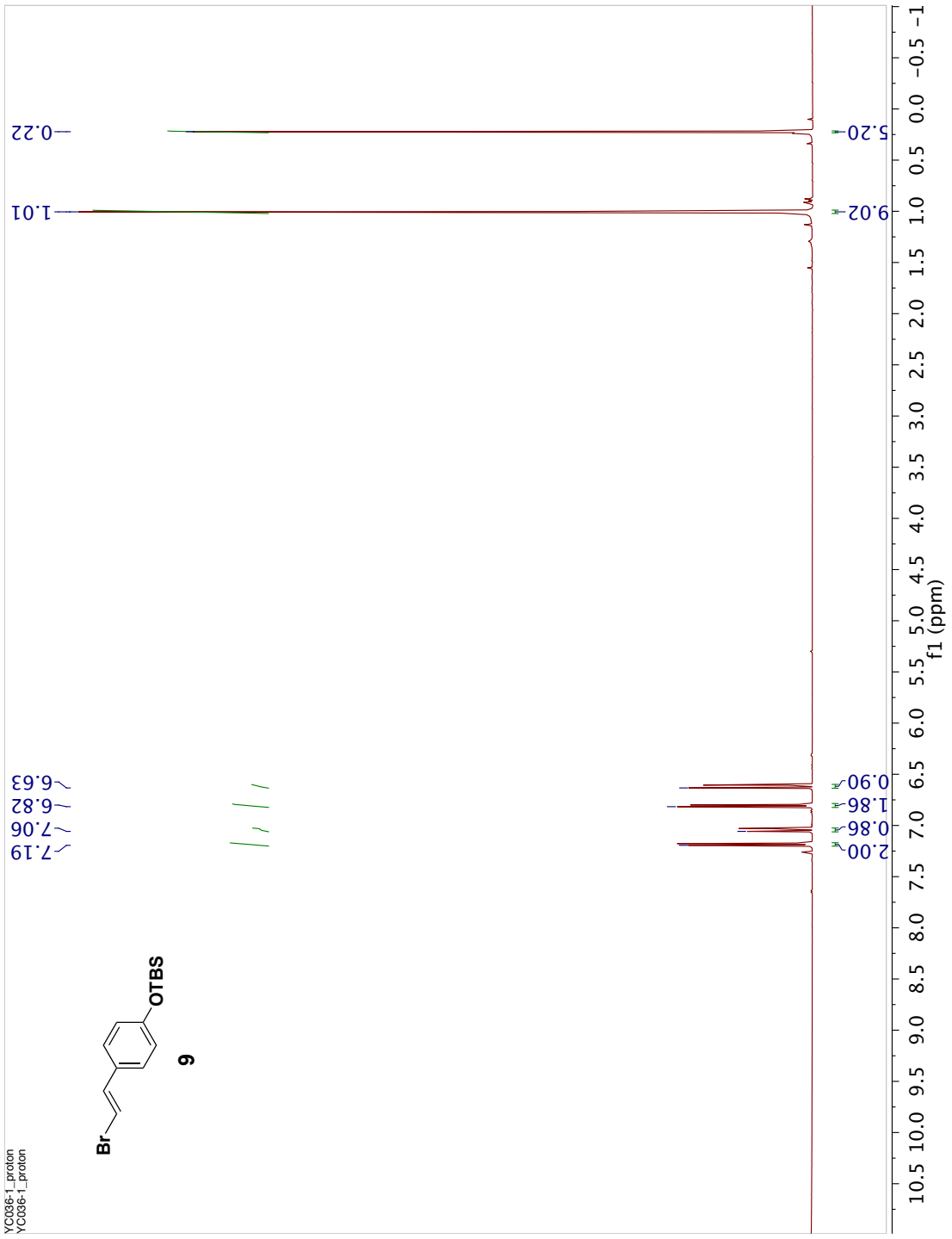

Figure 4A.8 ^{13}C- NMR of **13** in $CDCl_3$. 100 MHz

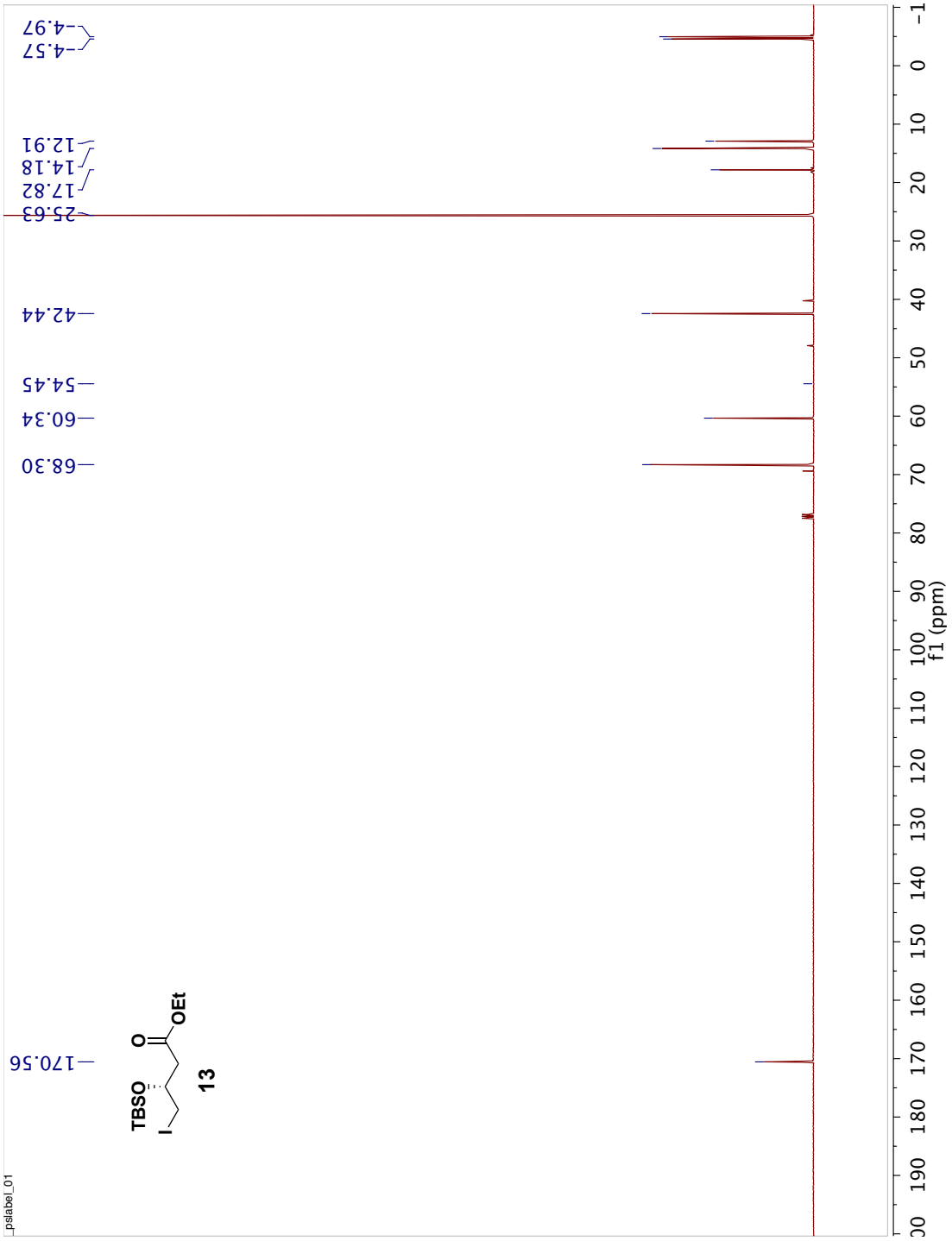

Figure 4A.9 ^{13}C- NMR of **9** in $CDCl_3$. 100 MHz